THE SILICATE MINERALOGY OF THE MG4 CHROMITITE PACKAGE IN THE EASTERN PART OF THE BUSHVELD COMPLEX, SOUTH AFRICA

BY

OLUTOLA O. JOLAYEMI

Submitted in partial fulfillment of the requirements for the degree Master of Science (Geology) in the Department of Geology, Faculty of Natural and Agricultural Sciences, University of Pretoria, South Africa

2011

UNIVERSITEIT VAN PRETORIA
UNIVERSITY OF PRETORIA
YUNIBESITHI YA PRETORIA

DECLARATION

I, Olutola O. Jolayemi declare that the thesis/dissertation,which I herby submit for the degree Msc: Geology at the University of Pretoria, is my own work and has not previously been submitted by me for a degree at this or any other tertiary institution.

Signature:.....

Date:.....

UNIVERSITEIT VAN PRETORIA
UNIVERSITY OF PRETORIA
YUNIBESITHI YA PRETORIA

DECLARATION OF ORIGINALITY

Full names of student:……..

Student number:……

Declaration

1. I understand what plagiarism is and I'm aware of the University's policy in this regard.
2. I declare that this …… (eg essay, report, project, assignment, dissertation, thesis, etc) is my own original work. Where other peoples' work has been used (either from a printed source, internet or any other source), this has been properly acknowledge and referenced in accordance with departmental requirements.
3. I have not used work previously published by another student or any other person to hand in as my own.
4. I have not allowed, and will not allow, anyone to copy my work with the intention of passing it off as his or her own work.

Signature of Student:……..

Signature of Supervisor:……

ACKNOWLEDGEMENT

Prof. and Dr. (Mrs.) Jolayemi generously provided financial support for this project. Their contributions and assistance are gratefully acknowledged.

I am indebted to my supervisor, Dr. James Roberts for his tremendous help over the years, particularly his assistance in the field and his patience in reviewing all my chapters. Many thanks to Prof. R Merkle for his advice and discussion especially in the early part of this project. Peter Gräser is thanked for his patience and assistance on the microprobe analysis of this project. My sincere thanks also go to Anja Roberts, Victor Tibane, Philane Mavimbela and John Bussio for their constructive reviews.

ABSTRACT

Stratiform chromitite layers are peculiar to large layered mafic intrusions. The origin of these chromitite layers has been widely debated. Some petrologists suggested that the layers formed as a result of the mixing of two compositionally different magmas whereas others suggest that the chromitite layers formed from changes in pressure. The former hypothesis is widely accepted, and states that chromitite forms when a more evolved magma is injected into the chamber occupied by a more primitive one. To evaluate this hypothesis, a study has been conducted on the silicate textures and major element geochemistry of the silicate-rich layers above and below the MG4 chromitite package in the Critical Zone of the Rustenburg Layered Suite, part of the Bushvel Complex in South Africa.The MG4 chromitite package consists of several chromitite seamsseparated by silicate layers. Orthopyroxene and plagioclase (interstitial plagioclase) are observed in large amounts throughout the silicate layer, with less abundant clinopyroxene and some trace amounts of biotite. Throughout the silicate-rich layers above and below the MG4 chromitite layers (MG4 pyroxenite), the orthopyroxene exhibits no major compositional variation in major elements (Mg#= 1.15-1.25). This is also observed in the clinopyroxene composition throughout the study area. However, plagioclase, which dominates the lower part of the stratigraphy, varies in composition with a decrease in the calcium content (Ca= 0.8-0.5) and a simultaneous increase in the sodium content (Na=0.2-0.5). These similarities between the rocks above and below the MG4 chromitite layers suggest that the chromitite layer originated from a single magma or a mixture of two magmas with similar composition. This model is supported by the observed thin sections where orthopyroxene occurs as euhedral grains throughout the section especially above the 63.13m depth lying above the plagioclase –rich layer. Trace element analysis further suggest that the magma that crystallized the plagioclase-rich lower part mixed with the influx of new magma rich in Mg to crystallize the rocks of the upper sequence dominated by orthopyroxene, clinopyroxene and Na-rich plagioclase.

Contents

DECLARATION 2
DECLARATION OF ORIGINALITY 3
ABSTRACT 5
LIST OF FIGURES 8
LIST OF TABLES 9
CHAPTER 1 10
1.1.1 THE MARGINAL ZONE 13
1.1.2 THE LOWER ZONE 13
1.1.3 THE CRITICAL ZONE 13
1.1.4 THE MAIN ZONE 14
1.1.5 THE UPPER ZONE 16
1.1.6 AIM OF THIS STUDY 16
CHAPTER 2 18
2.1 REVIEW OF CHROMITITE FORMATION MODELS 18
CHAPTER 3 23
3.1 METHODOLOGY 23
3.1 BOREHOLE STRATIGRAPHY 24
3.2 PETROGRAPHIC CHARACTER OF THE MG4 PYROXENITE 26
3.3 PETROGRAPHIC DESCRIPTION 28
3.4 Microprobe results 38
3.5 Trace element geochemistry on bulk rock samples 43
CHAPTER 4 45
4.1 DISCUSSION 45
4.1.1 THEORETICAL CRITERIA FOR DISTINGUISHING MAGMA INFLUX FROM FRACTIONAL CRYSTALLIZATION AND ASSIMILATION. 45
4.1.2 OBSERVATION ON BOREHOLE USED IN THIS PROJECT. 47
4.1.3 MAGMA INFLUX AT THE MG4 LEVEL? 54
CHAPTER 5 57
5.1 CONCLUSION 57
REFERENCES 59
APPENDIX I 63
APPENDIX II 70

APPENDIX III 76

LIST OF FIGURES

Figure 1 Generalized geological map of the Bushveld Complex with sample location at Steelpoort……11

Figure 2: Stratigraphic Column of the Bushveld Complex zones and their respective thickness based on Eales and Cawthorn, 1996……..15

Figure 3: Stratigraphic unit of the MG4 and the modal abundance of each thin section at the corresponding depth (m) as observed from the drill core. The blank space/column is a poorly prepared thin section……25

Figure 4: Mineral composition profiles through the MG4 sequence. Thick dark horizontal lines drawn across the graphs represent the chromitite layers……27

Figure 5: Photomicrographs of the MG4 chromitite rocks: (a) Interstitial orthopyroxene in the plagioclase-rich layer at the base of the stratigraphic sequence. (b) Na-rich plagioclase showing albite twinning at the upper part of the orthopyroxene-rich layers. (c) Ca-rich plagioclase observed at the lower part of the stratigraphy exhibiting carlsberg twinning. (d) Growth of interstitial clinopyroxene crystal around subrounded orthopyroxene crystals. (e) Large orthopyroxene crystal ……37

Figure 6: Plots of major elements against depth (m)……..40

Figure 7: Plots of some trace elements against depth (m)……..43

Figure 8: Variation in Mg# of both orthopyroxene (i) and clinopyroxene (ii) across the depth (m) of the MG4 section……48

Figure 9: Variation in NaO (i), CaO (ii) and Al_2O_3 (iii) composition of plagioclase across the depth (m) of the MG4 section……48

Figure 10**:** Compositional variation in the plagioclase at the 61.73m-64.12m , 61.09m-61.13m and 57.20m-60.68m……49

Figure 11: Compariso between some trace elements with compatible plagioclase elements(An%)….52

Figure 12: Comparison of some trace elements with compatible pyroxene compositions(Mg#)……..53

LIST OF TABLES

Table 1: Subdivisions of the Bushveld Complex (Johnson, Anhaeusser and Thomas, 2006) ……..12

Table 2: Average weight percent of major elements analysed. Blanks spaces are as a result of grain size too small to be analyzed or poor preparation of thin sections used in the microprobe analysis of major elements……38

Table 3: Trace elements analysis. Elements with an * can be regarded semi quantitative.....42

CHAPTER 1

INTRODUCTION

The Bushveld Complex is an igneous intrusion found in the northeastern region of South Africa. It intruded the sedimentary strata of the Transvaal Supergroup at 2.06Ga (Walraven and Cawthorn, 1998) and is currently the largest layered mafic-ultramafic intrusion known on earth. The Bushveld Complex covers an area of approximately 66000 km^2 (Wilson and Ahaeusser, 1998) and has a thickness that varies between 7000m and 9000m. This intrusion is exposed in four main localities, namely the northern, the eastern, the Bethal and the western limbs, as shown in figure 1. A fifth limb called the far western limb is also identified but far less prominent as the other four limbs. Gough and van Niekerk (1995), and Cawthorn, et al. (1998) proposed that the layers of the Bushveld Complex were nearly horizontal at the time of their formation, dipping inwards and towards the centre of the intrusion. Following this theory it was suggested that the entire intrusion is wide and shallow.

The Bushveld Complex contains the world's largest deposits of chromitite, vanadium and platinum group elements (PGEs). The chromitite occurs in stratigraphic layers. It has been suggested that these layers crystallize either from a single or from multiple injections of magma. This project aims to provide evidence that the chromitite layer examined for this study formed either as a result of multiple injections of magma, or just a single batch of magma, by studying the petrographic character of the rocks, as well as the major element geochemistry of these rocks within the MG4 stratigraphy.

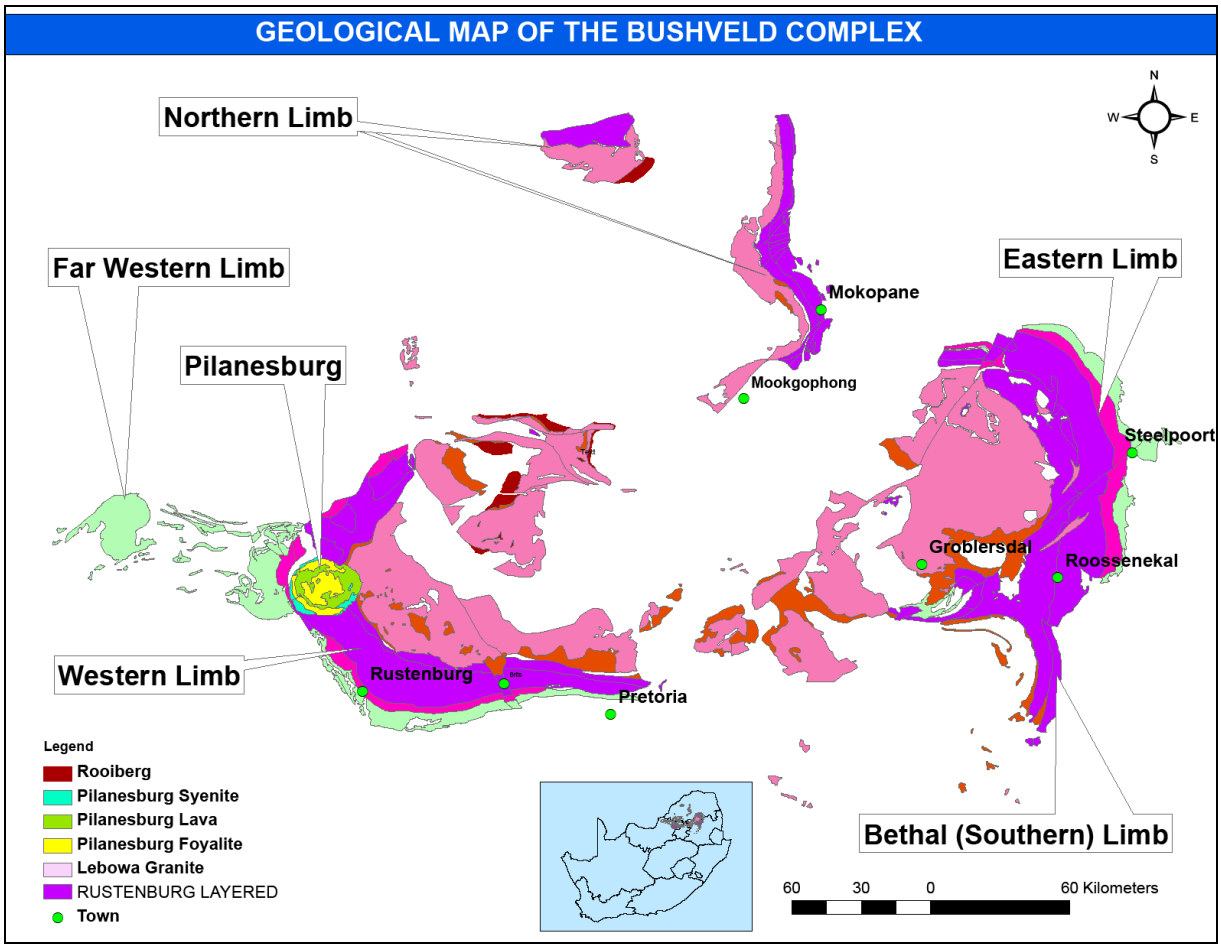

Figure 1: Generalized geological map of the Bushveld Complex with sample location at Steelpoort.

The Bushveld Complex is stratigraphically made up of five zones mainly on the basis of lithological and geological parameters peculiar to the different limbs. Hall (1932) distinguished these zones as the Marginal, Lower, Critical, Main and Upper zones. These zones have an unconformity which separates it from the overlying Rooiberg Group (Johnson et al., 2006).

Table 1: Subdivisions of the Bushveld Complex (Johnson, Anhaeusser and Thomas, 2006) .

LEBOWA GRANITE SUITE	Nebo, Makhutso, Klipkloop, Bobbejaankop, and Verena granites	
RASHOOP GRANOPHYRE SUITE	Stavoren and Diepkloop Granophyres, Rooikop Porphyritic Granite, Zwartbank Pseudogranophyre	
RUSTENBURG LAYERED SUITE	Upper Zone	Subzone C (Ol-Ap diorite) Subzone B (Ol-Mt gabbronorite) Subzone A (Mt gabbronorite)
	Main Zone	Upper subzone (gabbronorite) Lower subzone (gabbronorite, norite)
	Critical Zone	Upper subzone (norite , anorthosite, pyroxenite) Lower subzone (pyroxenite)
	Lower Zone	Upper pyroxenite subzone Harzburgite subzone Lower pyroxenite subzone
	Marginal Zone	Norite
ROOIBERG GROUP	Schrikloof Formation (flow-banded rhyolite) Kwaggasnek Formation (massive rhyolite) Damwal Formation (dacite, rhyolite) Dullstroom Formation (basaltic andesite)	

1.1.1THE MARGINAL ZONE

Medium to fine grained rocks, mainly norites, make up the Marginal Zone. This zone usually contains little or no pyroxenite but can consist of variable amounts of quartz and biotite, possibly reflecting assimilation of shale (Johnson et al., 2006). This sequence may reach 800m in thickness and is suggested to have resulted from multiple intrusions of magmas, making it inappropriate to be considered parental to the entire Rusternburg layered Suit of the Bushveld complex (Eales and Cawthorn, 1996).

1.1.2 THE LOWER ZONE

The Lower Zone consists of a sequence of pyroxenites, harzburgites and dunites. The lower zone in the eastern part of the Bushveld Complex is described by Cameron (1978) while its equivalent in the western limb is described by Teigler and Eales (1996). The thickness of the Lower Zone is influenced by structure of the floor topography and has an average of 1300m (Johnson et al., 2006). These rocks have been described by Hall (1932) as belonging to the Early Plutonic Phase. Cameron (1977) observes that the base of the Lower Zone, which he termed the Basal Subzone, is composed mainly of norites. Above this layer is the first appearance of cumulus bronzite(about 98.6%), which is called the Lower Bronzitite Subzone. This is overlaid by the appearance of olivine in the Harzburgite Subzone. This zone is very similar to the underlying Harzburgite Subzone due to the presence of cumulus bronzite. The final subzone is the Upper Bronzitite which shows lamination, and terminates at the appearance of feldspar-bearing bronzitite at the lower part of the Critical Zone.

1.1.3 THE CRITICAL ZONE

The lower part of the Critical Zone is composed of dunites, harzburgites and pyroxenites and hosts several chromitite layers. The upper part, however, is composed of pyroxenites, norites and anorthosites, but also bears chromitite layers. Based on this difference in composition, the Critical Zone has been further subdivided into the Upper and Lower Critical Zones. The Upper Critical Zone commences where there cumulus plagioclase first appears in the mafic stratigraphy (Boorman et al., 2003).

The layers of chromitite in the Critical Zone occur at different stratigraphic levels known as groups. These include the lower (LG), middle (MG) and upper (UG) group chromitite layers (Hatton and Von Gruenewaldt, 1987). Seven Lower Group chromitite layers (LGI-7) have been identified with the 6th layer (LG6) being more prominent and consistent. The Lower Critical Zone described by Wilson and Anhaeusser (1998) is separated from the overlying Upper Critical Zone at the boundary between the

MG2 and MG3 where there is the first appearance of cumulus plagioclase (Cameron 1980, 1982; Cawthorn and Walraven, 1998). Occurring near the top of the Critical zone are the UGI and UG2 layers where thick layers of chromitite are found which bear platinum group elements (PGE) in economic quantities. There are two cyclic units transitional to the Main Zone overlying the Critical Zone. These are the Merensky and Bastard Cyclic Units which have thick pyroxenite and anorthosite layers, and thin chromitite norite layers (Wilson and Anhaeusser 1998). The Merensky Cyclic Unit is host to the highly PGE enriched Merensky Reef, which is composed mainly of feldspathic pyroxenite and sulphide blebs. Immediately above this reef is the Merensky Pyroxenite Unit lying just below a layer of mottled anorthosite. The Bastard Cyclic Unit, although similar to the Merensky Cyclic Unit, has no economic mineralization and overlaid by unmottled anorthosite.

1.1.4 THE MAIN ZONE

The Main Zone is geochemically different from the underlying Critical Zone and is composed of gabbro, which consists of anorthosites and norites, grading up to gabbronorites,before reaching a distinctive pyroxenite layer called the Pyroxenite Marker about 500m below the footwall of the overlying upper zone. It suggested that the Main Zone formed from a different magma to the underlying Critical Zone (Eales et al., 1986). The Main Zone is subdivided into the upper subzone and the lower subzone (Johnson et al., 2006). The first appearance of cumulus clinopyroxene is found at the lower part of the Main Zone having a coarse-grained texture, at 200-400m above the Merensky Pyroxenite. Wilson and Anhaeusser (1998) described the occurrence of Pyramid Hills located in the South Western lobe to have formed as a result of the middle to upper zone part of the Main Zone being resistant to erosion. Sharpe (1985) in his study suggests a discontinuous relationship in the Sr/Al and Pt/(Pt+Pd) ratios. Also observed was the difference in Strontium (Sr) isotope in the Main Zone (Sharpe, 1985; Cawthorn et al., 1991) as compared to the overlying and underlying zones.

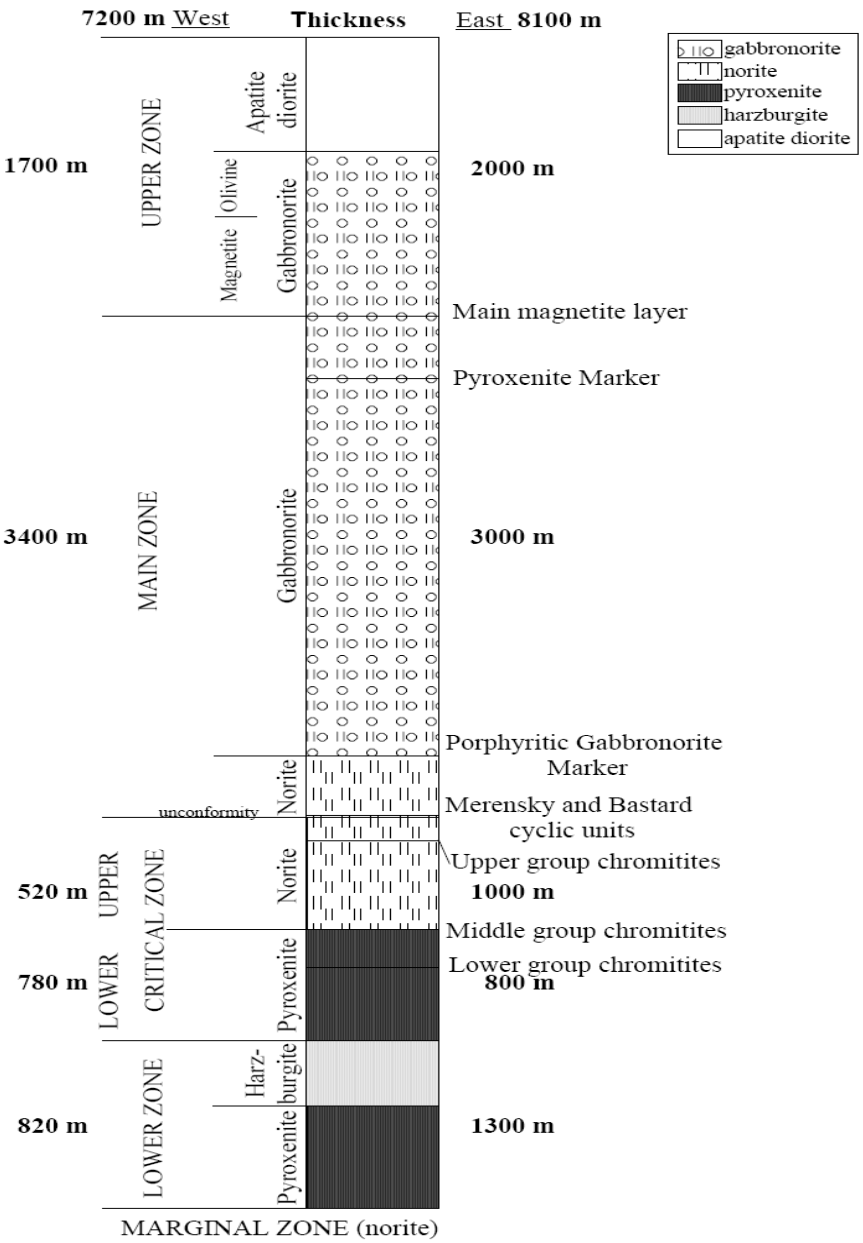

Figure 2: Stratigraphic Column of the Bushveld Complex zones and their respective thickness based on Eales and Cawthorn, 1996.

1.1.5 THE UPPER ZONE

The base of the Upper Zone is marked by the first appearance of cumulus magnetite. These magnetite layers are vanadiferous making it of economic value (Wilson and Anhaeusser, 1998). A total of 30 magnetite layers have been identified in the Upper Zone (Tegner et al., 2006). The Upper Zone is subdivided into four subzones (von Gruenewaldt, 1973, Molyneux, 1974), the first being a Basal Subzone A where there is, as mentioned earlier, the appearance of cumulus magnetite. This layer is then overlain by an olivine-free lithology termed Subzone B. Cumulus olivine reappears again in the Subzone C foolowed by the occurrence of apatite which forms subzone, D. These four lilthologies together are approximately 2000m thick (Johnson, Anhaeusser and Thomas 2006), and are comprised mainly of gabbro, gabbronorite, norite, anorthosite and ferrodiorite.

However, Wager and Brown (1968) and more recently Tegner et al, (2006) observed no cumulus mineralogical change in the cumulus and main magnetite layers, and suggested three subzones for the Upper Zone rather than four. These are the lowest appearance of the main magnetite layer forming subzone A, and the appearance of olivine and apatite as subzones B and C respectively. Sharp (1995) used strontium (Sr) isotopes to explain the preserved density stratification. He was able to use this isotope to explain the crystallization of the “U” (orthopyroxene) and “A” (anorthosites) liquids that evolved the Bushveld Complex.

1.1.6 AIM OF THIS STUDY

Various models have been suggested for chromitite crystallization in their respective mafic to ultramafic host rocks. Some of these models include change in total pressure, contamination of basic parental magma by silicic magma, changes in oxygen fugacities, the influx of new magma bearing chromite crystals, and the influx of new magma mixing with the fractionated resident magma in the chamber. The Bushveld chromitites have also been described by various researchers as originating from a combination of the above mentioned processes. This is especially important seeing as the Bushveld did not form from a single magma but from multiple injections of magma (Cawthorn and Walraven, 1998, Kruger, 2005).

This project will investigate the Middle Group Chromitites (MG4 to be precise), and aims to determine the origin of the chromitite, deciding whether it formed from a single magma or from multiple injections of different magma. This study involves proper investigation of the petrographic

character (majorly orthopyroxene, clinopyroxene and plagioclase) of the rocks, noting their relative abundances at various stratigraphic heights. Samples will thereafter be sent for electronmicroprobe analysis for major elements. The major element geochemistry will then be compared with the petrographic character.

CHAPTER 2

2.1 REVIEW OF CHROMITITE FORMATION MODELS

Chromitite origin has been studied by many igneous petrologists around the world and the study of the Bushveld Complex chromitite is no exception. Cameron and Emerson (1959) studied the chromitite seams in the eastern part of the Bushveld Complex, namely the Steelpoort Main seam and the Leader seam. Cameron and Emerson (1959) attributed the formation of chromitite-seams to not only a chromium-rich immiscible liquid, but rather a combination of several processes. These authors described magmatic differentiation as the main process of chromitite seam formation. Other factors described by Cameron and Emerson (1959) involved in the formation of chromitite are magma currents, crystallization of interstial liquid, magmatic sedimentation and diffusion. Chromitite seams were considered to be of magmatic origin replacing layers of sediments (pyroxenites and norites) as a result of fractional crystallization as well as the gravitational accumulation of chromitite crystals. Chromitite seams are observed in the pseudostratiformed layer of the Critical Zone of the Bushveld Complex (magmatic differentiation) within layers of norites or pyroxenites or both. Some of these seams were observed to be discontinuous, especially in anorthosites, which may result from magma current change. There is also some deformation which could possibly be due to the gravitational settling of the rocks. It should however be noted that the authors did not attribute the formation of chromitite seams to the multiple injection of magma of different composition, but believed their formation to have effected through the differentiation of a chromitite-rich liquid. However, this process of origin of chromitite layers only applies to the continuous and extensive Steelpoort and Leader seams and not to chromitite-rich seams alternating with non-chromitite or chromitite poor seams.

McDonald (1965) studied the formation of chromitite seam in the Bushveld Complex, and suggests that the presence of an immiscible chromitite liquid formed chromitites. Chromitites formed from immiscible liquid are suggested to be of two types based on analysis and observations. These are the inclusion-free chromitites and inclusion-bearing chromitites. These differences are consideres to have originated as chromitite-rich liquid (immiscible liquid) separates out from silicate magma. The chromitite-rich liquid separated out close to the floor of the magma chamber, began nucleating and simultaneously crystallizing. It was also noted that the silicate phase at this time is also crystallizing but not at same rate as the immiscible chromitite-rich liquid. This enhanced the separation of chromitite from the silicate liquid. The chromitite begins to nucleate on the magma chamber floor, but it is however noteworthy that the formation of the chromitite-bearing inclusions is as a result of

some degree of crystallization of the chromite-immiscible liquid before reaching the floor of the chamber. In contrast, chromitite-immiscible liquid while separating out of the silicate melt may contain some silicate-rich liquid. This liquid becomes an inclusion in the chromitite liquid if the chromitite-rich liquid begins to crystallize early as it moves down to the base of the magma chamber and on the final crystallization of the chromitite, the silicate-rich liquid trapped in the chromitite forms an inclusion.

Irvine and Smith (1969) described a crystallization and accumulation model for the formation of chromitite, which was used to explain the origin of the chromitite seam in the Muskox Intrusion of Canada. In this model, chromitite is formed between an underlying layer of olivine and an overlying orthopyroxenite. It was suggested that olivine and chromitite crystallize out first, but with a higher amout of olivine which will, as a result of greater density and gravity, settle below the chromitite crystals as finer particles which sink into the crystallizing pile slowly. Orthopyroxene forms at a slightly later stage above the chromitite grains. The orthopyroxenite compresses the chromitite crystals thereby forming a chromitite-rich seam as the orthopyroxenite appears as the process reaches its liquidus. Finally, a layer of orthopyroxene and clinopyroxene completes the crystallizing pile. This model however has failed to explain why the orthopyroxene which crystallized after the chromitite-rich layer does not mix to form a chromitite and orthopyroxene layer, especially considering the fact that orthopyroxene and chromitite have a good partition coefficient (Irvine and Smith, 1969).

Cameron and Desborough (1969) further criticized the theory that the process of magma differentiation is responsible for the origin of the chromitite and magnesium-rich, pyroxene layers. These authors put forward the idea that oxygen fugacity is responsible for the alternation of chromitite-rich layers with chromitite-poor, pyroxenites layers. They explained that chromium rich intervals originated from an increase in oxygen. An increase in oxygen fugacity increases the crystallization temperatures of both plagioclase and pyroxene. This results in the crystallization of chromitite occuring across different lithologies. Cameron and Desborough (1969) also explained that at short intervals, an increase in the oxygen fugacity resulted in a chromitite-rich phase which crystallized out alone yielding the chromitite layer.

Sharpe and Irvine (1983) described the origin of the chromitite layers of the Bushveld Complex to have resulted from two types of magmas, the “U” (ultramafic) and “A” (anorthosite) magmas in the Critical Zone, suggested to have mixed at the quartz-fayalite-magnetite buffer. The Lower Critical Zone was identified as crystallized from the U_{1b} magma which consists of olivine with minor

chromite, orthopyroxene and plagioclase. These three constituents produced the dunite, harzburgite and pyroxenite of the Lower Critical zone. Conversely, the Upper Critical Zone was considered to have crystallized from the A_1 magma. This is the plagioclase+chromitite, olivine, calcium-rich pyroxene and calcium-poor pyroxene magma that yielded the anorthosite, norite and pyroxenite of the Upper Critical Zone. Therefore, theformation of the Lower Critical Zone from the U_{1b} as opposed to the Upper Critical Zone which crystallized from the A_1 magma suggests two different magma types for the Critical Zone as a whole.

Pressure change has also been suggested to enhance the formation of chromitite seams. Lipin (1992) in his study of the Stillwater Complex determined that the change in pressure within the magma chamber favors the formation of chromitite layers (about 90% chromitite). Lipin (1992) explained that the addition of a more evolved magma into a chamber containing a primitive one will yield carbon dioxide (CO_2). This CO_2 when released in a cyclic unit of olivine + chromitite, olivine + chromitite + orthopyroxene and orthopyroxene + chromitite, rises through the different cumulate layers. At the point of CO_2 formation, olivine and chromitite begins to crystallize. As CO_2 rises through the overlying, new magma, its bubbles begin to increase and thus the pressure builds up in the chamber. This increase in pressure described by Lipin will favor the crystallization of the chromitite-rich phase at the expense of olivine, after which a decrease in pressure will crystallize olivine and chromitite. Furthermore, Lipin (1992) stated that carbon monoxide (CO) may also be evolved in the magma chamber as the new magma mixes with the resident magma in the chamber floor. The evolution of CO is considered to be a result of oxidation. This process is said to increase the oxygen fugacity which also favors chromitite crystallization from the crystal pile containing olivine, orthopyroxene or both in the chamber. However, very little was mentioned regarding the variation in the composition of the magmas involved in mixing, that is, the resident magma in the chamber and the new magma.

More recently, Spandler et al., (2005) described the formation of chromitite layers as a result of the injection of a primitive magma at the roof of the chamber followed by assimilation of the surrounding country rocks. This model was proposed after studying chromitite inclusions from experiments conducted that were similar to those of the Stillwater Complex, Montana. Spandler et al. (2005) observed that these inclusions observed chromitite grains are of three types. Type one, the inclusion contains quenched glass; type two, the inclusion contains one or more vapor bubbles within a spinifex texture; and type three contains one but large vapor bubble. The first and the second inclusions were observed to be similar with both types having low SiO_2, low CaO and high Na_2O. The third type of inclusion in contrast composed of low Na_2O and high CaO. It was proposed

that the first and second types of inclusions were formed from mixing of melted country rock with the primitive parent magma while the third type formed from fluid trapped within and during the growth of the chromitite crystal. After observing the three types of inclusions, Spandler et al. (2005) proposed that batches of high temperature and high Mg basaltic magma ascended to the roof of the magma chamber, and melted some of the rocks at the roof to produce trondhjemitic fluid rich in Na. This Na-rich fluid then mixed with the parent magma at the roof of the magma chamber to yield an over-saturated chromitite fluid that goes down to the magma chamber floor and commences crystallization.

Mondal and Mathez (2006) studied the silicate layers above and below the UG2 chromitite of the Bushveld Complex. They observed from its petrographic character that there are differences between the overlying and underlying pyroxenites of the UG2. One of the major differences observed include the abundance of phlogopite, k-feldpar and quartz in the UG2 footwall pyroxenite, three minerals which are generally absent in the rocks above the UG2. Another observation reveals that the plagioclase in the footwall pyroxenite is more sodic and potassic than the hanging wall pyroxenite. Mondal and Mathez (2005) also made clear that the amount of chromitite from the northwestern part of the Bushveld Complex where their research was conducted, contains an estimate of 1.40 wt% chromium (Cr_2O_3). This resulted in the conclusion that there is far too much chromium in the Bushveld Complex than has been accounted for as observed presently in preserved rocks. This led Mondal and Mathez (2005) to propose that the UG2 chromitite layer of the Bushveld Complex formed from the injection of a new batch of magma similar in composition to the resident magma in the chamber, but with suspension of chromitite and orthopyroxene crystals. As this new magma mixed with the resident magma in the chamber, chromitite crystals from the new magma separated from orthopyroxene sinking to the floor of the magma chamber and forming a dense, homogenous and relatively impermeable layer.

O'Driscoll et al. (2008) proposed that the unit 7-8 boundary of the Cr-spinel seam crystallized from the infiltration of a hot picritic fluid that partially melted and assimilated an olivine and plagioclase rich crystal mush. One important element, of the many observations, was the composition of the plagioclase crystals. It was observed that the plagioclase in the layer above the Unit7-8 boundary, anorthosite, is composed of a uniform core and a normally zoned rim. In the underlying troctolite however, plagioclase was observed to have a sodic core, mantled by a calcic zone, before eventually being rimmed by a thin sodic zone. Consequently, O'Driscoll et al. (2008) proposed that the infiltrating picrite became contaminated by assimilating olivine and plagioclase shifting the melt to an olivine-spinel cotectic while it mixes with the already crystallizing interstitial liquid in the

troctolite zone. He further proposed that the resuting late-stage liquid was saturated with clinopyroxene serving as a source for the abundance of Cr in the anorthosite and especially the spinel seam.

From a slightly different perspective, Voordouw et al., (2009) proposed that the chromitite seams of the Upper Group Chromitite (UG 1&2) crystallized from the intrusion of chromitite crystal slurries. Chromitite grains were suggested to have accumulated within a structural trap containing a melt composed of a mixture of chromium and silicate-rich fluid. This mixture was then transported through a conduit, which contained chromitite grains that have a volume of 53-62%, 38-47% noritic melt, trace amounts of immiscible sulphide liquid and hydrothermalfluids. Voordouw et al., (2009) further explains that the sulphide liquid and hydrothermal fluid aided the transport of materials through the conduit, and also that the small sizes and subrounded nature of the chromitite grains reduced the viscousity of the materials transported to the site of emplacement and subsequent crystallization.

In 2009, Filho and Araujo proposed that the formation of the main chromitite seam in the Bacuri mafic to ultramafic complex in Brazil to be underlain by rocks composed of pyroxene and plagioclase and overlain by rocks containing olivine and chromitite. It was proposed that a mixture of new primitive magma injected into the chamber with the fractionated resident magma in the chamber resulted in the cumulate pile of the Bacuri Complex. Filho and Araujo (2009) also studied the cumulate rocks of the Niqeulandia Complex in Brazil. In their study of the interlayered sequence of olivine and chromite, as well as olivine and chromite with some interstitial orthopyroxene and the main chromitite seam, Filho and Araujo (2009) observed that olivine in the rocks above the main chromitite seam is more magnesium-rich than the rocks below it, which they found consistent with the proposed parental primitive magma of the complex. As a result of this investigation, it was proposed that the magma chamber contained a resident, more fractionated magma, mixed with the influx of a new primitive magma.

CHAPTER 3

3.1 METHODOLOGY

Samples studied in this project were obtained from one of the many borehole cores drilled by the Dwars River Chrome Mine in Lydenburg. Core 109 was drilled by the Dwars River Chome mine through the entire set of the Middle Group chromitite layers, and is used for this project. Samples used for this analysis consist of pyroxenites and anorthosites under- and overlying the chromitite layers. The chromitite layers were not sampled but the rocks lying above and below them were sampled. Sample spacing is on average 2-3cm above and below the chromitite layer and between each sampled point within the silicate layers. A total of 33 samples were sent to the Council for Geoscience, South Africa, for the preparation of polished thin sections. Petrography of the different rock types was described using an optical microscope, grains were observed and modal abundance obtained. After optical observation using the microscope, the thin sections were sent for Electron Microprobe Analysis at the University of Pretoria.

The microprobe analysis was performed in the Department of Geology, University of Pretoria to determine major elements concentrations. These major elements include SiO_2, CaO, Na_2O, K_2O, FeO, Al_2O_3, Cr_2O_3, MgO, and TiO_2. In addition BaO was analysed although it is usually present only in trace amounts. Some results are not represented in the data as observed in the table. This is due to either the negligible amount of the element analyzed, small grain size used for the analyses or poor preparation of the thin section used in the analyses.

For major element analysis using the microprobe, the following quantitative procedure was followed. The quantitative electron microprobe analyses were performed using a CAMECA SX 100. The acceleration voltage was 20 kV and the beam current was 20 nA. Counting times were 20 seconds on peak position and 10 seconds on each background. The following X-ray lines, spectrometer crystals and standards (in brackets) were used: SiKα, TAP (KP Garnet); CaKα, PET (KP Garnet); AlKα, TAP (KP Garnet); MgKα, TAP (Diopside); FeKα, LLIF (KP Garnet); MnKα, LLIF (Rhodonite); TiKα, PET (Rutile); KKα, PET (KP Hornblende); NaKα, LTAP (KP Hornblende); CrKα, PET (Chromite); NiKα, LLIF (Olivine).

Trace elements were also prepared and analyzed by X-ray Flourescence (XRF) at the Geology Department, University of Pretoria. Pressed powder samples were prepared and analyzed using the Thermo-Scientific ARL 9400 and sequential XRF.

3.1 BOREHOLE STRATIGRAPHY

The borehole used for this study is composed mainly of norite, some pyroxenites and anorthosite. The core bears the MG4 chromitite package, which consists of five layers having varying thicknesses between 0.05m and 1.05m (fig3). The lowermost layer in the sequence is a chromitite layer about 0.16m thick. This layer is overlain by a thick succession of medium to coarse grain leucocratic rocks composed of anorthosite having a thickness of about 0.92m. Another chromitite layer of the MG4 overlies the anorthosite. This layer of chromitite is observed to be the thickest in this stratigraphic sequence having a thickness of about 1.05m. There is a sharp contact between this chromitite layer and the overlying thin layer of gabbro. This layer of gabbro is medium grained and is separated from the coarse gabbro just above it by a thin chromitite layer. The coarse gabbro is about 1.28m thick constituting larger grain sizes resulting in the coarse nature of the layer. Just immediately above the layer of coarse gabbro is another layer of chromitite with a hanging wall of medium to fine grain gabbro rocks. This is finally overlain by a chromitite layer which completes the stratigraphic sequence.

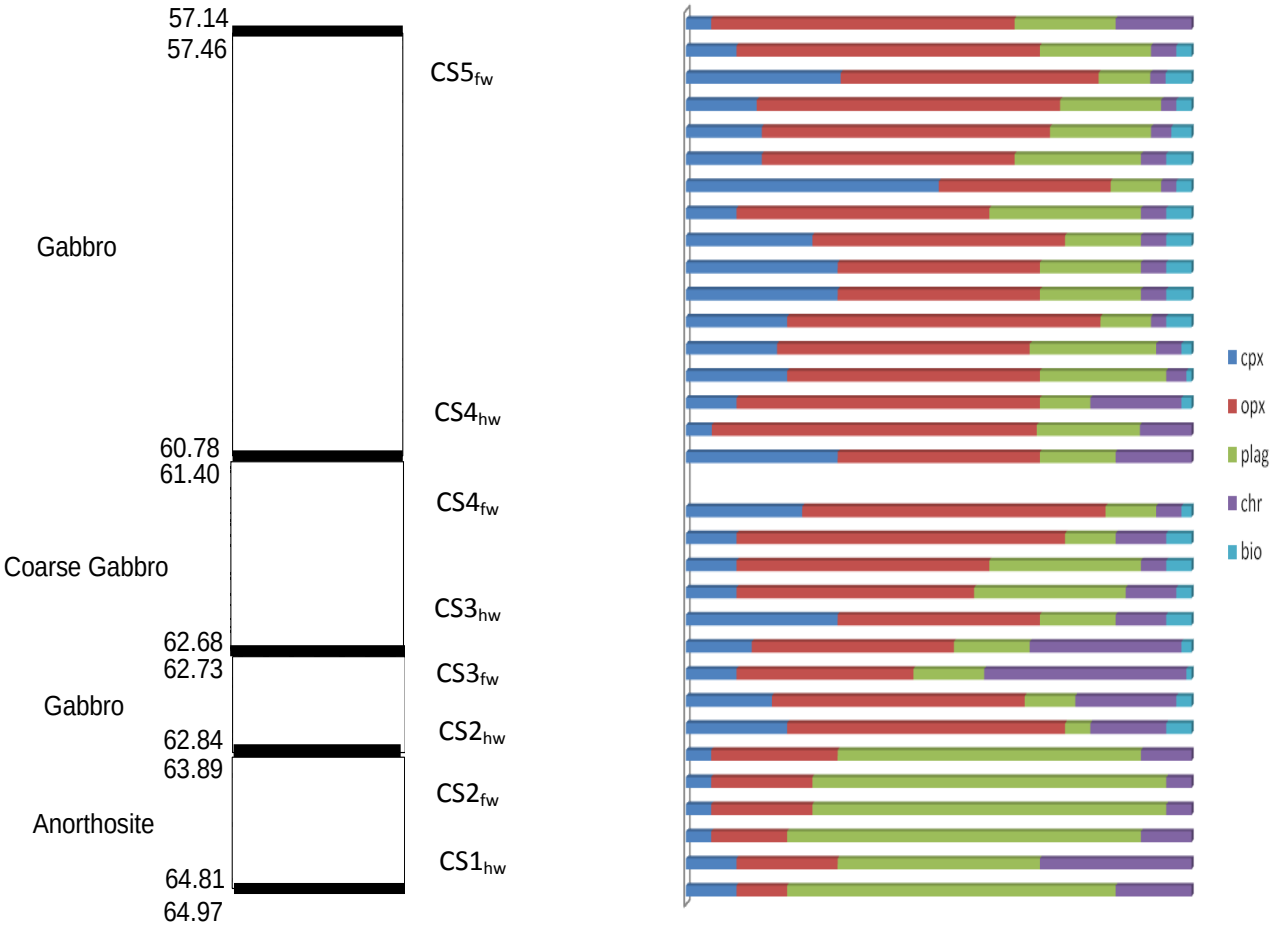

Figure 3: Stratigraphic unit of the MG4 and the modal abundance of each thin section at the corresponding depth (m) as observed from the drill core. The blank space/column is a poorly prepared thin section.

3.2 PETROGRAPHIC CHARACTER OF THE MG4 PYROXENITE

The MG4 pyroxenite is a plagioclase rich pyroxenite. This plagioclase pyroxenite is composed of orthopyroxene, clinopyroxene and plagioclase as the major phases with some minor amount of biotite occurring interstitially. The MG4 pyroxenite as observed in the thin sections is composed mainly of orthopyroxene rather than clinopyroxene throughout the entire sequence. Also noteworthy is the major occurrence of clinopyroxene crystals interstitially which in some sections are about 10µm. The plagioclase, on the other hand exhibit complex intergrowth especially in the footwall where they are modally more abundant. Visible on these plagioclase grains is the albite twinning, which lower down the sequence have the calsberg twining evident of calcium enrichment. This calcium enrichment can also be observed in the microprobe analysis with the CaO increasing from about 10.27 at the top of the sequence to 15.76 at depth. Although there are similarities between the footwall and hanging wall rocks of the MG4, the differences should not be ignored.

The first chromitite seam at 64.81m depth has a hanging wall ($CS1_{hw}$) composed mainly of a calcium-rich plagioclase (60%) with clinopyroxene and orthopyroxene occurring in similar amounts. Above the $CS1_{fw}$ is the footwall rock the second chromitite seam at 62.84m to 63.89m. At this depth, the orthopyroxene content is observed to increase slightly with a reduction in the amount of clinopyroxene and chromitite. This rock is however still plagioclase-rich. The hanging wall of this chromitite seam ($CS1_{hw}$) is, in contrast to the footwall, orthopyroxene-rich. In this hanging wall there is an increase in clinopyroxene, the appearance of biotite and a great reduction in the amount of plagioclase.

The footwall rocks of the third chromitite seam ($CS3_{fw}$) at 62.68m to 62.73m, is also observed to be orthopyroxene-rich, but with an increase in the amount of chromitite. From this stratigraphic position upward in the sequence, the rock composition remains similar above and below the chromitite layers. That is, the hanging wall of the chromitite ($CS3_{hw}$) layer at 62.68m to 62.73m, the footwall ($CS4_{fw}$) and hanging wall ($CS4_{hw}$) of the chromitite seam at 60.78m to 61.40m and the footwall ($CS5_{fw}$) of the chromitite seam at 57.46m are orthopyroxene-rich with clinopyroxene increasing with the decrease in depth. The amount of chromitite remains fairly constant while plagioclase concentration reduces and is observed to be more sodic.

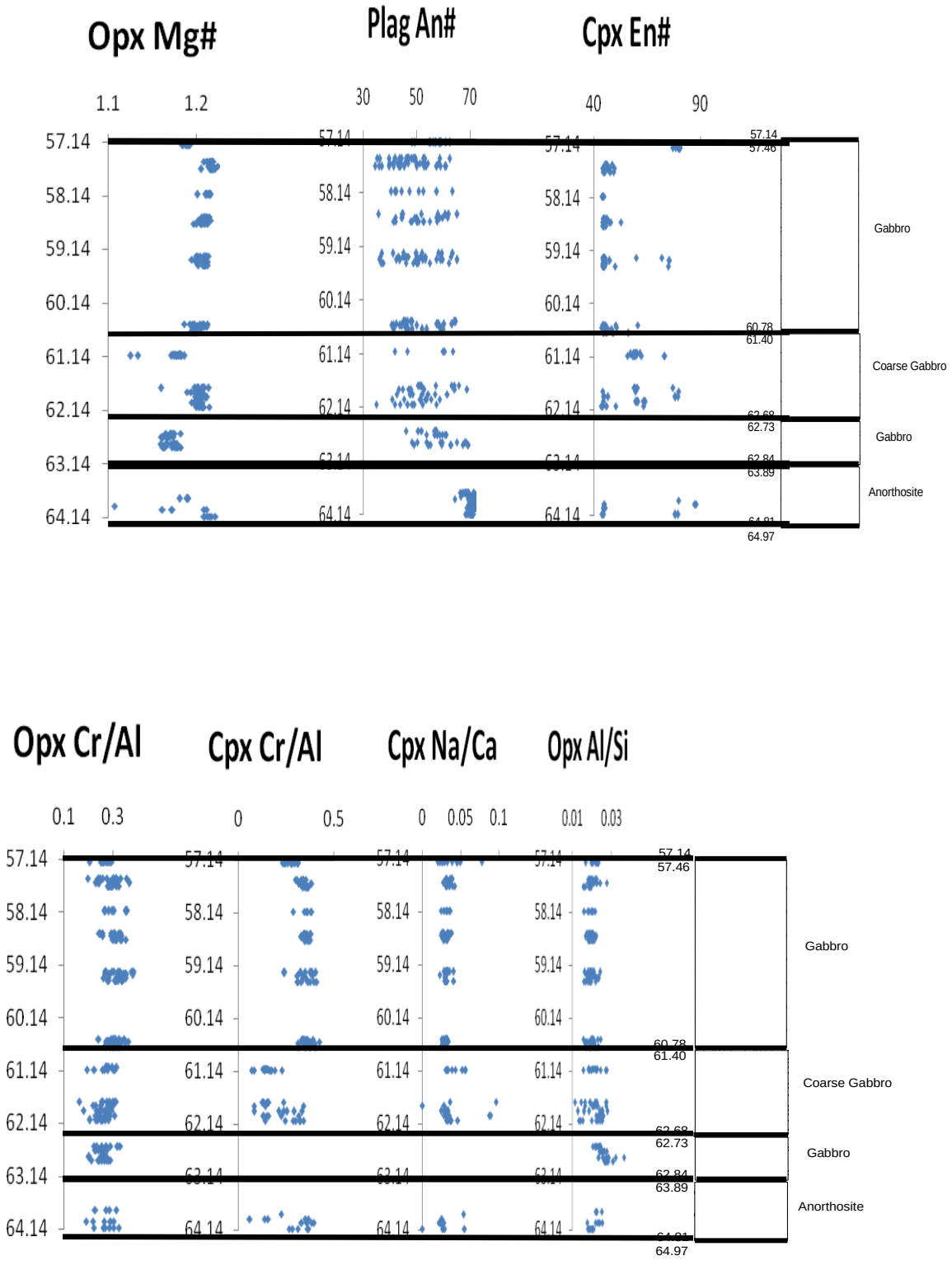

Figure 4: Mineral composition profiles through the MG4 sequence. Thick dark horizontal lines drawn across the graphs represent the chromitite layers.

3.3 PETROGRAPHIC DESCRIPTION

As mentioned earlier, the rocks studied are mainly pyroxenites with some anorthosite and accessory biotite. The rocks are medium to coarse grained and at the studied interval in the stratigraphic sequence, thin sections were prepared and observed under the optical microscope. In total, 33 thin sections were prepared. Noteworthy in some of the thin sections is the occurrence of large interstitial clinopyroxene crystals. The petrographic character of each thin section is described below.

Section 01 (57.20m):

As described earlier, this section consists mainly of orthopyroxene, clinopyroxene, plagioclase and some biotite. The plagioclase crystals are anhedral occurring interstitially between orthopyroxene and clinopyroxene crystals. Also found similar to the plagioclase is interstitial biotite but far fewer grains. Chromite grains occur as stains on other grains in the section, especially on orthopyroxene and clinopyroxene crystals. These chromite grains occur as clusters, with very few scatteredgrains, in the section.

Section 02 (57.51m):

Most of the chromitite in the section also occurs interstitial to the pyroxene crystals and are euhedral. In a particular orthopyroxene crystal there are two chromitite inclusions, suggesting a different generation of crystals to the other pyroxene crystals. The plagioclase grains are anhedral, occupying spaces between the pyroxene crystals. Some pyroxene crystals have grown around the edges of chromitite crystals. The chromitite crystals are euhedral and quite large in size. This may indicate a more favorable condition of solidification or crystallization and hence, crystal growth. The chromite probably formed first and its growth was not inhibited by the presence of other grains. These chromite crystals are not nucleated, but occur all around the section.

Section 03 (57.59m):

Many orthopyroxene crystals in the section are euhedral with the exception of some occurring interstitially. About 2-3 orthopyroxene grains are twinned. The few plagioclase grains are isotropic and anhedral. This texture as observed in the section suggests that themore abundant and surroundindg pyroxene crystals inhibited the growth of the plagioclase grains The section is sparsely populated by the chromitite crystals. The chromitite grains are small in size with only a few found as inclusions in some interstitial clinopyroxene and are absent in others.

Section 04 (57.65m):

As observed in the previous thin sections, the dominant grain is orthopyroxene with few twinned crystals and some chromite inclusions. In comparison, clinopyroxene has no inclusions occurring interstitially. The plagioclase grains are anhedral and found interstitial to the orthopyroxene crystals only. The absence of plagioclase interstitial to clinopyroxene may indicate a different time of growth of clinopyroxenecompared to plagioclase and orthopyroxene.

Section 05 (58.12m):

Orthopyroxene crystals in the section are equigranular with some alterations visible on some grains. The interstitial clinopyroxenes are again devoid of chromitite inclusions. The plagioclase grains are slightly deformed as the twin lamellae are very visible in the section. This texture may indicate a late stage of formation of the plagioclase grains. The chromitite grains as seen in section 003 are very few and found all around the section with no preferred orientation or nucleation.

Section 06 (58.54m):

There are some sub-rounded orthopyroxene grains surrounded by elongate ones. The orthopyroxene crystals found in interstitial clinopyroxene are equigranular, Subhedral and subrounded. As observed in section 005, there is a visible and clear albite twinning on the plagioclase crystals. Chromite grains are observed between orthopyroxene with about 8grains occurring as inclusions. There is an inclusion of chromitite in biotite. The chromite have well developed euhedral crystal phases (majorly tetragonal in appearance). The chromite inclusions in orthopyroxene and plagioclase are subhedral, but the inclusions are larger in plagioclase, and more abundant in orthopyroxene. Also visible are the observed large interstitial biotite grains between the orthopyroxene crystals in the section.

Section 07 (58.60m):

Orthopyroxene in this section is subhedral to anhedral. There are some orthoyroxenes found as inclusions in plagioclase. Plagioclase can be found along the rims of some of the orthopyroxene grains. Clinopyroxene are interstitial and very few. Chromite is anhedral and its growth appears to have been disturbed by orthopyroxene grains.

Section 08 (57.67m):

Some orthopyroxene grains, as seen in the section, are observed to be poikilitic as exhibited by the growth around other orthopyroxene crystals. Most of the large orthopyroxene crystals are elongated

with high birefringence. Plagioclase is not as light colored as observed in previous slides, but dark in cross-polarized light (xpl). This may be as a result of the alterations or other processes the grains were subjected to after formation. Thus the plagioclase grains in this section are not as fresh or well preserved as described in earlier sections. Chromite can be seen as inclusions, or between pyroxenes (especially orthopyroxene crystals), and absent in plagioclase. Where it is occasionally found in contact with plagioclase, chromite is found between plagioclase and pyroxene.

Section 09 (59.27m):

Again orthopyroxene dominates the section. They are euhedral to subhedral, equigranular with the exception of some elongated grains. Clinopyroxenes are interstitial and quite large in size. Plagioclase crystals in the section have well developed and exposed lamellae. About half of the total constituting plagioclase grains exhibit the tappard structure. This texture in plagioclase is evidence of deformation. Chromite occurs as inclusions in pyroxene grains (especially orthopyroxene), and between the pyroxene grains. The chromites that occur as inclusions are observed to be smaller in size compared to those found between pyroxene crystals. This texture suggests that either the two different chromitite grains mentioned crystallized from different source or the growth of the chromitites found as inclusions was inhibited by the pyroxene crystals in which it formed.

Section 10 (59.33m):

This section is dominated by euhedral orthopyroxene growing around crystals of plagioclase and clinopyroxene, forming a poikilitic texture. Clinopyroxene is not a major face in this section as only one fairly large interstitial grain exists. Chromitite grains are mostly interstitial between orthopyroxene crystals, very few of which are euhedral . There are chromite inclusions in the orthopyroxene and plagioclase, with a few in clinopyroxene. The chromite inclusions in plagioclase when observed have better developed crystal faces than that observed in orthopyroxene.

Section 11 (59.39m):

Orthopyroxene in the section is subhedral to euhedral showing good cleaveges. There are also grains of orthopyroxene in the interstitial pyroxene. These garins of orthopyroxene are usually subrounded. This texture may be as a result of the interstitial pyroxene's rapid growth inhibiting the otherwise slow growth of the orthopyroxene grains. There is also in the section a twinned plagioclase grain bounded by orthopyroxene grains. One of the bounding orthopyroxene grains include two chromitite crystals with a very small plagioclase grain occurring as the matrix. Chromite is observed to form heavily along the crystal edges of the pyroxene crystals.

Section 12 (59.44m):

Orthopyroxene have poor cleavage in many of the grains while in some others, cleavages meet at about 60^0 and 120^0. Quite a number of orthopyroxene have also been inverted to pigeonite. Plagioclase in the section is dark colored. Chromitite grains are found between orthpopyroxene crystals with very few occurring as inclusions.

Section 13 (60.54m):

The crystals in this section are dark colored. This character may be due to the high concentration of basic elements in the section as compared to the other sections described. Chromitite are few but concentrated in two main regions of the slide. Very few chromitite crystals are found as inclusions while many others are found in between the pyroxene crystals. The plagioclase have poorly formed or deformed lamellae. This may also be due to the presence of basic minerals in the section.

Section 14 (60.59m):

Similar to the previous slide, the section constitute more mafic minerals as evident by the general dark color exhibited by the slide. Chromite grains are dispersed in this section and not in clusters with most of them occurring between the pyroxene grains. This dispersion may support the idea that chromite in the section grew at a different time or rate to the growth of the pyroxene crystals. To further support this idea, there is quite a large grain of chromite observed to have grown round an orthopyroxene grain forming an inclusion in the chromite grain.

Section 15 (60.61m):

In this thin section, there are very few, interstitial clinopyroxene grains compared to chromitite and orthopyoxene. This texture may be due to the compatible partition coefficient between chromitite and orthopyroxene. Chromite here is equigranular and euhedral, which may imply that the chromite formed before clinopyroxene. Also noteworthy in the section is the observed amount of chromite in plagioclase which appears to be greater when compared to that in pyroxene.

Section 16 (60.68m):

This section is quite similar to the one described previously. Chromite grains are also numerous and found around the orthopyroxene grains. The orthopyroxene crystals have well developed cleavage and crystal faces.

Section 17 (61.09m):

There is an increase in the amount of plagioclase in this section. There are chromitite crystals occurring around both the pyroxene and plagioclase grains. The chromite crystals around the plagioclase grains are better formed in that the crystal faces are well formed and euhedral. The chromitite crystals around the pyroxene grains on the other hand are anhedral and exist as interstitial grains. Orthopyroxene have few inclusions of chromitite and few clear and distinct cleavages.

Section 18 (61.13m):

Large orthopyroxene crystals are observed surrounding smaller ones already present by forming a poikilitic texture. A unique feature in this slide is the growth of chromitite crystals along the well formed, euhedral edges of a pyroxene crystal. This texture may imply that the orthopyroxene was crystalline while the chromite grains were growing along its edges. This almost crystalline nature of the pyroxene grain can also be supported by the absence of chromite inclusions, and to some extent any cleavages in it.

Section 19 (61.73m):

In this section, orthopyroxene grains are very large and dominant. These large crystsals have poorly formed cleavages and very well formed crystal faces (euhedral). Some of these crystals are also observed to have broken into two parts. This division might be due to some stress or strain which may be as a result of deformation in the system. This deformation that is suggested to have occurred in the system could also be the result of the poor twin lamellae exhibited by plagioclase.

Section 20 (61.80m):

Just as in some of the sections described above, the chromitite grains observed here are better formed in or around the plagioclase than in or around the orthopyroxene. The chromite grains found around plagioclase are euhedral while that around orthopyroxene are mainly anhedral. This may suggest that chromite crystals are better formed around plagioclase than pyroxene despite the compatible partition coefficient of both orthopyroxne and chromite.

Section 21 (61.90m):

Orthopyroxene grains are also large in this section, equant with very few or no chromitite inclusions. Some plagioclase show well formed lamellae, while in others a tappard structure evident of deformation is observed. The orthopyroxene in this section can be divided into two main groups. These are the grains

with low birefringence and those with high birefringence. The reason for this observed texture is uncertain.

Section 22 (61.99m):

Orthopyroxene is equigranular with little chromite inclusions, they have poorly formed cleavages which mostly run across the width of the grain. Plagioclase is anhedral and with clearly formed twin lamellae. There is a particular plagioclase grain observed to grow into one of the orthopyroxenes, breaking up a bit of it and thus forming an inclusion of orthopyroxene in chromitite.

Section 23 (62.08m):

Chromitite is observed to nucleate in two main regions of the section. The chromite crystals are anhedral. Plagioclase grains consist of at least two chromite inclusions. There is an exception with one plagioclase grain having no chromite inclusion. The nucleation of the chromite crystals in the two sections seem to have been caused by the growth of the pyroxene crystals while the chromitite grains were crystallizing.

Section 24 (62.57m):

There are lots of equant chromite grains around the plagioclase and with some occurring as inclusions. These chromitite grains are not as large as those found between the pyroxene crystals. Some of the chromite crystals are observed to merge together which may be due to some changes in the system while crystallizing.

Section 25 (62.65m):

The crystals in this section are large with more abundant chromite crystals. Chromite crystals occur mostly in plagioclase especially as inclusions. The chromite grains are equigranular, and scattered throughout the slide.

Section 26 (62.78m) and Section 27 (62.84m):

Orthopyroxene crystals are large in this section. They have poorly developed cleavages. This may imply a slow time of cooling thereby enhancing the growth of the crystal. These large crystals of orthopyroxene rarely bear chromite inclusions, but visible along the rim of the orthopyroxene grains are numerous chromites. This may be favored by the partition coefficient between the two grains.

Section 28 (63.72m):

This section observed under the microscope displays a different texture to what has been previously described. Here, the grains sizes are smaller with plagioclase appearing as the most abundant. Plagioclase grains have got clear and well exposed twin lamellae. Chromitite in the section are observed to occur more around plagioclase than pyroxene (mainly orthopyroxene) as described in previous sections. There are some plagioclase grains exhibiting the Carlsberg twinning, which is evidence of calcium enrichment. These plagioclase grains as usual are anhedral. It is also observed that where there's pyroxene, there is at least a chromite grain along its rim.

Section 29 (63.79m):

In this section, orthopyroxne is interstitial and fewer in grain number. Also reduced is the amount of chromite in the section. This corresponding reduction in the amount of chromite may be as a result of the reduced orthopyroxene. Chromite grains are also observed to be larger in size than that of orthopyroxene. Plagioclase is the most abundant in the section, more abundant than in previous sections, and is subhedral, with well developed lamellae.

Sections 30 (63.85m), 31 (63.93m), 32 (64.00m) and 33 (64.12m):

These sections are all the same in petrography. Orhtopyroxene is less abundant, anhedral, and interstitial with little or no interstitial clinopyroxene. Biotite is completely absent in the sections. Chromite seldomly occurs as inclusion in the interstitial orthopyroxene or clinopyroxene where found. Some chromites also exist interstitially and anhedral while others are euhedral or subheral. Plagioclase in these sections can be subdivided based on the type of twinning that exists. The two types of twinning observed are the albite and calsberg twinning which represent sodium and calcium enrichment respectively.

As presented in fig. 4 the MG4 is composed of an anorthosite-rich layer having a thickness of about 0.5m. In this layer orthopyroxenes are interstitial with little or no chromite inclusion. Clinopyroxene is not a major occurrence in this region but where found, it is also interstitial. Biotite is also not observed at this level. A chromitite layer separates this layer from the overlying succession. The overlying layer is a pyroxene rich layer with orthopyroxene as the major constituent. The orthopyroxene has large grain sizes with poorly developed cleavage. Clinoproxene is an interstitial constituent with very little

chromitite inclusions compared with those found in orthopyroxene. Plagioclase is also present with chromitite inclusions. Plagioclase is anhedral with well and clearly developed twinning. Some plagioclase grains are dark colored resulting in poor visibility of twinning. Biotite is also observed in this layer occurring interstitially with no inclusions of chromitite. This layer is very rich in chromitite observed to occur as inclusions in other grains, interstitially (anhedral) and or as euhedral grains between pyroxene and plagioclase. There are some thin chromitite layers intruding into this layer. Overlying this layer is a more leucocratic pyroxene dominant layer. Unlike the orthopyroxene of the underlying layer, orthopyroxene is subhedral to euhedral, smaller in size and poikilitic. While some are of low order of birefringence, other orthopyroxene grains are of high order. Orhtopyroxene in this region is pleochroic.

Interstitial clinopyroxene is large with some subrounded orthopyroxene found as inclusions in it. Clinopyroxene in this layer is also pleochroic. Plagioclase is anhedral with chromitite inclusion. Twinning is well developed in plagioclase. Also present is interstitial biotite with no chromitite inclusion.

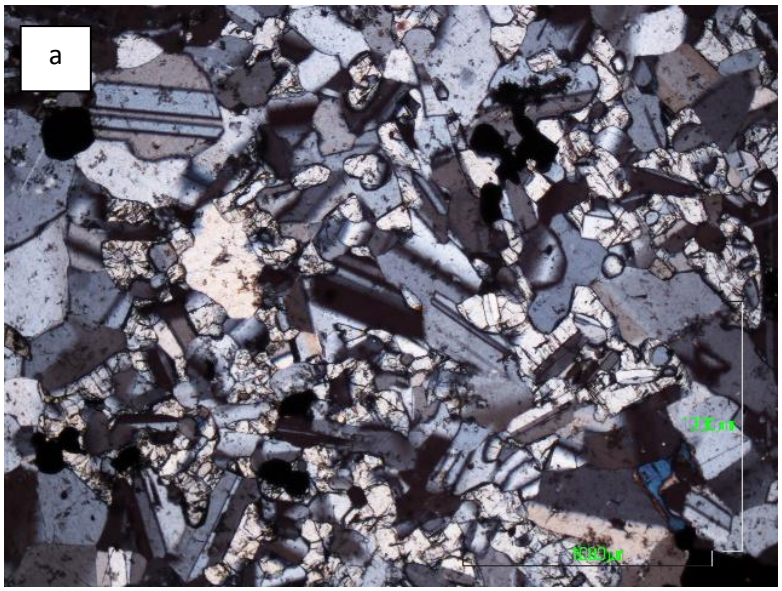
a


b

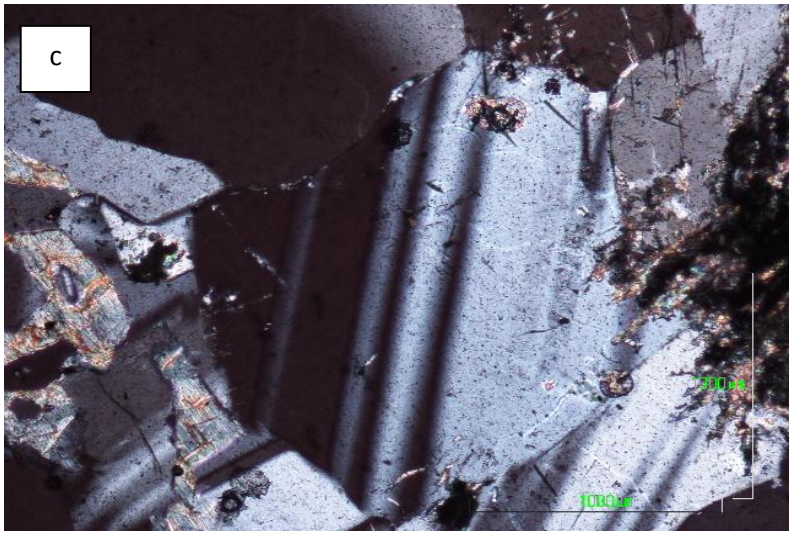
c

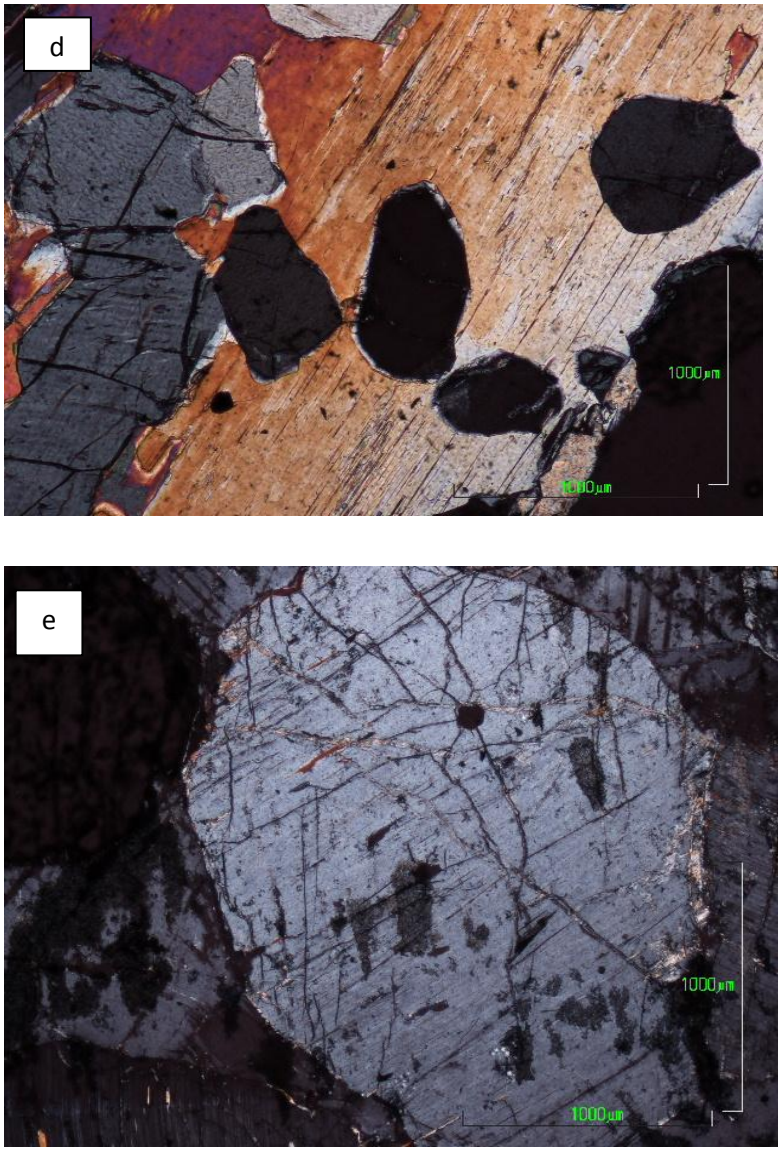

Figure 5: Photomicrographs of the MG4 rocks: (a) Interstitial orthopyroxene in the plagioclase-rich layer at the base of the stratigraphic sequence. (b) Na-rich plagioclase showing albite twinning at the upper part of the orthopyroxene-rich layers. (c) Ca-rich plagioclase observed at the lower part of the stratigraphy exhibiting carlsberg twinning. (d) Growth of interstitial clinopyroxene crystal around subrounded orthopyroxene crystals. (e) Large orthopyroxene crystal.

Table 2: Average weight percent of major elements analyzed

Depth(m)	cpx(Mg#)	opx(Mg#)	Mg#	An#	Na2O	MgO	Al2O3	SiO2	K2O	CaO	TiO2	Cr2O3	MnO	FeO	BaO
57.20	70.84	70.93	70.88	77.25	1.39	19.58	11.02	54.06	0.07	5.14	0.10	0.28	0.18	8.10	0.006
57.51	75.03	67.14	71.09	71.08	2.25	12.62	14.40	53.85	0.14	10.27	0.17	0.30	0.13	5.72	0.015
57.59	74.73	66.64	70.68	72.45	1.68	14.74	10.70	53.72	0.10	11.54	0.20	0.43	0.15	6.56	0.009
57.65	74.76	67.06	70.91	70.84	1.69	14.76	10.65	53.72	0.10	11.62	0.21	0.41	0.14	6.49	0.015
58.12	76.24	67.02	71.63	73.67	1.80	13.66	11.75	53.45	0.11	11.87	0.19	0.37	0.13	5.98	0.010
58.54	75.35	67.30	71.32	75.99	1.51	14.45	10.73	53.28	0.10	12.22	0.20	0.39	0.14	6.25	0.012
58.60	73.02	67.37	70.19	74.96	1.71	13.87	11.96	53.31	0.15	11.37	0.21	0.40	0.13	6.24	0.008
58.67	75.69	67.64	71.67	74.12	2.09	12.40	14.09	53.45	0.20	11.09	0.16	0.30	0.12	5.48	0.011
59.27	74.36	67.52	70.94	74.96	1.55	14.98	10.68	53.67	0.11	11.20	0.20	0.41	0.14	6.47	0.008
59.33	72.21	67.68	69.95	73.93	2.30	12.26	15.19	53.67	0.24	9.68	0.16	0.27	0.12	5.63	0.014
59.39	74.61	67.70	71.16	75.66	2.50	10.58	17.81	53.38	0.15	9.87	0.13	0.21	0.11	4.93	0.015
59.44	73.47	67.54	70.50	73.35	1.79	14.35	11.77	53.73	0.12	10.72	0.20	0.37	0.13	6.34	0.014
60.54	75.03	68.22	71.63	74.98	1.56	14.72	10.74	53.55	0.15	12.01	0.20	0.41	0.14	6.17	0.015
60.59	76.42	68.23	72.32	76.43	1.49	14.62	10.83	53.44	0.10	12.36	0.20	0.42	0.14	6.02	0.009
60.61	75.45	68.53	71.99	72.13	1.67	13.93	10.47	56.07	0.11	10.87	0.19	0.39	0.13	5.84	0.013
60.68	76.38	68.99	72.69	74.99	1.53	15.15	10.61	53.59	0.15	11.55	0.18	0.38	0.13	6.06	0.012
61.09	75.33	71.99	73.66	75.78	1.86	15.74	12.71	52.34	0.21	8.80	0.57	0.61	0.12	5.82	0.015
61.13	70.59	71.56	71.08	79.31	0.11	23.59	6.23	47.94	0.06	4.71	0.07	0.47	0.30	9.81	0.015
61.73	72.92	68.47	70.69	77.41	1.55	15.78	12.13	52.83	0.16	8.70	0.25	0.48	0.13	6.74	0.015
61.80	73.30	68.73	71.02	75.56	1.69	13.91	13.89	51.39	1.08	9.31	0.81	0.52	0.11	5.87	0.039
61.90	70.73	68.16	69.44	74.80	1.41	16.19	10.40	51.04	0.61	8.05	0.47	0.37	0.15	7.30	0.030
61.99	77.27	68.34	72.81	74.71	1.62	15.46	11.42	53.55	0.11	9.48	0.20	0.43	0.12	6.18	0.018
62.08	74.69	67.99	71.34	72.40	1.70	14.86	10.73	53.49	0.07	11.18	0.17	0.42	0.15	6.39	0.010
62.57		72.53	72.53	76.05	2.11	14.63	15.64	53.68	0.07	7.38	0.08	0.23	0.13	5.61	0.024
62.65		73.38	73.38	78.19	1.94	14.65	15.93	53.51	0.08	7.79	0.08	0.23	0.12	5.37	0.020
62.78		72.17	72.17	79.14	1.88	14.23	15.96	53.15	0.09	8.10	0.08	0.26	0.13	5.56	0.012
62.84		71.96	71.96	80.21	2.06	9.62	17.44	52.94	0.12	8.00	0.06	0.18	0.09	3.84	0.010
63.72				84.14	2.91	0.02	31.68	49.25	0.09	15.43	0.03	0.01	0.01	0.16	0.019
63.79		70.48	70.48	84.75	2.09	7.32	24.28	50.74	0.13	11.77	0.06	0.11	0.07	3.16	0.010
63.85	69.04		69.04	84.74	2.38	3.21	28.73	49.45	0.15	14.11	0.04	0.05	0.03	1.56	0.013
63.93	80.43	80.00	80.22	84.82	1.56	11.26	17.31	52.13	0.11	11.05	0.06	0.26	0.04	2.84	0.004
64.00	78.00	70.79	74.40	85.10	1.48	10.09	16.60	51.25	0.08	15.76	0.13	0.33	0.10	3.56	0.013
64.12	70.30	66.79	68.55	84.82	1.35	13.32	15.43	52.05	0.08	10.70	0.11	0.27	0.15	6.11	0.017
Average	74.30	69.32	71.64	76.93	1.76	13.35	14.24	52.75	0.16	10.41	0.19	0.33	0.12	5.58	0.01

Note: Blanks spaces are as a result of grain size too small to be analyzed or poor preparation of thin sections used in the microprobe analysis of major elements.

3.4 Microprobe Results

Fig 6 (i-vi) shows the variation in weight percent versus depth of major elements analysed. MgO at depth decreases from about 13wt% down to zero between 64.12m to 63.72m. After this decline is a rise in the concentration to about 14wt%. This concentration is just about constant (between 14wt% and 16wt %) up till some few meters above the 62m mark. At this depth, a sudden increase in MgO to about 24wt% is observed after which it decreases back to about 15wt%. This sharp increase and subsequent decrease in MgO is observed to occur about 1m (between 62m and 61m) apart. From this depth upward, the concentration is constant, 15wt% and 12wt% for about 3.5m decrease in depth. It is

noteworthy that at a depth of 59.4m however, there is a decrease up to about 10wt%. Towards the top of the MG4 at about 57.5m, there is an increase in MgO from about 13wt% to about 19.5wt%.

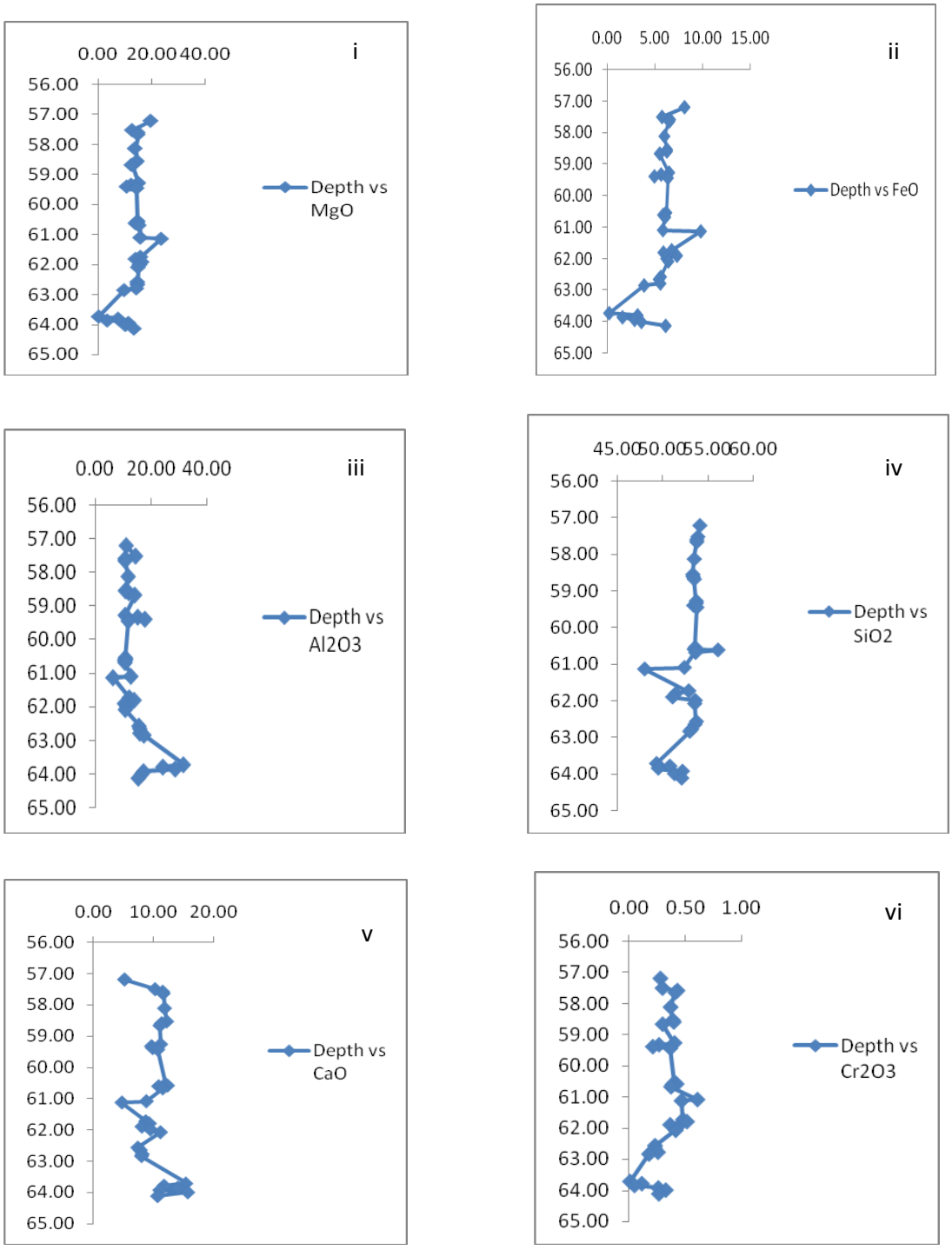

Figure 6: Plots of major elements against depth (m) showing differentiation or crystallization trend of the magma that crystallized the MG4 chromitite package. .

Similar to the trend exhibited by MgO is FeO. FeO (fig 6ii) also decreases at depth from about 6wt% to zero before gradually increasing to about 5.8wt% some few meters above the 63m mark. After this point, a slightly sharp increase is observed to about 6.3wt% after which it remains constant between 6.3wt% and 7wt% for about 0.5m. There are some concentrations as low as 5.9wt%. At this

point, there is a sharp increase in t 0wt% before decreasing almost the same way it increased back to about 5.9wt%. This trend is observed at a depth between about 61.8m and 61.1m. From 61.1m, the FeO ranges between 4.8wt% to 6.4wt% for about 3.5m decrease in depth before increasing to about 8wt% at the top of the sequence. This similar increase and corresponding decrease between MgO and FeO may be as a result of the fact that both are major constituents of mafic rocks and pyroxene. From the depth of 64.12m to 61.09m, Al_2O_3 is observed to decrease from 30wt% to 10wt% before maintain a fairly constant composition of 10wt% above this depth (60.68m to 57.20m).

SiO_2 (fig 6iv) decreases from about 52wt% to 49wt% at depth (64.12m), before increasing to about 53.7wt% at 62.6m. At this point, SiO_2 begins to decrease at the interval where an increase in MgO and FeO was observed. This is the 61.1m mark. From this point, there is increase in SiO2 from about 47.9wt% to 52.3wt% over a very short height between 61.13m and 61.09m after which a sharper increase from 52.3wt% to 53.6wt% is observed. Moreover, further increase in SiO_2 to 56.07wt% is observed with no change in stratigraphic height. SiO_2 decreases back to 53.6wt% at this same interval and remains fairly constant as the height decreases to the top of the sequence at 57.2m. Fig 6iv shows the decrease in CaO from 10wt%-15wt% at 64.12m to 5wt% at 61.09m and thereafter maintaining a fairly constant composition upwards to the 57.20m mark. Cr_2O_3, however, increases up the stratigraphy. Cr_2O_3 increases from 0.3wt% at 64.12m to between 0.4wt% and 0.5wt% at 61.09m and thereafter maintaining this composition upward the sequence.

Table 3: Trace elements analysis. Ele d semi-quantitative.

ppm	GSN cert		T1	T2	T3	T4	T5	T6	T7	T8	T9	T10
	GSN	Depth (m)	57.20	57.51	58.54	58.67	59.39	60.54	60.68	61.09	61.73	61.80
As	1.6	3.00	3.00	3.00	3.00	3.00	3.00	3.00	3.00	3.00	3.00	3.00
Cu	20	71.62	7.44	9.24	14.49	12.00	14.50	14.53	17.07	20.92	11.96	11.51
Ga	22	18.45	5.98	2.98	3.70	3.54	2.63	3.78	4.93	12.89	4.04	4.48
Mo	1.2	1.00	1.53	1.00	1.00	1.00	1.10	1.06	1.72	5.08	1.00	1.00
Nb	21	19.78	4.30	2.80	2.48	2.00	2.47	2.00	2.52	5.52	2.76	2.62
Ni	34	29.61	576.73	505.91	514.06	527.04	517.79	522.77	556.62	680.22	493.84	498.78
Pb	53	46.51	8.30	3.00	9.36	7.76	3.00	3.00	3.00	3.00	3.00	3.00
Rb	185	179.34	7.65	4.13	5.31	5.85	6.80	5.81	4.36	8.99	5.33	5.92
Sr	570	566.17	52.71	66.97	64.17	63.23	64.16	58.94	55.20	50.13	50.31	66.15
Th	42	41.66	3.00	3.00	3.00	3.00	3.00	3.00	3.00	8.64	3.00	3.00
U	8	3.00	3.00	3.00	3.00	3.00	3.00	3.00	3.00	7.44	3.00	3.00
W*	450	494.89	1123.91	217.13	166.32	363.17	197.60	114.55	302.32	182.70	125.01	113.90
Y	19	12.18	14.29	9.71	9.13	9.56	8.31	9.57	8.85	13.20	8.29	9.36
Zn	48	66.94	103.10	83.37	89.56	93.92	88.18	85.43	95.07	176.59	85.43	86.01
Zr	235	209.22	36.26	19.19	24.69	24.66	21.05	21.33	20.67	21.78	16.73	29.50
Cl*	450	574.78	7.58	166.87	7.58	7.58	7.58	7.58	40.43	97.66	226.54	251.87
Co	65	64.90	217.22	109.07	110.97	135.82	116.18	106.14	118.82	125.66	95.99	96.32
Cr	55	64.23	22373.47	3755.63	3667.39	3635.04	3861.19	3918.36	10572.04	72465.07	6722.76	7401.94
F*	1050	940.27	100.00	100.00	100.00	100.00	100.00	100.00	100.00	100.00	100.00	100.00
S*	140	83.83	16.00	16.00	26.49	16.00	16.00	16.00	16.00	22.98	16.00	61.32
Sc	7	3.51	30.15	28.93	25.07	26.93	23.34	25.00	25.78	22.01	25.36	26.55
V	65	60.81	229.61	131.08	125.46	122.62	121.06	116.11	155.49	587.19	139.65	150.05
Cs	5	9.43	9.43	9.43	9.43	9.43	9.43	9.43	9.43	9.43	9.43	9.43
Ba	1400	1299.92	38.17	41.30	62.89	50.39	53.81	58.46	36.27	32.09	29.91	39.26
La	75	61.53	18.20	17.27	20.32	18.34	19.04	22.64	16.75	17.66	17.75	14.48
Ce	135	150.80	4.88	4.88	4.88	4.88	4.88	4.88	4.88	4.88	4.88	4.88
ppm	GSN cert		T11	T12	T13	T14	T15	T16	T17	T18	T19	T20
	GSN	Depth (m)	61.90	61.99	62.08	62.57	62.65	62.84	63.79	63.93	64.00	64.12
As	1.6	3.00	3.00	3.00	3.00	3.00	3.00	3.00	3.00	3.00	3.00	3.00
Cu	20	71.62	21.41	10.05	11.17	26.47	15.64	11.78	4.58	3.67	9.81	4.87
Ga	22	18.45	3.24	5.28	5.52	13.28	12.42	7.95	18.14	17.15	17.47	19.44
Mo	1.2	1.00	1.48	1.00	1.00	5.70	5.43	2.80	1.00	1.00	1.00	1.00
Nb	21	19.78	2.84	2.78	2.23	5.45	5.12	6.11	2.03	2.00	2.46	2.57
Ni	34	29.61	544.83	507.54	484.76	630.96	624.15	546.25	87.94	36.21	55.11	49.19
Pb	53	46.51	3.00	3.00	6.42	7.00	3.00	4.27	3.00	3.00	3.00	3.00
Rb	185	179.34	8.81	7.58	4.49	8.87	6.49	14.82	13.13	16.63	8.10	8.91
Sr	570	566.17	49.05	82.40	90.39	91.87	77.45	77.72	431.80	468.77	422.58	426.00
Th	42	41.66	3.00	3.00	3.00	9.45	6.92	4.28	3.00	3.00	3.00	3.00
U	8	3.00	3.00	3.00	3.00	6.73	3.00	3.00	3.00	3.00	3.00	3.00
W*	450	494.89	63.63	59.52	267.76	148.85	138.31	144.36	498.13	433.08	280.15	284.64
Y	19	12.18	10.63	8.37	8.53	13.83	11.25	13.65	4.57	4.14	5.55	5.42
Zn	48	66.94	88.63	87.26	95.37	151.71	161.46	114.44	77.12	52.34	60.21	61.79
Zr	235	209.22	29.05	41.83	19.74	25.32	21.90	30.01	11.96	19.23	14.85	15.26
Cl*	450	574.78	323.50	27.35	253.38	7.58	83.92	173.77	7.58	80.89	7.58	7.58
Co	65	64.90	97.12	94.12	107.75	114.49	114.71	104.73	93.29	70.49	58.49	61.29
Cr	55	64.23	7730.82	8854.18	10110.29	60417.83	56256.79	33739.00	24515.16	9516.67	13620.38	14163.39
F*	1050	940.27	100.00	100.00	100.00	100.00	100.00	100.00	100.00	100.00	100.00	100.00
S*	140	83.83	376.56	20.36	90.36	16.00	36.77	16.00	16.00	16.00	16.00	16.00
Sc	7	3.51	29.78	25.42	24.72	22.25	24.65	26.10	0.65	0.65	0.65	1.11
V	65	60.81	162.32	157.12	161.59	569.03	538.73	355.82	207.10	101.87	159.13	163.57
Cs	5	9.43	9.43	9.43	9.43	9.43	9.43	9.43	9.43	9.43	9.43	9.43
Ba	1400	1299.92	46.38	58.44	41.26	58.36	39.84	45.06	118.65	139.07	92.57	86.99
La	75	61.53	18.29	17.15	15.76	21.19	17.22	19.75	24.21	23.49	25.89	24.84
Ce	135	150.80	4.88	4.88	4.88	4.88	4.88	4.88	4.88	4.88	4.88	4.88

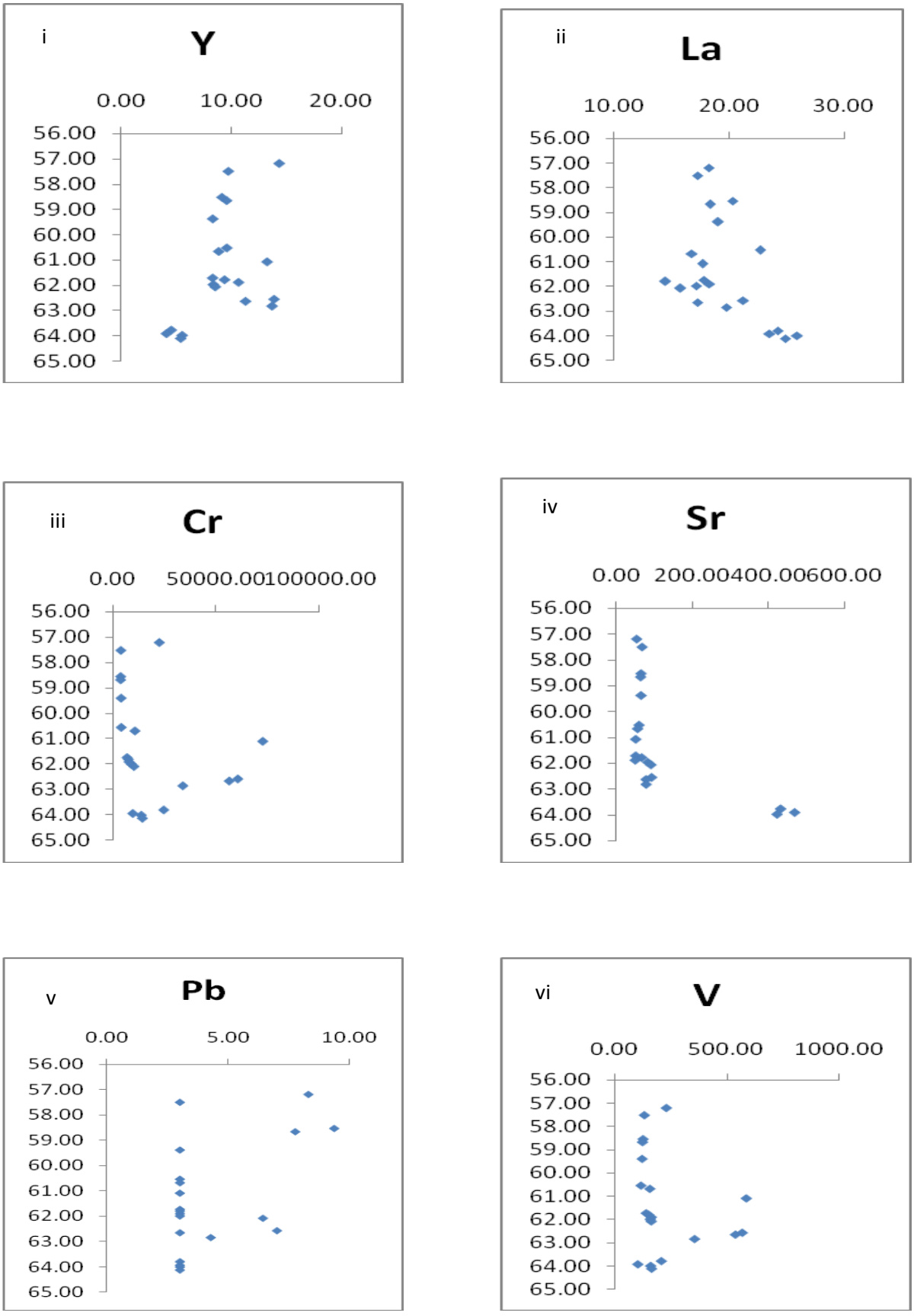

Figure 7: Plots of some trace elements against depth (m).

3.5 Trace element geochemistry on bulk rock samples

From Fig. 7 it is observed that the concentration of Y (fig.7i) increases from depth towards the top of the section used for this study. This increase in concentration is from ± 4ppm to 13ppm. Across the section, there is an observable variation in the concentration at the depth between 63.79m and 62.84m. It is at this depth that the variation in concentration is observed to be sharp and greatest. Cr and V (figs iii and vi respectively) are observed, in contrast, to decrease in concentrations. But at same depth between 63.79m and 62.84m Cr and V are observed to also have a major variation in the stratigraphy where there is a sudden decline in their concentrations, both trace elements are observed to increase upward the sequence from 64.12m to 63.79m where there's a decrease in their concentrations. Sr also displays a reduction in its concentration from about 426ppm at 64.12m to about 53ppm at 57.12m. Within this variation is also the sharp decline from about 431ppm at 63.79m to about 78ppm at 62.84m. Pb however is observed to retain a constant composition throughout the studied section with just some variation at 63.79m where the concentration increases from 3ppm to 7ppm at 62.57m and reducing back to its original composition of about 3ppm. This composition remains constant up until 58.67m where it increases to about 8ppm.

4.1 DISCUSSION

4.1.1 THEORETICAL CRITERIA FOR DISTINGUISHING MAGMA INFLUX FROM FRACTIONAL CRYSTALLIZATION AND ASSIMILATION.

The influx of a new batch of magma has been widely accepted as a medium for the formation of chromitite seams in layered mafic-ultramafic intrusions. Influx of new magma, either primitive or more evolved, has the can to alter the composition of the crystallizing magma to a greater or lesser degree. The degree of change in the composition of the final crystallizing magma relies on whether the new magma has a similar composition or a totally different one to the original resident magma in the chamber. For example, Spandler et al. (2005) interpreted the G chromitite seam of the Stillwater Complex as forming from the mixture of resident fractionating magma with magma which had assimilated part of the Na-rich country rocks at the chamber's roof. This however did not yield a great change in the composition of the resulting magma; this may be due to the fact that the magma involved in the assimilation of the country rocks is of same composition as the resident fractionating magma. Another example of magma influx is found in the explanation by Sharpe and Irvine (1983) for the formation of chromitites in the Critical Zone of the Bushveld Complex. This, unlike at Stillwater, is a good example of magma influx yielding quite a different magma in composition to the resident one in the chamber.

Sharp and Irvine (1983) ascribed the lower Critical Zone as crystallizing from olivine- and orthopyroxene-rich magma which is poor in plagioclase magma and chromitite (A-type magma). This composition is different from that which crystallized the overlying upper Critical Zone, with the boundary between these two compositions lying halfway into the middle group chromitites (between MG2 and MG3 chromitite layers) and marked by the appearance of cumulus plagioclase (Boorman et al., 2003). The upper Critical Zone was interpreted to form from chromite-rich, plagioclase, olivine and calcium-rich magma (U-type magma). One essential observation supporting the influx of new magma is the difference in the rocks of the lower Critical Zone to that of the upper Critical Zone. Rocks of the lower Critical Zone appear to have crystallized from a plagioclase-poor magma in contrast to rocks of the upper Critical Zone which crystallized from plagioclase-rich magma.

Similarly, Naldrett et al. (2009) observed PGE content and ratios in the Critical Zone of the Bushveld Complex. In the lower part of the Critical Zone between LG1-LG4, (Pt+Pd)/(Rh+Ru+Ir+Os) was observed to be low, in the order of 0.1 to 0.3. This ratio however increases above this zone especially in the LG5 where it ranges between 0.9 and 10. The increase in (Pt+Pd)/(Rh+Ru+Ir+Os) was explained to be as a result of mixing of new influx of magma with the resident fractionating magma in the chamber. Naldrett et al., (2009) further explained that the low (Pt+Pd)/(Rh+Ru+Ir+Os) at LG1-LG4 was due to the rapid influx of new primitive magma which surpressing fractional crysatallization. At LG5 where there is increase in (Pt+Pd)/(Rh+Ru+Ir+Os), the effect of influx of the new magma decreased favoring subsequent fractional crystallization of the magma.

A major identifier for magma influx is the use of isotopes. A good example of this is the decrease in the $^{87}Sr/^{86}Sr$ in the rocks above the Pyroxenite Marker of the Main Zone of the Bushveld Complex compared to the rocks below it. This suggested the influx of a new batch of magma at the level of the Pyroxenite Marker. Cawthorn et al., (1990) reported the decrease in the $^{87}Sr/^{86}Sr$ from 0.7082 in the rocks below the pyroxenite magma to about 0.7067 in the rocks above it. The use of isotopes is widely accepted for the determination of influx of new magma; however, in this project it is excluded.

Fractional crystallization, however, may yield similar results to contamination and influx of magma depending on the mineral crystallizing out of the magma. The variation observed in a fractionally crystallized pile of rocks is generally gradual. For example, a melt or magma containing Mg-rich, Na-rich, and Ca-rich elements crystallizing out orthopyroxene will lead to depletion in the Mg content of the melt resulting to a Na-rich, Ca-rich and Mg-poor melt. Similarly, crystallization of plagioclase will deplete the melt of Na and or Ca resulting in Mg-rich and Na-poor (or Ca-poor) melt. This idea can be compared to the proposed model of Mondal and Mathez (2006). These authors suggested that chromitite layers in the Critical Zone of the Bushveld Complex crystallized from a magma mainly composed of Mg and Na with chromitite crystals suspended in the melt. As orthopyroxene (and minor clinopyroxene) crystallized out from the melt, the melt became more Na- and chromitite-rich. Almost immediately, the crystallization of plagioclase commenced which becomes a cumulus phase between the MG2 and MG3 chromitite layers. The crystallization of the chromite-rich magma was suggested to be responsible for the chromitite layers of the Critical Zone. The melt soon got depleted in chromite resulting in a residual chromite-poor melt. This is supported with the absence of chromitite layers above the Critical Zone of the Bushveld Complex.

Assimilation can occur at any time when magma is fractionally crystallizing. This occurs when magma partially melts or dissolves surrounding (country) rocks. Assimilation to a large extent also alters the

composition of the melt but greatly ted material is of same or different composition as the magma assimilating it. For example Spandler et al. (2005) observed the types of inclusions found in chromitite grains from the Stillwater Complex. They observed three different types of inclusions in the chromitite grains; the first type of inclusion containing just quenched glass; the second containing a number of vapor bubbles; and the third containing just a large vapor bubble. The first and the second types of inclusions observed were proposed to have crystallized from the assimilation of the country rocks at the roof of the chamber by the resident Mg-rich magma during which there was also exolution of Ca-rich fluid as chromitite crystallized. This resulted in the low CaO content of these two types of inclusions. This assimilation resulted in a Na-rich trondhjemitic melt which is now different in composition from the resident magma. The third inclusion inclusion bearing a large bubble was proposed to crystallize from a Ca-rich fluid phase trapped during chromitite crystallization. It must be noted that assimilation described above resulted in a magma composition different to that of the "original" resident magma in the chamber and this is due to the difference in composition between the resident magma and the assimilated country rocks.

4.1.2 OBSERVATION ON BOREHOLE USED IN THIS PROJECT.

The rocks above and below the MG4 chromitite layers studied in this project, as mentioned earlier and presented by graphs from the microprobe analysis, are quite similar especially in the Mg# of orthopyroxene as shown in fig 7. The Ca content however decreases upward in the sequence but remains fairly similar in composition both above and below the chromitite layers. Noteworthy is the 61.09m and 61.13 marks where there is observable change in the concentration of elements. At these depths, the concentration of all the major elements is altered by either a sharp increase or decrease in their concentration. This implies that at these depths, there was a change in either the physical or chemical condition of the chamber from which crystallization occurs. The Mg# of orthopyroxene and clinopyroxene as shown in fig 7, exhibit no significant variation either above or below the chromitite layers.

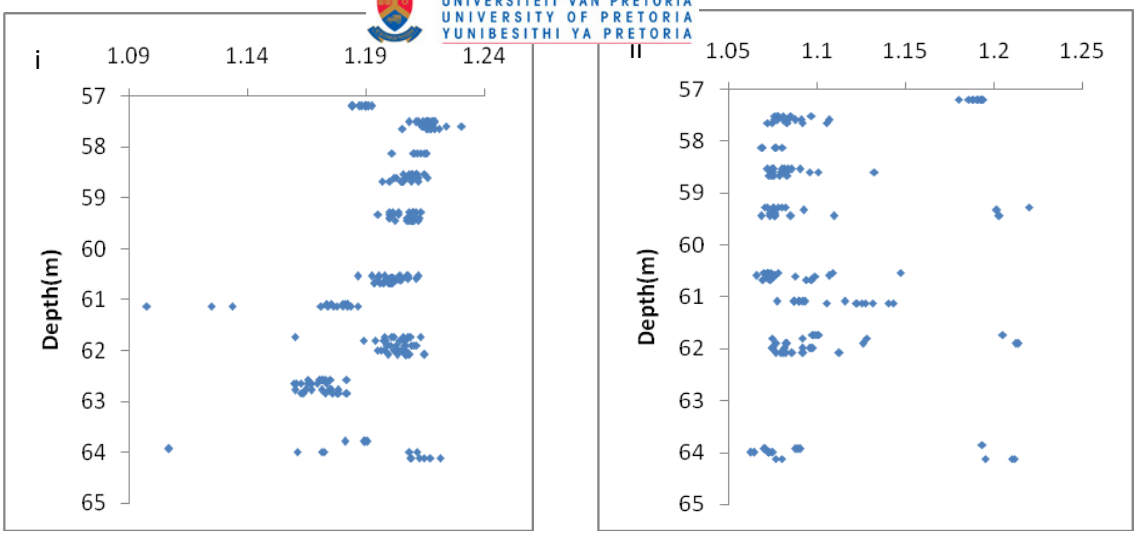

Figure 8: Variation in Mg# of both orthopyroxene (i) and clinopyroxene (ii) across the depth (m) of the MG4 section.

The plagioclase content however changes from depth upward the sequence. The plagioclase content changes from calcium-rich plagioclase to a more sodic plagioclase.

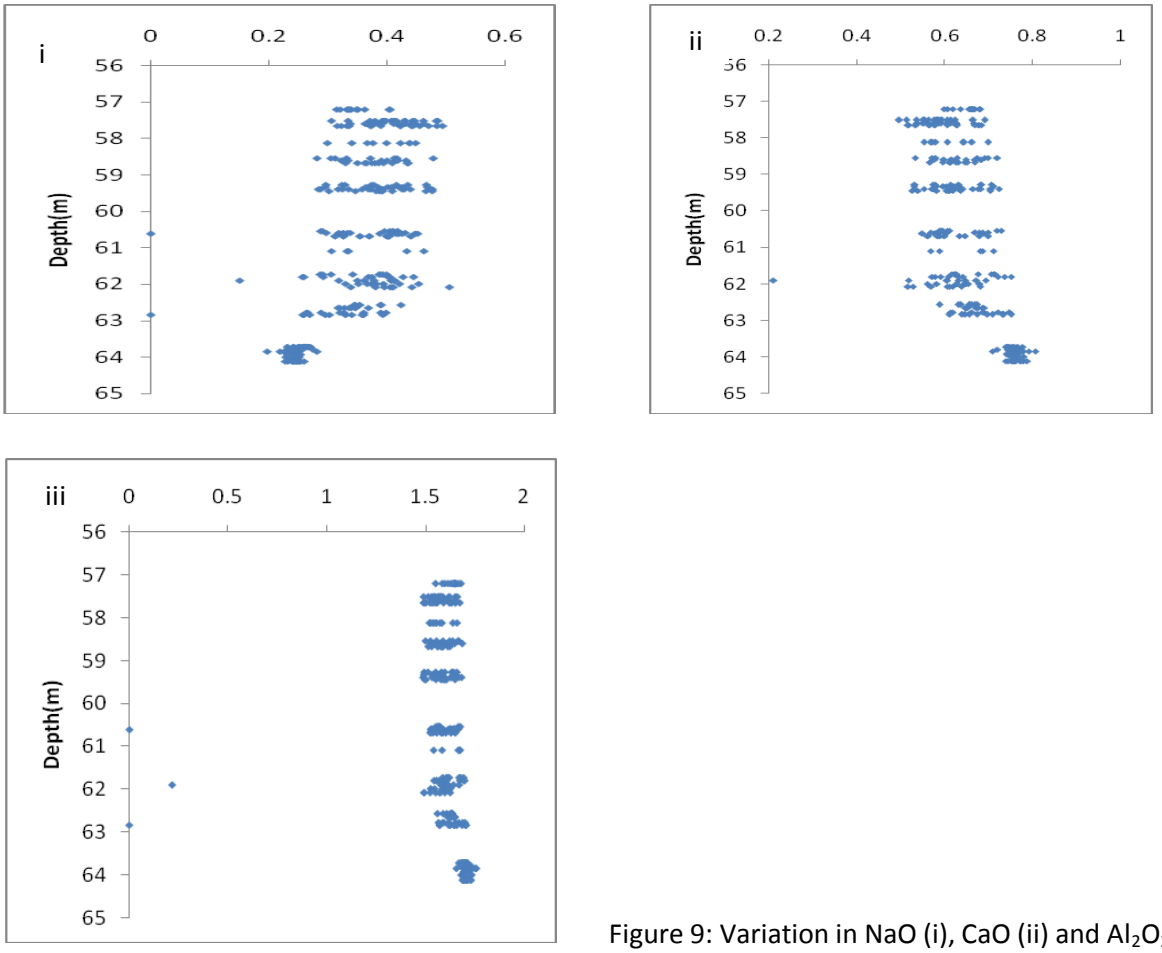

Figure 9: Variation in NaO (i), CaO (ii) and Al_2O_3 (iii) composition of plagioclase across the depth (m) of the MG4 section.

This change is observed to take place at the 61.09m and 61.13m depths as shown in fig 8. Fig 8 shows the composition of plagioclase above and below the 61.09 and 61.13m mark where the major variation is observed.

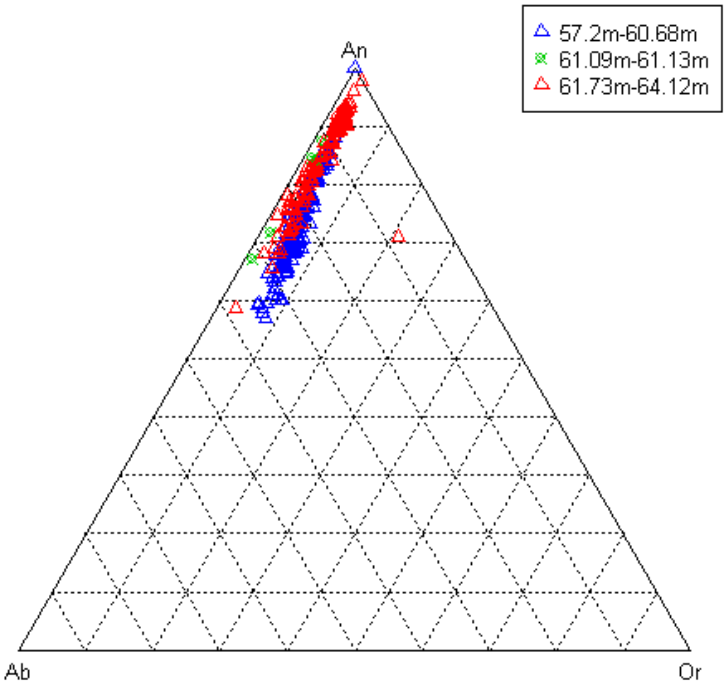

Figure 10: Compositional variation in the plagioclase at 61.73m-64.12m, 61.09m-61.13m and 57.20m-60.68m.

Another significant variation above and below the 61.09m and 61.13m depths is the abundance of interstitial biotite. Biotite is more abundant above 61.09m than below and at 61.09m and 61.13m absent. The presence of biotite below the depths may be attributed to metasomatic infiltration down the stratigraphy assisted by gravity.

Data also reveal that the Mg# of orthopyroxene ranges from 1.18 to 1.23 ($En_{73.96-80.51}$, $Fs_{17.86-22.76}$, $Wo_{1.07-7.36}$) at 57.20m to 60.68m, 1.10 to 1.18 ($En_{57.15-81.34}$, $Fs_{14.46-19.59}$, $Wo_{0.14-28.39}$) at 61.09m to 61.13m and 1.09 to 1.22 ($En_{69.02-87.84}$, $Fs_{11.18-22.04}Wo_{0.20-15.10}$) at 61.73m to 64.12m. These compositions are

similar especially with the middle se has been observed and described as the section with major variation. This similarity in orthopyroxene composition may suggest similar origin (possibly same magma) for the formation of the MG4 pyroxenite. The clinopyroxene composition of $En_{43.73-80.39}$, $Fs_{6.66-21.84}$, $Wo_{1.09-49.06}$ at 57.20m to 60.68m, $En_{55.78-73.19}$, $Fs_{9.07-16.23}$, $Wo_{10.57-30.33}$ at 61.09m to 61.13m and $En_{43.35-88.07}$, $Fs_{6.29-20.83}$, $Wo_{0.13-49.23}$ at 81.73m to 64.12m however, are not akin across the section especially in the 61.09m to 61.13m where there is increase in calcium from $Wo_{0.13}$ to $Wo_{10.57.}$ This may also be another reason for the decrease in the calcium content of the rocks in this section of study especially plagioclase which varies from being calcium-rich at depth (64.12m-61.73m) to a sodium-rich plagioclase from 61.13m depth upward in the stratigraphy.

Chromium content of orthopyroxene however, is similar across the MG4 pyroxenites observed in this study. At 57.20m to 60.68m, Cr_2O_3 is averagely 0.005897, at 60.09m to 61.13m, Cr_2O_3 is 0.007. In contrast, Cr_2O_3 is about 0.00724 at 61.73m. This similarity in the Cr_2O_3 of orthopyroxene highlights the fact that chromitite and orthopyroxene were once in equilibrium (coexisted) in the magma chamber. Similarly, the Cr/Al of orthopyroxene through the entire section shows no significant variation especially at the 61.09m and 61.13m mark. This similar Cr/Al ratio is a good evidence of no pressure change in the magma chamber from which the chromitite layer of the MG4 was formed (Mathez and Modal, 2006). In otherwords, if the MG4 chromitite layers formed from a closed system, the solubility of Cr should increase the pressure in the system which will crystallize rocks above the chromitite layers different to rocks below it especially in terms of the Cr/Al.

One main observation about the 61.09m and 61.3m depths is the fact that these are the depths at which there is an increase in sodium content and a corresponding decrease in the calcium content of the rocks (especially plagioclase). One important question to answer, however, is why the change in the sodium and calcium content of the rocks (plagioclase) affect the composition of orthopyroxene as well at this same depth. In an attempt to explain this, it must be noted that it is at 61.09m and 61.13m depths that orthopyroxene and clinopyroxene grains are large in size. The appearance of large clinopyroxene grains contain greater amount of calcium as it crystallizes. The calcium crystallizing in clinopyroxnene will however affect (possibly reduce) the calcium content crystallizing in the plagioclase grains. Another explanation comes from the formation or crystallization of biotite in the mineral assemblage. Biotite as is a secondary mineral formed during crystallization, as this mineral form, the potassium in it has the ability to be replaced by either sodium or calcium. The plagioclase at these depths and below is calcium-rich and this calcium content could have been trapped in the formation of biotite. Another explanation is that as orthopyroxene and clinopyroxene crystallize, Mg and Fe will be extracted out with little Ca. Either of these processes or a combination

of these can be responsible for th simultaneous calcium depletion of plagioclase.

The Ca-rich plagioclase observed in the rocks at the base of the stratigraphy suggests that the melt which produced the chromitite layers at this depth (61.13m-64.12m) was Ca-rich crystallizing a small amount of chromitite. However, above this depth (57.12m-60.68m), plagioclase is Na-rich. This is suggested by Spandler et al., (2005) to be as a result of the mixing of partially melted surrounding country rocks with the parent magma which resulted in the melt being oversaturated with chromitite. This is assumption is supported by the petrographic character of the rocks lying above or below the chromitite layers. At depth, especially at 63.85m-64.12m, Ca-rich plagioclase is cumulus with little chromitite crystals. However, higher up in the stratigraphy where there is abundance of Na- rich plagioclase, there is also an increase in the chromite abundance suggesting that the fluid which crystallized the rocks observed was either saturated or oversaturated with chromitite. Converse to the idea of mixing of two magmas to form chromitite and hence chromitite layers, it should be made clear that the proposed formation of chromitite seam is from a single parent magma that was however, contaminated.

With the study of the trace elements plots, it is observed that a major change also occurs in the lower part of the studied stratigraphy between the depths of 63.79m and 62.84m. In the plot of some compatible trace elements with plagioclase composition (An%) in fig. 11(i-iv), it is observed that these elements substitute for plagioclase and thus crystallize along with plagioclase. For example, in the plot of La against depth (m) compared with the plot of An% there is a similar trend observed with a major observation about the depth between 65.70m and 63.80m.

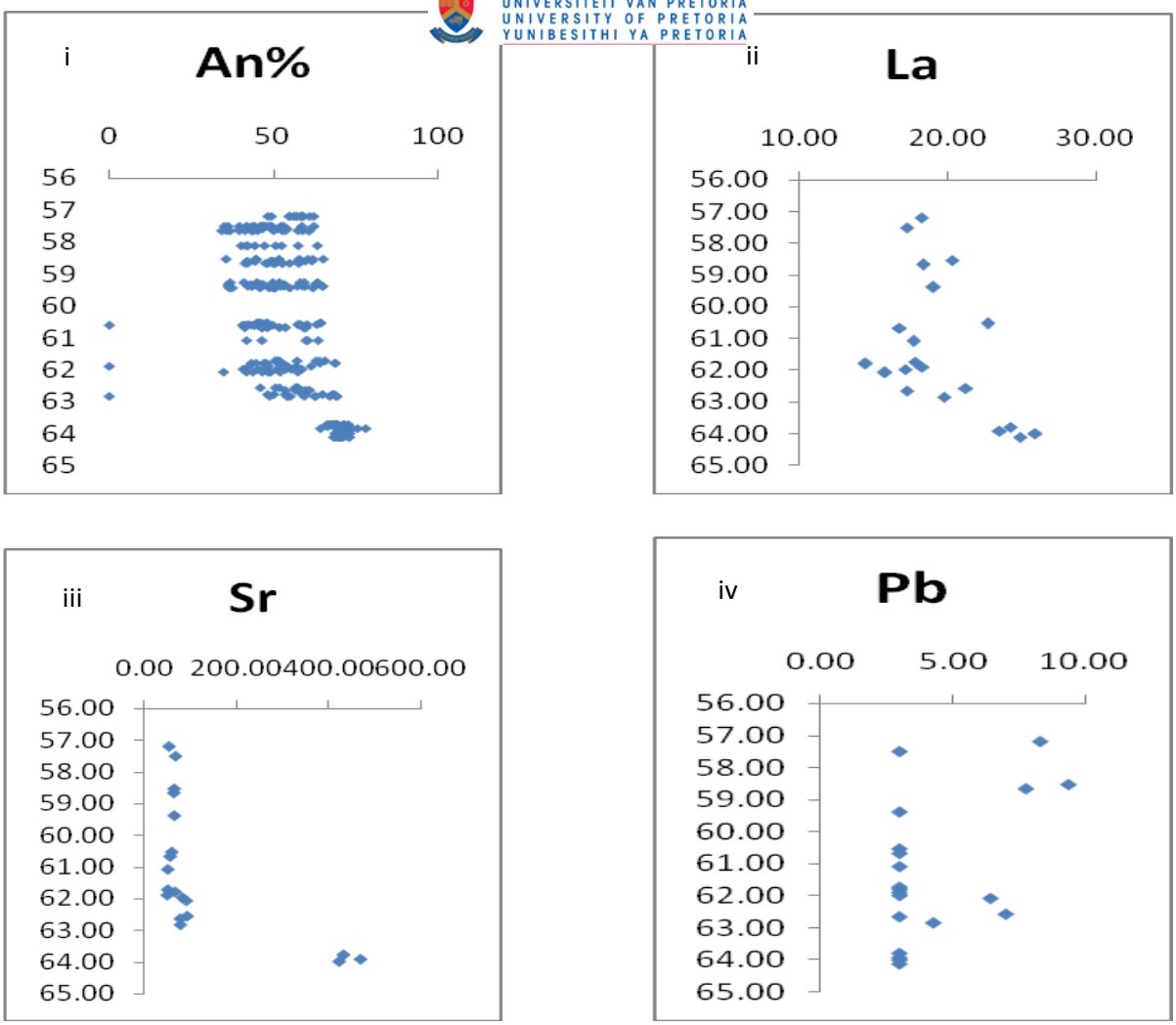

Figure 11: Comparison between some trace elements with compatible plagioclase elements (An%).

The observed change is similar to the trend of the major elements plots as shown earlier which shows a major reversal at the mentioned level. Also exhibiting this trend is the plot of Sr. This major change observed at this depth occurs where there is the change from a plagioclase-rich (especially the calcium-rich plagioclase) layer to a pyroxene-rich layer. However Pb which is also compatible with plagioclase has a constant composition. It would have been easy to suggest that the reduction of the Ca-rich plagioclase was due to the crystallisation of plagioclase-rich fluid but as observed in thin section and major element analysis there is clinopyroxene, also containing Ca, above this depth.

Therefore it is suggested that at the depth of about 63.70m where there is the observed reduction of Ca-rich plagioclase, magma rich in Na entered into the chamber which commenced the crystallization of Na-rich plagioclase. This suggestion is also supported by the increase in the Na content of clinopyroxene at this same interval of depth where the change in plagioclase compositions is observed. In other words, the depth of about 63.70m is where magma rich in Mg, (Fe), and Na was injected into the magma chamber. To further confirm this suggestion, some

compatible trace elements with both pyroxene were also plotted as shown in fig 12 (i-v). The plots of Co, Ni, Sc, all of which are compatible with orthopyroxene, show a similar crystallization sequence to that of the orthopyroxene Mg#. The compatible trace elements with the orthopyroxene composition suggest that they crystallized together from the melt.

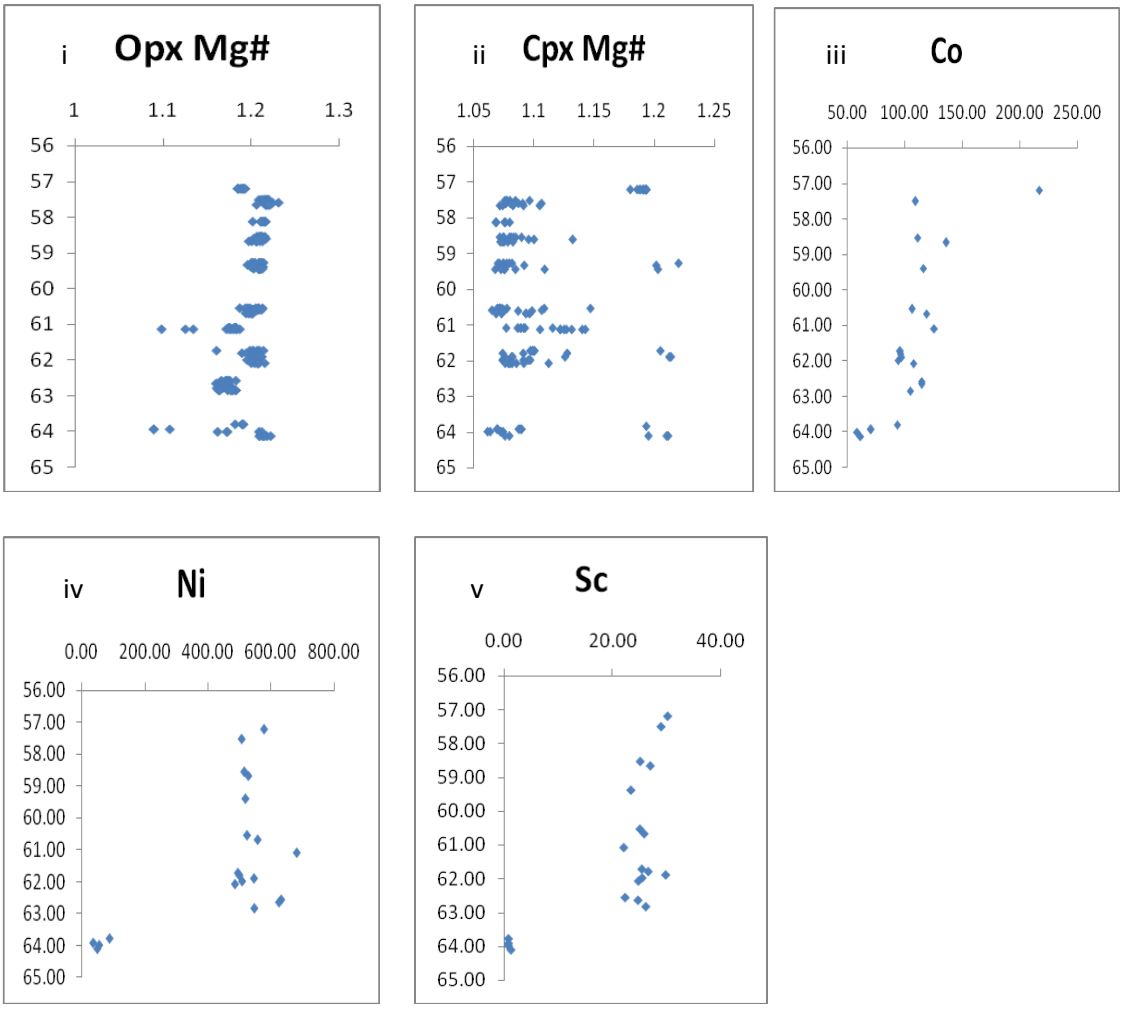

Figure 12: Comparison of some trace elements with compatible pyroxene compositions(Mg#).

Between the depths of 63.79m and 62.84m there is a distinctive increase in the crystallization of the compatible elements with pyroxene compositions. This sudden increase suggests variation in the magma composition crystallizing at this level.

In summary, the change in composition of plagioclase might be the depth at which there is a change in the composition of the magma crystallizing from the chamber. In contrast, the Mg# of both orthopyroxene and clinopyroxene do not show a significant variation at the depth as observed in the plagioclase compositions but increases steadily upward the sequence.

If however, the increase in the Mg# from depth upward the sequence is evaluated, the model proposed by Filho and Araujo (2009) will be supported. The Mg# of orthopyroxene is higher in the rocks above than those underlying the layers of chromitite used in this study. This supports the idea of the mixture between a primitive magma and a fractionating resident magma in the chamber. Also supporting this idea is the observation of chromium-rich rocks where there is abundance of orthopyroxene and especially large (interstitial) clinopyroxene crystals. Filho and Araujo (2009) suggested that calcium-rich clinopyroxene from mafic to ultramafic layered intrusions have more chromium (Cr) content than orthopyroxene due to higher partition coefficients. A possible suggestion of the Cr-poor plagioclase-rich layer in the lower part of the stratigraphic sequence studied in this project may be as a result of crystallization from the resident magma while the pyroxene-rich layers interlayered with the chromitite seams might have crystallized from the influx of a new primitive magma into the chamber.

In other words, the analysis used in this project supports the idea of all the mentioned authors which suggest a single batch of magma or the mixing of a resident magma with a more primitive magma with similar composition or with very little contamination as suggested by Spandler et al. (2005).

4.1.3 MAGMA INFLUX AT THE MG4 LEVEL?

From the above observations made from petrographic, major element and trace elemen geochemistry analyses, one of the major trends observed is the decrease in the Ca content with a subsequent increase in Na content. It will be hard to ascribe this change in composition to magma influx. Similar to the report by Mathez and Mondal (2006) about the rocks above and below the chromitite layers in the lower part of the Critical Zone, the rocks above and below the MG4 chromitite layers studied in this project are also identical suggesting that crystallization of these rocks and the stratiformed chromitite layers contained within them crystallized from a single batch of magma.

However, chromite crystals are not as abundant in the lower part of the stratigraphy as they are in the upper part. This suggests that the magma crystallizing the plagioclase-rich lower part of the layers used in this study was chromite-poor. At the 63.72m mark (fig 6vi), it is observed that Cr_2O_3 begins to increase, leading to the suggestion that the magma at this level is chromitite-rich. This can be compared to the idea proposed by Mondal and Mathez (2006) that the magma which crystalized the UG2 chromitite layer composed of suspended chromite crystals abundant enough to form the

chromitite layers. However, an impo there are very few chromite crystals in the lower part of the stratigraphy in contrast to the upper part if the magma which crystallized the MG4 contained suspended chromite crystals?

The boundary between the upper and lower Critical Zone is marked by the appearance of cumulus plagioclase. This formed from a melt over-saturated with respect to plagioclase and thus shifts the crystallizing mineral proportions, favoring the crystallization of plagioclase. The crystallization of plagioclase out of the melt will result to a pyroxene-rich melt which is compatible with suspended chromitite crystals injected into the chamber. Thus, formation of chromitite layers is through fractional crystallization.

In contrast to the proposed idea of influx of magma with suspended particles to form the MG4 chromitite is the idea of Kinnaird et al. (2002) and more recently Spandler et al. (2005). They proposed mixing magma which assimilated part of the surrounding country rocks with the resident magma in the chamber. Spandler et al. (2005) in describing the formation of chromitite seams of the Stillwater Complex proposed that magma similar in composition to the resident magma in the chamber ponded in the roof of the chamber, assimilating part of the surrounding country rocks. This assimilation led to a Na-rich magma. This proposition is very similar to what is observed in the rocks studied in this project. The rocks studied here are calcic in the lower part of the stratigraphy as opposed to the more sodic rocks in the upper part as shown in fig 9i and ii. The Na-rich rocks in the upper part might have resulted from the assimilation of the surrounding country rocks. The surrounding rocks to the Bushveld Complex are the rocks of the Pretoria Group of the Transvaal Supergroup. These rocks are rich mainly in Ca and some Na (unpublished thesis by Reczko, 1994). Assimilation of Ca-rich rocks will have little or no effect on the melt owing to the similar composition of the assimilated rocks and the resident magma. Ca-rich plagioclase does crystallize under high temperature thus proposing another possible explanation for the crystallization of Ca-rich plagioclase first at the base of the stratigraphy. Clinopyroxene also contains Ca and thus its crystallization will also reduce the Ca content of the melt resulting in a Ca-poor melt and as described in the petrographic character of the rocks studied, clinopyroxene does appear as large interstitial grains.

The assimilation of the Na-rich country rocks will however alter (contaminate) the composition of the melt. Na is not a major constituent of pyroxene and will only be crystallized out of the melt during the crystallization of plagioclase. As a result, the Ca-depleted melt will commence the crystallization of Mg and Na contained in the melt. As orthopyroxene and clinopyroxene crystallize simultaneously with chromitite due to the good partition coefficient between chromium and orthopyroxene, plagioclase will also start to crystallize containing Na. In other words, the Idea of

mixing of magma with assimilated agma might be responsible for the formation of the MG4 chromitite layers studied in this project.

As a result, the similarity between the MG# of orthopyroxene and clinopyroxene across the studied depth suggests that a single magma or magma of similar composition injected into the chamber crystallized the MG4 package. Although the plagioclase composition differs across depth, it does not imply magma with different composition mixing, but rather the crystallization sequence observed. That is the crystallization of Ca-rich plagioclase first, followed by the crystallization of Na-rich plagioclase. However the plots of the compatible trace elements with both pyroxene and plagioclase compositions suggest that there was possible magma mixing. This is due to the fact that the compositions of both orthopyroxene and clinopyroxene (Mg#) do not change in contrast to that observed in the plagioclase compositions (Ca to Na). It can therefore be suggested that at the depth of 64.12m, the magma crystallizing was mainly Ca-rich forming the Ca-rich plagioclase. However, at the depth between 63,79m and 62.84m, it is suggested that a Mg-rich (also Na-rich) magma entered into the chamber and mixed with the resident Ca-rich magma which at this time had a smaller volume compared to the new magma. This idea is supported by the presence of Ca-rich clinopyroxene in the upper part of the studied section.

5.1 CONCLUSION

The major aim of this project is to observe, if any, the variation in magma composition that crystallized the rocks above and below the MG4 chromitite seams. Although the rocks of the MG4 sequence used in this project at depth (64.12m) grade upwards from a plagioclase-rich (anorthosite) layer to a pyroxene-rich (pyroxenite) layer, this does not necessarily imply different magma injection observed in some other Bushveld chromitites such as the UG2 (Mathez and Mondal, 2006) and the E-pyroxenites described by Cameron (1980, 1982). Also, the similarity in the magnesium number (Mg#) of orthopyroxene as well as that of the clinopyroxene across the studied section does not support that the emplacement of the pyroxenite above and below the MG4 chromitite layer was as result of injection of magma of different types. Also similar in composition is the Cr/Al of both orthopyroxene and clinopyroxene. Difference in the Cr/Al (figure 4) would have resulted from pressure change in the magma chamber which would probably be brought about by influx of a new batch of magma either more primitive or evolved. At the 61.09m and 61.13m depths, the Cr/Al for both orthopyroxene and clinopyroxene remain similar each across the section of study.

However, the major variation in the section is observed in the plagioclase composition (figure 9). This difference is observed at the 61.09m and 61.13m depths at which the calcium and sodium content decreases and increases respectively and where the grain sizes of orthopyroxene and clinopyroxene increases with a slight reduction in the modal abundance of plagioclase. This decrease in plagioclase is attributed not only to the increase in the abundance of pyroxene especially clinopyroxene with increasing calcium content but also to the larger grain sizes. Calcium is a major constituent of clinopyroxene and is one of the factors distinguishing clinopyroxene from orthopyroxene. The crystallization and growth of clinopyroxene within the assemblage therefore, will subsequently extract calcium from the melt. This can cause a reduction in the amount of calcium remaining to form other minerals including plagioclase.

Another mineral formed other than plagioclase and clinopyroxene that contains calcium is Biotite. Biotite constitutes potassium which can be replaced by either sodium or calcium. At 61.09m, 61.13m and below in the stratigraphy, the plagioclase content is calcium-rich, potassium in plagioclase could have been replaced by calcium which is a major constituent of plagioclase at these depths and hence the melt. This replacement will cause a reduction in the amount of calcium left in the melt and hence, the calcium content of other minerals. In other words, calcium is extracted simultaneously with the crystallization of plagioclase (which probably crystallized first), then clinopyroxene before the formation of biotite, a secondary mineral formed in the assemblage. It should be noted that the

similarities argued for above also s[illegible] of magma influx into the melt. But new magma influx should result in difference in the compositions of the rocks above and below the chromitite layers (Mathez and Mondal, 2006). Trace elements geochemistry have also helped to suggest that the variation observed at the 61.09m and 61.13m marks might be due to the observed variation at 63.79m and 62.84m. Below the depth of 63.79m it is observed that there was the crystallization of Ca-rich plagioclase indicating that the melt was composed of it. Between 63.79m and 62.84m it is suggested that there was the influx of new batch of magma into the chamber. With the evidence shown above by the increase orthopyroxene and clinopyroxen and hence the Mg#, the new magma is proposed to be Mg-rich that mix with the resident Ca-rich magma which at this level had a lower quantity compared with the new magma. The proposed idea of magma mixing is preferred to influx of new magma because of the presence of Ca-rich clinopyroxene at above this level. It is evidence that Ca was still present and in sufficient quantity to support the crystallization of clinopyroxene.

In conclusion, it is proposed the MG4 chromitite package crystallized from the mixture of a resident Ca-rich magma with the influx of a Mg- (and Na-) magma at the depth of 63.79m and 62.84m which eventually mixed to start crystallization of the Mg-rich layers at 61.09m and 61.13m.

REFERENCES

Boorman, S, Boudreau, A, Kruger, F.J., 2003, The Lower Zone Critical Zone Transition of the Bushveld Complex: A Quantitative Textural Study, Journal of petrology, p. 1209-1235.

Cameron, E.N., 1977, The Lower Part of the eastern part of the Bushveld Complex in the Olifants River Trough, Journal of petrology, p. 437-462.

Cameron, E.N., Desborough, G.A., 1969, Occurrence and characteristics of chromite deposites-Eastern Bushveld Complex, Economic Geology Monogram, volume 4, p.23-40.

Cameron, E.N., Emerson, M.E., 1959, The origin of certain chromite deposits of the eastern part of the Bushveld Complex. Economic Geology, volume 54, p. 1151-1213.

Cawthorn, R.G., 2002, Delayed accumulation of plagioclase in the Bushveld Complex. Mineralogical Magazine, December 2002, vol 66(6), p 881-893.

Cawthorn, R.G.,nd, Controls on platinum mineralisation in the Bushveld complex.

Cawthorn R.G., Cooper G.R.J. & Webb S.J., 1998, Connectivity between the western and eastern limbs of the Bushveld Complex, South Africa Journal of Geology, 101, 291-298.

Cawthorn, R.G., Meyer, S.P., Kruger, F.J., 1991. Major addition of magma at the Pyroxenite Marker in the western Bushveld Complex, South Africa, Journal of Petrology, p. 739-763.

Cawthorn, R.G., Meyer, P.S., Kruger, F.J., 1990, Major addition of magma at the Pyroxenite Marker in the western Bushveld Complex, South Africa, Journal of petrology, p.738-763.

Cawthorn, R.G., Walraven F., 1998, Emplacement and crystallization time for the Bushveld Complex, Journal of Petrology, volume 39, p. 1669–1687.

Eales, H.V., Cawthorn, R.G., 1996, The Bushveld in the layered intrusions. Cawthorn, R.G. (ed), Elservier science B.V., Amsterdam, p. 181-229.

Eales, H. V., de Klerk, W. J., Teigler, B., 1990, Evidence for magma mixing processes within the Critical and Lower Zones of the Northwestern Bushveld Complex, South Africa, Chemical Geology, volume 88, p. 261–278.

Eales, H.V., Marsh, J.S., Mitchell, A.A., de Klerk, W.J., Kruger, F.J., Field, M., 1986, Some geochemical constraints upon models for the crystallization of the Upper Critical Zone-Main Zone interval, Northwest Bushveld Complex, Mineral magazine , volume 52 , p. 63-79.

Filho, C.F.F, Araujo, S.M., 2009, Re[illegible]s deposits associated with layered intrusions: geological and petrological constraints for the origin of stratiform chromitites, Transactions of the Institute of Mining and Metallurgy, Section B: Applied Earth Science, volume 118, p. 86-100.

Gain, S.B., 1980, The Geology and PGE distribution in the Upper Group Chromitite Layers at Maandashoek 254KT, Eastern Bushveld Complex.

Gough, D.I., van Nierkerk, C.B., 1959, A study of the paleomagnetism of the Bushveld Complex, Philosophical Magazine, p. 126-136.

Hall, A.L., 1932, The Bushveld Igneous Complex in the central Transvaal, Geological magazine, p237-238.

Hulbert, L.J., von Gruenewaldt, G., 1984, Textural and Compositional features of Chromite in the Lower and Critical Zones of the Bushveld complex South of Potgietersrus, Economic Geology, volume 80, p. 872-895.

Irvine, T.N., Smith, C.H., 1969, Primary oxide minerals in the layered series of the Muskox Intrusion. In Wilson, H.D.B. (Ed.) Magmatic Ore Deposits, A symposium. Economic Geology, p. 4, 76-94.

Johnson, M.R., Anhaeusser, C.R. and Thomas R.J. (eds), 2008, The Geology of South Africa. Geological Society of South Africa, Johannesburg/Council for Geoscience, Pretoria

Kinnaird, J.A., Kruger, F.J., Nex, P.A.M., Cawthorn, R.G., 2002. Chromite formation- a key to understanding processes of platinum enrichment, Transactions of the Institute of Mining and Metallurgy, Section B: Applied Earthscience, volume 111, p. B23-B35.

Kruger, F.J., 2005, Filling the Bushveld complex magma chamber: lateral expansion, roof and floor interaction, magmatic unconformities, and the formation of giant chromitite, PGE and Ti-Vmagnetite deposits. Mineral Deposits, p. 40, 451–472.

Lee, A.C., Sharpe, M.R., 1979, The “Boulder Bed” and Merensky reef- further examples of silicate liquid immiscibility and spherical aggregation in the Bushveld Complex, Earth and Planetary Science Latters, volume48, p. 131-147.

Lipin, B.R., 1992, Pressure increases, the Formation of Chromite Seams, and the Development of the Ultramiafic Series in the Stillwater Complex, Montana, Journal of Petrology, volume 34, p. 955-976.

McDonald,J.A., 1965, Liquid immiscibility as one factor in chromitite seam formation in the Bushveld Igneous Complex: Econnomic Geology, volume 60, p. 1674-1685.

R.K.W. Merkle, G. von Gruenewaldt, Valuation of proposed platinum group element contents in the parental magmas of the Bushveld complex, Journal of African Earth Sciences, Volume 21, Pages 607-613

Molyneux, T.G., 1974. A geological investigation of the Bushveld Complex in Sekhukhuneland and part of the Steelport valley. Trans Geology Society South Africa, p. 7, 329-338.

Mondal, S. K., Mathez, E.A., 2006, Origin of the UG2 chromitite layer, Bushveld Complex, Journal of Petrology, volume 48, p. 495-510.

Naldrett, A.J., Kinnaird, J., Wilson, A., Yudovskaya, M., McQuade, S., Chunnett, C., Stanley, C., 2009, Chromite composition and PGE content of Bushveld Chromitites: Part 1- The lower and Middle Groups, Transactions of the Institutions of mining and Metallurgy, Section B Applied Science volume 118, p. 131-161.

O'Driscoll, B., Donaldson, C.H., Daly, J.S., Emeleus, C.H., 2008, The roles of melt infiltration of anorthosite and a Cr-spinel seam in the Rum Eastern Layered Intrusion, NW Scottland, Lithos 111, p. 6-20.

Reczko, B.F.F., 1994, The geochemistry of the sedimentary rocks of the Pretoria Group, Transvaal Sequence, *Ph. D. dissertation*, University of Pretoria, Pretoria, South Africa

Sharpe, M.R., 1985, Strontium isotope evidence for preserved density stratification in the main zone of the Bushveld Complex, South Africa, Nature 316, p. 119-126.

Sharpe, M.R., Irvine, T.N., 1983, Melting relations of two Bushveld chilled margin rocks and implications for the origin of chromitite, Carnegie Institution Geophysical Laboratory Yearbook 82, 295-300.

Spandler, C., Mavrogenes, J., Arculus, R., 2005, Origin of chromities in layered intrusions: Evidence of chromit-hosted melt inclusions from the Stillwater Complex. Geology 2005, p. 33, 893-896.

Tegner, C., Cawthorn, R.G., Kruger, F.J., 2006, Cyclicity in the Main and Upper Zones of the Bushveld South Africa: Crystallization from a Zoned Magma Sheet, Journal of Petrology, volume 47, p. 2257-2279.

Teigler, B., Eales, H.V., 1996, The Lower and Critical Zones of the Western Limb of the Bushveld Complex as intersected by the Nooitgedagt boreholes, Bulletin- Geophysical Survey volume 111, p. 126.

Voordouw, R., Gutzmer, J., Beukes, ן for the Upper Group (UG1, UG2) chromitite seams in the Dwars River area, Bushveld Complex, South Africa, Mineralogy and Petrology volume 97, p.75-94.

Von Gruenwaldt, G., Webber-Diefenbach, K., 1977, Co-existing calcium poor pyroxenes in the main zone of the Bushveld Complex, Contributions to Mineralogy and Petrology, volume 65, p.11-18.

Von Gruenewaldt, G., 1973, The Main and Upper Zones of the Bushveld Complex in the Roossenekal area, Eastern Transvaal, Transactions of the Geological Society of South Africa, p. 76, 207-227.

Wilson M G C, Anhaeusser C R (eds), 1998, The Mineral Resources of South Africa, Council for Geoscience, Pretoria

APPENDIX I: Major Element Data of Plagioclase

Depth (m)	Na2O	Al2O3	SiO2	K2O	CaO	TiO2	Cr2O3	MnO	FeO	Ab	An	Or
57.2	0.337199	1.652574	2.311268	0.018817	0.662157	0	0	0	0.006835	10.296	58.931	2.228
57.2	0.338079	1.655785	2.326253	0.022778	0.666536	0.000683	0	0	0.007975	9.993	58.45	2.683
57.2	0.333677	1.656855	2.334426	0.020797	0.657292	0	0	0	0.007595	11.22	59.109	2.452
57.2	0.405871	1.599593	2.398451	0.018817	0.60718	0.000683	0.002154	0	0.006076	15.042	49.381	2.21
57.2	0.40411	1.586214	2.409349	0.02773	0.597936	0.001025	0.000718	0.000385	0.005316	15.164	48.333	3.256
57.2	0.332797	1.642406	2.310814	0.020797	0.668969	0.000683	0	0	0.005316	10.224	58.739	2.464
57.2	0.351285	1.630097	2.328069	0.020797	0.655346	0.000342	0	0.001154	0.006835	11.014	56.263	2.458
57.2	0.349525	1.647223	2.339421	0.020797	0.66313	0.001708	0.000359	0	0.006076	10.772	56.955	2.447
57.2	0.315188	1.681473	2.303095	0.018817	0.679672	0	0	0	0.005696	9.269	62.294	2.222
57.2	0.336318	1.653644	2.336696	0.018817	0.661671	0.001025	0	0.000385	0.006456	11.369	58.753	2.216
57.2	0.321351	1.668629	2.313084	0.018817	0.680645	0	0	0.000385	0.006456	9.673	60.976	2.222
57.2	0.362731	1.615648	2.336242	0.017826	0.636858	0.001025	0.000718	0	0.006835	12.597	54.794	2.116
57.2	0.33984	1.649898	2.331248	0.017826	0.664103	0	0	0	0.007215	11.017	58.34	2.104
57.2	0.348644	1.641336	2.322166	0.018817	0.657778	0.001025	0.001077	0.000769	0.005696	10.719	57.187	2.228
57.2	0.333677	1.552499	2.261773	0.024759	0.61837	0.001708	0.001077	0.000769	0.013671	10.512	55.147	3.026
57.51	0.334558	1.651504	2.333518	0.020797	0.66459	0.001708	0	0.000769	0.006835	10.987	58.693	2.452
57.51	0.380339	1.619929	2.383921	0.024759	0.624208	0.001708	0	0.000385	0.006076	13.363	52.364	2.902
57.51	0.396187	1.546077	2.414344	0.032682	0.576043	0	0	0	0.007595	17.175	47.129	3.883
57.51	0.411154	1.569624	2.421609	0.029711	0.582367	0.002733	0	0.000769	0.006076	16.316	46.764	3.493
57.51	0.371535	1.623675	2.402084	0.02872	0.613018	0.000342	0.000718	0.000385	0.005696	14.307	53.066	3.363
57.51	0.429642	1.551964	2.46066	0.037633	0.554149	0	0.000718	0.000385	0.005316	17.751	43.544	4.414
57.51	0.486869	1.515038	2.510609	0.038624	0.513768	0.001366	0.001077	0.000769	0.002658	20.198	36.178	4.503
57.51	0.443729	1.537515	2.441589	0.033672	0.554636	0.001708	0	0	0.006456	17.325	41.913	3.965
57.51	0.306384	1.662207	2.289472	0.018817	0.690375	0.001366	0	0.000385	0.006456	9.097	62.391	2.234
57.51	0.412914	1.568019	2.417523	0.037633	0.581394	0.001025	0.000359	0	0.006456	14.964	46.039	4.426
57.51	0.393545	1.58996	2.403446	0.030701	0.590638	0.001708	0.000718	0	0.007215	15.154	49.444	3.617
57.51	0.462218	1.530558	2.475191	0.034662	0.535175	0.00205	0	0.000385	0.006076	18.866	39.609	4.06
57.51	0.407632	1.577652	2.410712	0.023768	0.5848	0	0	0	0.005316	16.419	47.989	2.801
57.51	0.447251	1.546612	2.46066	0.034662	0.551717	0.000342	0	0	0.005696	17.61	41.797	4.06
57.51	0.416436	1.574441	2.428421	0.02872	0.585773	0	0.000359	0.000769	0.004557	16.07	46.46	3.368
57.51	0.484228	1.491491	2.517874	0.043576	0.49674	0.001366	0	0.000769	0.006076	21.27	35.043	5.106
57.51	0.431403	1.563202	2.441589	0.032682	0.56388	0.002391	0	0	0.005696	16.781	44.265	3.829
57.51	0.392665	1.583003	2.402538	0.02674	0.606694	0.00205	0	0.000769	0.006456	15.045	49.331	3.144
57.51	0.398828	1.580863	2.41616	0.025749	0.593558	0	0.000359	0.000385	0.005696	16.146	48.715	3.032
57.59	0.365372	1.614043	2.38165	0.031691	0.625668	0.001708	0	0.000769	0.005696	13.06	53.125	3.723
57.59	0.363611	1.615113	2.365758	0.022778	0.627128	0.000342	0.000359	0.000769	0.006456	13.577	54.133	2.689
57.59	0.378578	1.611902	2.386191	0.024759	0.612532	0.001366	0	0	0.007595	14.28	52.274	2.913
57.59	0.431403	1.558921	2.453395	0.029711	0.573124	0.001366	0	0.000385	0.005696	17.426	44.11	3.475
57.59	0.391784	1.598523	2.389824	0.02674	0.622749	0.00205	0.000359	0.000385	0.006835	13.466	50.093	3.138
57.59	0.449011	1.545007	2.476553	0.040604	0.552203	0.001366	0.000359	0	0.007215	17.368	41.009	4.728
57.59	0.412034	1.571765	2.428421	0.02872	0.592098	0.001025	0	0	0.004937	16.123	46.715	3.368
57.59	0.463098	1.534839	2.472921	0.031691	0.538094	0.001366	0	0.000385	0.004937	18.908	39.927	3.711
57.59	0.387382	1.58996	2.407533	0.02773	0.603774	0.001025	0.000359	0.000385	0.008734	15.219	50.069	3.262
57.59	0.441968	1.562667	2.45612	0.030701	0.560474	0.00205	0	0.000385	0.004937	17.394	43.262	3.587
57.59	0.44549	1.558921	2.453849	0.031691	0.551717	0.001025	0	0	0.006456	17.476	42.775	3.705
57.59	0.386502	1.610296	2.395273	0.025749	0.621289	0.000342	0.000359	0	0.008354	13.618	51.152	3.014
57.59	0.338079	1.648828	2.331248	0.020797	0.667022	0.001708	0.001077	0.000385	0.007595	10.585	58.199	2.452
57.59	0.419958	1.55571	2.424334	0.023768	0.585773	0.001025	0	0	0.006456	16.878	45.611	2.801

Depth (m)	Na2O	Al2O3	SiO2	K2O	[illegible]	[illegible]	2O3	MnO	FeO	Ab	An	Or
57.59	0.428762	1.535374	2.442951	0.02872	0.536148	0.001366	0	0	0.022785	15.868	43.22	3.363
57.65	0.494793	1.491491	2.518783	0.037633	0.51766	0.001025	0.001436	0.000769	0.005696	20.704	34.283	4.391
57.65	0.423479	1.559991	2.422518	0.029711	0.575556	0.001708	0.000718	0	0.005316	16.442	45.191	3.498
57.65	0.441968	1.553034	2.445676	0.023768	0.566312	0.001025	0	0.000385	0.007975	17.888	43.319	2.789
57.65	0.323112	1.675051	2.319896	0.018817	0.67578	0.002391	0.001077	0.000385	0.007595	10.015	61.006	2.216
57.65	0.332797	1.652039	2.328069	0.018817	0.678212	0.000683	0	0	0.007215	10.426	58.955	2.216
57.65	0.390024	1.592636	2.394819	0.02773	0.606694	0.000342	0	0.000769	0.006456	14.521	50.067	3.262
57.65	0.316069	1.65418	2.309906	0.021788	0.684537	0.001025	0	0	0.007975	9.561	60.656	2.577
57.65	0.422599	1.541261	2.429783	0.035653	0.577502	0.00205	0.000718	0	0.007595	16.248	43.913	4.202
57.65	0.336318	1.634379	2.345324	0.021788	0.669942	0.000683	0.000359	0	0.006456	11.448	57.534	2.565
57.65	0.372415	1.626886	2.387099	0.021788	0.626641	0.001366	0.001077	0	0.006456	13.847	53.591	2.553
57.65	0.471022	1.499518	2.484273	0.041595	0.534202	0.001366	0	0.000385	0.009494	18.592	36.767	4.875
57.65	0.374176	1.622605	2.397543	0.02674	0.627614	0	0.000359	0	0.007595	13.484	52.768	3.126
57.65	0.456055	1.523601	2.4929	0.037633	0.532742	0.00205	0	0	0.004177	19.795	39.579	4.403
57.65	0.485108	1.503264	2.518783	0.036643	0.516687	0.000683	0	0.000769	0.004937	20.916	35.83	4.273
57.65	0.444609	1.531628	2.460206	0.032682	0.56388	0.001708	0	0.000769	0.006076	17.816	41.381	3.829
58.12	0.376817	1.574976	2.3594	0.025749	0.642696	0.00205	0	0	0.004557	12.826	50.739	3.049
58.12	0.399708	1.557851	2.404354	0.030701	0.605234	0	0.000359	0	0.006835	15.12	47.273	3.623
58.12	0.34072	1.640265	2.333518	0.021788	0.662644	0.001708	0.000359	0.000769	0.006076	11.016	57.551	2.571
58.12	0.299341	1.661137	2.274942	0.014855	0.699133	0.00205	0.000359	0	0.007975	8.984	63.41	1.773
58.12	0.449011	1.525741	2.463839	0.039614	0.553176	0.002391	0	0.000385	0.007595	17.503	40.267	4.645
58.12	0.439327	1.521995	2.423426	0.032682	0.570204	0.002391	0.000359	0	0.004557	16.708	41.726	3.865
58.12	0.423479	1.547683	2.423426	0.032682	0.579448	0.002733	0.000359	0.001154	0.007595	16.068	44.342	3.847
58.12	0.367133	1.584609	2.347594	0.021788	0.64075	0.000342	0.000359	0	0.007215	12.915	52.534	2.588
58.12	0.438446	1.537515	2.456574	0.032682	0.569718	0.001708	0.001795	0	0.008354	17.427	42.222	3.829
58.54	0.331916	1.62314	2.318079	0.019807	0.672861	0.001366	0	0	0.007595	10.985	57.9	2.352
58.54	0.372415	1.589425	2.364849	0.02872	0.628101	0.000683	0	0	0.004937	13.075	51.717	3.404
58.54	0.417316	1.557316	2.433416	0.042585	0.579448	0.000683	0	0	0.004937	15.203	44.684	5
58.54	0.478945	1.501124	2.499257	0.047537	0.533229	0.00205	0.000359	0	0.007595	18.187	35.617	5.543
58.54	0.281733	1.670234	2.266314	0.018817	0.720053	0.000683	0	0.000769	0.004937	7.57	65.209	2.24
58.54	0.312547	1.63866	2.289472	0.020797	0.691835	0.001025	0	0.000769	0.008734	8.966	60.556	2.476
58.54	0.305504	1.665418	2.31036	0.021788	0.698646	0.001708	0	0.001154	0.006076	9.052	62.024	2.571
58.54	0.412914	1.526812	2.412528	0.031691	0.571177	0.002391	0.001436	0	0.006835	17.245	44.68	3.77
58.6	0.400589	1.600664	2.395727	0.017826	0.614965	0.002733	0	0	0.005316	14.983	49.955	2.092
58.6	0.323112	1.648828	2.32035	0.019807	0.682591	0.00205	0	0	0.006835	10.324	59.756	2.34
58.6	0.328395	1.68736	2.296737	0.017826	0.649021	0.000683	0	0	0.007595	9.844	61.692	2.11
58.6	0.326634	1.627422	2.318533	0.018817	0.683564	0.001708	0.000718	0	0.006835	10.722	58.562	2.234
58.6	0.433164	1.529487	2.442951	0.038624	0.577016	0.002391	0	0	0.007215	16.266	42.031	4.539
58.6	0.334558	1.626351	2.324436	0.023768	0.669942	0	0.001077	0	0.005696	10.605	57.478	2.819
58.6	0.417316	1.53698	2.406625	0.035653	0.597936	0.002733	0	0	0.007975	14.619	44.248	4.208
58.6	0.419077	1.543937	2.421155	0.031691	0.595504	0	0	0	0.006835	15.573	44.585	3.729
58.6	0.390904	1.577117	2.388008	0.02773	0.616911	0.001366	0	0.001154	0.007595	14.016	49.216	3.268
58.67	0.350405	1.614043	2.354406	0.02773	0.646588	0.001025	0.000718	0.001154	0.006076	12.092	54.972	3.274
58.67	0.380339	1.578187	2.380288	0.024759	0.612045	0.001708	0.000718	0	0.006456	15.003	50.677	2.937
58.67	0.436686	1.532163	2.45839	0.033672	0.565339	0.00205	0	0.000385	0.005316	18.024	42.131	3.954
58.67	0.394426	1.562667	2.385737	0.02773	0.613505	0.001708	0	0	0.004937	14.549	48.311	3.286
58.67	0.386502	1.585679	2.395273	0.029711	0.611072	0.000683	0	0.000769	0.006835	14.302	49.904	3.498
58.67	0.409393	1.588355	2.413436	0.030701	0.59599	0	0	0.000769	0.007215	14.502	47.664	3.593
58.67	0.434925	1.515573	2.43614	0.037633	0.566312	0.00205	0	0.001154	0.005316	16.959	41.433	4.45
58.67	0.330155	1.624746	2.324436	0.024759	0.669455	0.00205	0	0.000769	0.006456	10.687	57.744	2.937
58.67	0.375057	1.563202	2.375293	0.02872	0.627128	0.000683	0	0	0.006456	14.034	50.163	3.41
58.67	0.362731	1.588355	2.357584	0.02674	0.65194	0	0.000359	0	0.005316	12.177	52.594	3.162

Depth (m)	Na2O	Al2O3	SiO2	K2C			2O3	MnO	FeO	Ab	An	Or
58.67	0.366252	1.586749	2.347594	0.020797	0.631506	0.001366	0	0.000385	0.016709	13.084	52.765	2.47
59.27	0.329275	1.634379	2.329885	0.022778	0.681132	0.001708	0.001077	0.001154	0.006456	10.461	58.202	2.689
59.27	0.4675	1.494702	2.493808	0.042585	0.531769	0	0.000718	0	0.005696	19.473	36.816	5
59.27	0.323993	1.642941	2.315355	0.020797	0.684051	0.000683	0.000718	0.000385	0.004177	10.073	59.431	2.464
59.27	0.435805	1.513968	2.449762	0.038624	0.572637	0.001366	0.000359	0	0.006456	17.081	41.052	4.55
59.27	0.2967	1.660066	2.280845	0.014855	0.705944	0	0.000718	0.000385	0.006456	8.983	63.51	1.767
59.27	0.374176	1.598523	2.378472	0.02674	0.632479	0.001366	0	0	0.005316	13.277	51.871	3.15
59.27	0.378578	1.581933	2.39936	0.038624	0.613505	0.001025	0.000359	0	0.005696	13.591	49.855	4.545
59.27	0.416436	1.552499	2.422972	0.036643	0.577989	0.002391	0	0	0.006456	15.729	45.014	4.314
59.33	0.409393	1.55464	2.404354	0.030701	0.59599	0.001025	0.000359	0	0.005696	15.303	46.255	3.629
59.33	0.385622	1.580328	2.377564	0.02773	0.619343	0.000683	0	0	0.007215	13.747	49.996	3.28
59.33	0.420838	1.558921	2.452941	0.033672	0.581394	0.001366	0.001795	0	0.004557	16.935	44.817	3.936
59.33	0.427001	1.53698	2.428875	0.037633	0.579448	0.00205	0	0	0.007595	15.755	43.141	4.432
59.33	0.372415	1.583003	2.370752	0.024759	0.632966	0.001025	0.000718	0.000769	0.006456	13.697	51.565	2.931
59.33	0.469261	1.493096	2.488359	0.045556	0.53031	0.001366	0.000718	0	0.007215	18.76	36.394	5.348
59.33	0.295819	1.645082	2.273125	0.015846	0.711296	0.002391	0.000718	0	0.006456	8.756	62.896	1.891
59.33	0.401469	1.558921	2.4039	0.033672	0.603288	0.001366	0.000359	0	0.009873	14.492	46.91	3.971
59.33	0.373296	1.583538	2.366666	0.022778	0.631506	0.001708	0	0.000385	0.006076	13.783	51.68	2.701
59.33	0.411154	1.541796	2.418431	0.032682	0.595504	0.00205	0.001077	0	0.005316	15.819	45.219	3.853
59.33	0.364492	1.642406	2.494262	0.030701	0.622262	0.00205	0.000359	0	0.007215	16.941	53.33	3.51
59.33	0.407632	1.560527	2.422518	0.038624	0.59745	0.001708	0	0.000769	0.008734	14.446	45.911	4.527
59.39	0.390904	1.580863	2.395273	0.021788	0.617884	0.001025	0	0	0.004177	15.261	49.772	2.571
59.39	0.31783	1.644012	2.322166	0.023768	0.682591	0.001025	0.000359	0.001154	0.006456	10.103	59.783	2.807
59.39	0.373296	1.570695	2.381196	0.02674	0.636858	0	0	0.000769	0.007215	13.901	50.648	3.162
59.39	0.429642	1.535909	2.44613	0.02674	0.572151	0.001708	0.000359	0.000385	0.005696	18.321	43.502	3.15
59.39	0.477185	1.488815	2.506522	0.031691	0.53031	0.000683	0	0.000385	0.006076	21.264	36.224	3.717
59.39	0.392665	1.596917	2.396635	0.030701	0.614478	0.00205	0	0	0.007215	13.557	49.668	3.599
59.39	0.358329	1.595847	2.35486	0.030701	0.64075	0.00205	0.000359	0	0.007595	12.101	53.203	3.634
59.39	0.287896	1.683613	2.28811	0.018817	0.704971	0.001025	0	0.000385	0.007215	8.518	65.014	2.228
59.39	0.324873	1.632238	2.324436	0.018817	0.67578	0.001025	0.000359	0	0.007215	11.222	58.965	2.228
59.39	0.426121	1.536444	2.441589	0.032682	0.57361	0	0.000718	0	0.007215	17.227	43.495	3.847
59.39	0.284374	1.670234	2.253146	0.017826	0.724432	0.00205	0	0	0.006835	6.777	65.082	2.122
59.39	0.368894	1.58889	2.378926	0.023768	0.632479	0.00205	0.000359	0.000385	0.007975	14.079	52.13	2.807
59.39	0.440207	1.557851	2.524232	0.037633	0.553663	0.000683	0	0	0.009114	19.416	42.213	4.338
59.39	0.335438	1.628492	2.330339	0.024759	0.665076	0.001708	0	0.001154	0.007215	10.703	57.335	2.931
59.44	0.387382	1.598523	2.383921	0.030701	0.610586	0.001025	0.001436	0.000385	0.006076	13.461	50.454	3.617
59.44	0.391784	1.580328	2.410257	0.033672	0.609613	0.000342	0.001077	0	0.007975	14.401	48.746	3.954
59.44	0.477185	1.496843	2.506068	0.032682	0.526417	0.001708	0.000359	0.000385	0.005316	21.171	36.57	3.829
59.44	0.3821	1.589425	2.384375	0.030701	0.617884	0.003074	0	0.000385	0.006456	13.665	50.475	3.617
59.44	0.346883	1.608156	2.355314	0.030701	0.635885	0.000342	0	0.000385	0.004557	12.627	55.002	3.64
59.44	0.46662	1.503264	2.496079	0.038624	0.539554	0.001366	0.000359	0.000385	0.004557	19.544	37.478	4.521
59.44	0.392665	1.600664	2.396181	0.030701	0.602801	0.001708	0.000359	0.000385	0.004937	14.072	49.981	3.605
59.44	0.409393	1.554105	2.432507	0.032682	0.582367	0.002391	0	0	0.006076	16.838	45.94	3.847
59.44	0.301982	1.650969	2.295829	0.018817	0.703998	0	0	0	0.008354	9.061	62.105	2.234
60.54	0.396187	1.569624	2.385737	0.030701	0.610099	0.001366	0	0	0.005696	14.026	48.279	3.629
60.54	0.418197	1.554105	2.425696	0.034662	0.589665	0.001025	0	0.000385	0.005696	15.526	44.954	4.072
60.54	0.287896	1.668094	2.266314	0.018817	0.71908	0.001025	0.000718	0	0.004557	7.501	64.513	2.24
60.54	0.404991	1.575511	2.403446	0.025749	0.605234	0.000683	0	0.000769	0.006456	14.996	47.872	3.032
60.54	0.419077	1.564273	2.441135	0.032682	0.591125	0.001025	0	0	0.005316	16.011	45.31	3.818
60.54	0.409393	1.57123	2.428875	0.035653	0.595017	0.001025	0.001077	0	0.006456	15.098	46.439	4.172
60.54	0.411154	1.561062	2.421609	0.036643	0.592584	0.001708	0	0.001154	0.003797	15.029	45.83	4.302
60.54	0.291417	1.676656	2.267222	0.019807	0.728811	0.00205	0	0.000385	0.006456	6.349	64.232	2.346

Depth (m)	Na2O	Al2O3	SiO2	K2C			2O3	MnO	FeO	Ab	An	Or
60.59	0.409393	1.565343	2.447492	0.041595	0.585287	0.000683	0.000359	0	0.004937	15.748	45.713	4.864
60.59	0.326634	1.624746	2.331702	0.021788	0.669942	0.001708	0.001077	0	0.004937	11.719	58.271	2.583
60.59	0.338079	1.641336	2.330793	0.019807	0.678699	0.001708	0	0.000769	0.006076	10.482	57.85	2.334
60.59	0.29758	1.669699	2.287656	0.023768	0.69816	0	0	0	0.005696	8.175	63.221	2.819
60.59	0.31871	1.647758	2.306273	0.020797	0.68697	0	0	0.001154	0.004937	9.531	60.234	2.464
60.59	0.414675	1.562667	2.428421	0.032682	0.585773	0.000683	0	0	0.005316	15.947	45.829	3.841
60.59	0.333677	1.627957	2.334426	0.024759	0.669455	0.000342	0.001436	0.000769	0.004937	10.868	57.447	2.925
60.59	0.431403	1.531093	2.455211	0.036643	0.568745	0.000683	0	0	0.006456	17.372	42.387	4.302
60.61	0	0.001605	4.521276	0	0.000487	0.00205	0	0	0.00038	0	0.055	0
60.61	0.452533	1.535374	2.466563	0.025749	0.547338	0.000342	0	0	0.004557	19.553	41.371	3.026
60.61	0.448131	1.527882	2.474283	0.036643	0.54977	0.001366	0.000359	0.001154	0.005316	18.57	40.625	4.29
60.61	0.418197	1.561062	2.424788	0.036643	0.582367	0.000342	0	0	0.006076	15.307	45.209	4.302
60.61	0.415556	1.541261	2.430691	0.040604	0.577989	0.001366	0.000718	0.001538	0.006835	15.828	44.258	4.781
60.61	0.388263	1.594242	2.414798	0.030701	0.603774	0.001366	0	0	0.005316	15.144	49.939	3.599
60.61	0.426121	1.535909	2.440681	0.032682	0.575556	0.000683	0	0.001154	0.006456	17.16	43.455	3.847
60.61	0.420838	1.549823	2.442043	0.036643	0.585287	0.001025	0	0	0.006456	16.012	44.245	4.296
60.61	0.324873	1.615113	2.289018	0.024759	0.688916	0.000342	0	0	0.006456	8.732	58.082	2.955
60.68	0.326634	1.652039	2.318079	0.024759	0.678699	0.001025	0	0.000385	0.005696	9.477	59.284	2.919
60.68	0.400589	1.581933	2.405717	0.033672	0.588692	0.00205	0.000718	0.000769	0.005316	14.889	48.187	3.965
60.68	0.441088	1.526276	2.450671	0.036643	0.561934	0.001708	0	0.000385	0.006076	17.351	41.318	4.308
60.68	0.370655	1.603875	2.382559	0.034662	0.632966	0.001025	0	0.000769	0.004557	12.347	51.874	4.072
60.68	0.312547	1.630097	2.293559	0.023768	0.699619	0.000342	0.000718	0.000385	0.005696	8.726	59.892	2.831
60.68	0.354807	1.58889	2.339421	0.02674	0.646102	0.001025	0.000718	0.000385	0.006456	12.067	53.648	3.185
60.68	0.40323	1.53805	2.407533	0.02773	0.584314	0.001708	0.000718	0.000385	0.006456	17.089	46.366	3.298
60.68	0.40411	1.558386	2.400722	0.033672	0.599882	0.001025	0	0	0.006456	14.501	46.717	3.977
60.68	0.326634	1.652039	2.318079	0.024759	0.678699	0.001025	0	0.000385	0.005696	9.477	59.284	2.919
60.68	0.400589	1.581933	2.405717	0.033672	0.588692	0.00205	0.000718	0.000769	0.005316	14.889	48.187	3.965
60.68	0.441088	1.526276	2.450671	0.036643	0.561934	0.001708	0	0.000385	0.006076	17.351	41.318	4.308
60.68	0.370655	1.603875	2.382559	0.034662	0.632966	0.001025	0	0.000769	0.004557	12.347	51.874	4.072
60.68	0.312547	1.630097	2.293559	0.023768	0.699619	0.000342	0.000718	0.000385	0.005696	8.726	59.892	2.831
60.68	0.354807	1.58889	2.339421	0.02674	0.646102	0.001025	0.000718	0.000385	0.006456	12.067	53.648	3.185
60.68	0.40323	1.53805	2.407533	0.02773	0.584314	0.001708	0.000718	0.000385	0.006456	17.089	46.366	3.298
60.68	0.40411	1.558386	2.400722	0.033672	0.599882	0.001025	0	0	0.006456	14.501	46.717	3.977
61.09	0.332797	1.667559	2.304457	0.008913	0.68697	0.000342	0.001795	0	0.006456	10.002	60.506	1.052
61.09	0.463098	1.542866	2.452487	0.006932	0.568745	0	0	0	0.007595	19.755	41.863	0.816
61.09	0.306384	1.676121	2.268584	0.009904	0.711296	0.000342	0.001436	0	0.004557	8.133	63.657	1.176
61.09	0.335438	1.675586	2.323074	0.014855	0.680645	0.000342	0	0.000385	0.007215	9.818	59.989	1.743
61.09	0.434044	1.585144	2.420247	0.009904	0.589179	0.002733	0	0.000769	0.005316	17.18	46.5	1.158
61.73	0.393545	1.609226	2.385283	0.012875	0.620316	0.000683	0	0	0.004937	15.028	51.451	1.513
61.73	0.387382	1.607086	2.38165	0.013865	0.627128	0.000683	0	0	0.005696	14.67	51.855	1.631
61.73	0.390024	1.588355	2.372569	0.019807	0.622749	0.000683	0	0.000385	0.005316	14.083	50.488	2.34
61.73	0.287015	1.694317	2.267222	0.017826	0.710809	0.001025	0.000718	0	0.008734	7.157	65.796	2.11
61.73	0.291417	1.671305	2.271763	0.020797	0.715188	0.001366	0	0	0.007595	7.201	64.059	2.47
61.73	0.399708	1.618324	2.397089	0.013865	0.615451	0.000683	0.001077	0.000385	0.005696	14.932	51.076	1.619
61.73	0.305504	1.679867	2.298554	0.016836	0.706917	0.000342	0	0.000769	0.006456	8.371	63.033	1.986
61.73	0.342481	1.621535	2.311268	0.012875	0.676753	0.001708	0.000718	0	0.007975	10.83	57.233	1.531
61.8	0.368894	1.598523	2.371661	0.024759	0.631993	0	0	0.000385	0.005696	13.561	52.633	2.925
61.8	0.404991	1.55678	2.401176	0.02674	0.591611	0	0	0	0.008354	15.962	47.113	3.168
61.8	0.292298	1.675051	2.276304	0.017826	0.721026	0.001025	0	0	0.008734	7.382	64.206	2.11
61.8	0.257081	1.699668	2.233166	0.024759	0.737082	0.000683	0	0	0.007595	4.655	68.741	2.949
61.8	0.375057	1.607621	2.356676	0.021788	0.64221	0.000683	0.000718	0	0.008734	12.155	52.623	2.571
61.8	0.402349	1.571765	2.408895	0.025749	0.608153	0.001708	0	0	0.006835	15.301	47.877	3.026

Depth (m)	Na2O	Al2O3	SiO2	K2O	[illegible]	[illegible]	2O3	MnO	FeO	Ab	An	Or
61.8	0.44549	1.545007	2.437502	0.013865	0.572151	0.001366	0.000718	0	0.006835	18.731	43.296	1.631
61.8	0.427881	1.557316	2.440227	0.025749	0.577989	0.003074	0.000359	0	0.004557	17.448	44.708	3.02
61.8	0.259722	1.696457	2.225901	0.015846	0.750704	0.000683	0.000359	0	0.006456	4.865	68.895	1.891
61.9	0.378578	1.60548	2.365758	0.023768	0.630533	0.002391	0	0.000385	0.006456	12.944	52.085	2.801
61.9	0.36185	1.616718	2.355768	0.021788	0.647562	0.001708	0	0	0.005696	12.427	54.334	2.571
61.9	0.407632	1.589425	2.415706	0.019807	0.603774	0.000683	0	0	0.005696	15.946	48.552	2.322
61.9	0.31871	1.671305	2.300824	0.016836	0.693295	0.000683	0.000359	0	0.006076	8.925	61.493	1.986
61.9	0.350405	1.642941	2.330339	0.016836	0.672374	0.001025	0	0	0.006076	10.567	56.973	1.98
61.9	0.413795	1.579257	2.409803	0.017826	0.606207	0.00205	0.000359	0.000385	0.006835	15.866	47.631	2.092
61.9	0.150551	0.21781	0.291974	0.004952	0.211151	0.000342	0	0.002308	0.037215	0	0	0
61.9	0.412034	1.585679	2.398451	0.108939	0.518147	0.003074	0	0.001154	0.023924	4.815	42.491	12.694
61.99	0.374176	1.607621	2.358492	0.005942	0.649021	0	0	0.000385	0.006456	14.322	53.766	0.703
61.99	0.3821	1.587285	2.36712	0.015846	0.626155	0	0	0.001154	0.006456	14.596	51.525	1.879
61.99	0.330155	1.626886	2.301732	0.015846	0.680159	0	0.000359	0	0.006076	10.499	58.666	1.885
61.99	0.394426	1.599593	2.358492	0.009904	0.628101	0.001025	0	0	0.005696	14.191	51.327	1.17
61.99	0.367133	1.606015	2.35486	0.024759	0.642696	0	0	0.000769	0.006456	12.073	53.175	2.925
61.99	0.454294	1.526812	2.450671	0.025749	0.560474	0.001708	0	0	0.006076	18.323	40.792	3.026
61.99	0.421719	1.547683	2.432053	0.019807	0.581881	0.00205	0.000718	0	0.006456	18.178	45.306	2.334
61.99	0.352166	1.615648	2.329885	0.020797	0.653886	0.000683	0.000718	0.001538	0.009873	11.22	55.468	2.464
62.08	0.506238	1.494702	2.507885	0.015846	0.517173	0.000683	0	0.000769	0.005696	22.765	34.84	1.856
62.08	0.405871	1.572835	2.373931	0.006932	0.61837	0.000683	0	0	0.005696	15.969	49.14	0.821
62.08	0.381219	1.599593	2.360763	0.014855	0.638804	0.00205	0	0	0.006456	13.596	52.143	1.755
62.08	0.409393	1.553034	2.397997	0.023768	0.606207	0.001366	0	0	0.005696	15.531	46.609	2.813
62.08	0.33896	1.626351	2.322166	0.015846	0.681132	0	0	0.000769	0.006076	10.803	57.472	1.873
62.08	0.396187	1.576046	2.398905	0.030701	0.612045	0.002391	0	0.000769	0.008354	14.044	48.362	3.611
62.08	0.442848	1.524671	2.431145	0.024759	0.569718	0.001366	0	0.001154	0.009494	16.686	41.816	2.913
62.08	0.411154	1.493632	2.361217	0.022778	0.527877	0.000683	0	0.003077	0.069114	14.326	43.744	2.724
62.57	0.345122	1.631168	2.326253	0.011884	0.669455	0.000342	0.001436	0.000385	0.005696	11.825	57.441	1.406
62.57	0.346003	1.634379	2.327161	0.016836	0.660698	0.000683	0	0.000385	0.006456	11.444	57.22	1.992
62.57	0.389143	1.608691	2.362579	0.013865	0.637345	0	0.000718	0.000769	0.006076	13.245	51.843	1.631
62.57	0.353927	1.638125	2.339875	0.012875	0.656805	0.000683	0.000359	0	0.004937	12.336	56.779	1.519
62.57	0.346003	1.626351	2.304003	0.011884	0.67432	0.000683	0	0	0.004557	10.828	57.358	1.412
62.57	0.353927	1.637054	2.33261	0.010894	0.656805	0.001366	0.001436	0.000769	0.005316	12.275	56.927	1.288
62.57	0.390904	1.590496	2.384375	0.014855	0.63102	0.001708	0	0.000385	0.005316	14.742	50.62	1.749
62.57	0.42436	1.561597	2.411166	0.016836	0.589179	0.000342	0.000359	0	0.005696	16.901	46.031	1.986
62.65	0.328395	1.647758	2.314901	0.012875	0.68697	0.001708	0.000718	0	0.004937	10.721	59.706	1.525
62.65	0.33984	1.634379	2.328523	0.016836	0.672374	0	0.000359	0	0.003797	11.298	57.733	1.992
62.65	0.31783	1.648293	2.311722	0.009904	0.687456	0.001025	0.000359	0	0.004177	11.406	61.06	1.176
62.65	0.368894	1.614578	2.358038	0.019807	0.645615	0	0	0.000385	0.004177	12.591	53.691	2.334
62.65	0.346883	1.629027	2.3426	0.017826	0.652427	0.000342	0.000718	0.000385	0.004557	12.428	56.757	2.11
62.65	0.320471	1.650433	2.28811	0.015846	0.689889	0.001366	0.002154	0	0.004937	9.215	60.694	1.885
62.65	0.346883	1.649363	2.328069	0.018817	0.649508	0.000683	0	0.000385	0.003418	11.322	57.772	2.222
62.65	0.336318	1.646152	2.325344	0.016836	0.675293	0.000683	0	0	0.004937	10.74	58.566	1.986
62.78	0.265885	1.6895	2.242702	0.012875	0.746326	0.001025	0.000359	0	0.006076	6.347	68.052	1.531
62.78	0.288776	1.67077	2.265406	0.011884	0.722486	0.000342	0	0	0.005316	8.121	65.006	1.412
62.78	0.264124	1.701274	2.238615	0.015846	0.746812	0.000342	0.001795	0.000385	0.005696	5.412	68.553	1.885
62.78	0.327514	1.654715	2.319896	0.016836	0.689402	0.000342	0	0	0.006076	9.968	59.717	1.986
62.78	0.36097	1.594777	2.345778	0.018817	0.662644	0.001366	0	0	0.004937	12.327	53.62	2.228
62.78	0.320471	1.619929	2.303095	0.019807	0.687456	0.001025	0	0	0.004937	10.285	58.965	2.364
62.78	0.390024	1.58782	2.383467	0.022778	0.619343	0.00205	0	0	0.004937	14.319	50.174	2.683
62.78	0.398828	1.568019	2.396635	0.023768	0.612532	0.001025	0	0.000385	0.006456	15.109	48.273	2.807
62.84	0.302863	1.661137	2.284477	0.019807	0.697673	0	0.000359	0	0.005316	8.645	62.654	2.352

Depth (m)	Na2O	Al2O3	SiO2	K2C			2O3	MnO	FeO	Ab	An	Or
62.84	0.269407	1.686824	2.248605	0.018817	0.732216	0.000683	0	0.000385	0.006835	6.302	67.245	2.24
62.84	0	0.000535	4.51174	0	0	0.001366	0	0	0.001899	0	0	0
62.84	0.36097	1.627957	2.383921	0.022778	0.647562	0.001708	0.001077	0	0.003797	13.193	54.549	2.665
62.84	0.257961	1.703949	2.235891	0.016836	0.733676	0.001708	0.000359	0.001154	0.005316	6.017	69.425	2.009
62.84	0.358329	1.619394	2.335788	0.018817	0.655346	0.00205	0.000718	0	0.005316	11.704	55.138	2.228
62.84	0.393545	1.5723	2.39164	0.025749	0.612045	0	0.001795	0.001154	0.006835	14.688	48.903	3.043
62.84	0.295819	1.645617	2.277212	0.015846	0.70789	0	0.000718	0	0.004557	9.081	62.962	1.891
62.84	0.330155	1.649898	2.31036	0.017826	0.673834	0.001708	0.000359	0	0.004557	10.264	59.466	2.11
62.84	0.259722	1.708231	2.234983	0.017826	0.750704	0	0.001077	0.000385	0.006076	4.685	69.129	2.116
62.84	0.34072	1.573906	2.295375	0.024759	0.638804	0.001366	0	0.001154	0.022785	7.312	54.252	2.949
63.72	0.261483	1.699668	2.222268	0.019807	0.746326	0.001708	0.000718	0.000385	0.005696	4.383	68.686	2.358
63.72	0.257961	1.700739	2.254054	0.015846	0.743406	0.000342	0.000718	0.000769	0.005696	6.513	69.003	1.879
63.72	0.263244	1.682008	2.244518	0.019807	0.745839	0	0.000718	0	0.006076	5.664	67.49	2.358
63.72	0.242114	1.705555	2.205921	0.012875	0.767246	0.000342	0.000359	0	0.006835	4.217	71.401	1.542
63.72	0.250038	1.690035	2.234074	0.015846	0.752164	0.000683	0.001077	0	0.006456	5.839	69.53	1.891
63.72	0.260603	1.694317	2.241794	0.017826	0.747785	0.00205	0	0.000385	0.006835	5.54	68.386	2.116
63.72	0.265885	1.695387	2.241794	0.013865	0.740974	0.000342	0.000359	0	0.006076	6.156	68.302	1.649
63.72	0.260603	1.683613	2.242702	0.017826	0.742433	0.001025	0	0.000385	0.006456	6.104	68.019	2.127
63.72	0.253559	1.694852	2.232712	0.015846	0.753137	0.001708	0	0	0.006456	5.438	69.341	1.885
63.72	0.252679	1.700203	2.234528	0.017826	0.75557	0.00205	0.000718	0	0.006835	5.006	69.436	2.122
63.72	0.241234	1.711442	2.217727	0.013865	0.764327	0.001025	0	0.000769	0.005696	4.596	71.52	1.655
63.72	0.266766	1.686824	2.249967	0.020797	0.74292	0.000342	0	0	0.005316	5.606	67.211	2.47
63.72	0.270287	1.670234	2.2536	0.016836	0.739514	0.00205	0	0	0.006835	6.779	66.401	2.003
63.72	0.231549	1.714653	2.18685	0.014855	0.777463	0.000342	0.000718	0.000769	0.004937	2.833	72.879	1.779
63.72	0.261483	1.693781	2.251329	0.014855	0.741947	0.001025	0	0.000385	0.004937	6.612	68.467	1.767
63.72	0.259722	1.706625	2.239523	0.015846	0.758489	0.000342	0	0	0.006076	4.807	69.023	1.879
63.79	0.240353	1.724286	2.229079	0.018817	0.759462	0.001366	0.000718	0	0.009494	4.3	71.643	2.234
63.79	0.235951	1.731778	2.219998	0.014855	0.760435	0	0.000359	0.000769	0.008354	4.341	72.831	1.767
63.79	0.247396	1.714118	2.242248	0.018817	0.756543	0	0	0	0.006835	4.988	70.398	2.228
63.79	0.232429	1.704485	2.207284	0.016836	0.773084	0.001366	0	0	0.008354	3.867	71.947	2.009
63.79	0.249157	1.711977	2.229988	0.016836	0.759462	0.000683	0	0.000385	0.006456	4.602	70.397	1.997
63.79	0.235951	1.724821	2.224085	0.017826	0.754596	0.000342	0.000718	0	0.007975	4.621	72.37	2.122
63.79	0.245636	1.700739	2.226355	0.023768	0.745353	0.00205	0.000359	0.000385	0.006835	4.583	70.01	2.837
63.79	0.274689	1.682543	2.261319	0.017826	0.720053	0.001366	0	0.000385	0.006076	7.371	66.553	2.122
63.79	0.257081	1.710371	2.243156	0.015846	0.753137	0.000683	0.000359	0.001154	0.006076	5.199	69.456	1.879
63.79	0.242114	1.72375	2.23362	0.016836	0.758975	0.000683	0	0.000385	0.006835	4.669	71.536	1.997
63.79	0.240353	1.721075	2.23362	0.016836	0.752164	0.000683	0	0.000385	0.006835	5.147	71.712	1.997
63.79	0.237712	1.711977	2.229534	0.015846	0.760435	0.001366	0	0.000385	0.007975	5.002	71.599	1.885
63.85	0.197213	1.759071	2.154156	0.015846	0.806654	0	0	0.000385	0.012911	0	78.183	1.835
63.85	0.246516	1.721075	2.224539	0.014855	0.753137	0	0	0.000385	0.007215	4.814	71.361	1.767
63.85	0.219223	1.753184	2.183671	0.011884	0.791086	0	0.000359	0.000385	0.011392	1.785	75.712	1.412
63.85	0.245636	1.731243	2.237707	0.014855	0.751677	0.001708	0.000359	0.000385	0.007595	5.208	71.659	1.761
63.85	0.228027	1.730707	2.2091	0.018817	0.774544	0.001025	0.000718	0.001154	0.006456	3.098	73.286	2.24
63.85	0.250918	1.694852	2.239069	0.018817	0.753623	0.001366	0.001077	0	0.007975	5.352	69.296	2.24
63.85	0.226267	1.737129	2.210916	0.013865	0.775517	0.000342	0	0	0.008734	3.622	74.04	1.649
63.85	0.245636	1.710371	2.234983	0.016836	0.757029	0	0	0	0.007215	5.052	70.661	1.997
63.85	0.247396	1.70502	2.228171	0.017826	0.753623	0.001708	0	0.000769	0.007595	4.858	70.286	2.122
63.85	0.232429	1.718399	2.22136	0.016836	0.778923	0	0	0	0.006076	3.82	72.26	1.997
63.85	0.237712	1.70609	2.218636	0.015846	0.762381	0	0.000718	0.000385	0.008734	4.617	71.514	1.891
63.85	0.235071	1.708766	2.204105	0.015846	0.77503	0	0	0	0.007975	3.468	71.948	1.891
63.85	0.231549	1.709301	2.19911	0.014855	0.769192	0.000342	0	0	0.006835	3.865	72.583	1.779
63.85	0.242114	1.692711	2.218182	0.019807	0.751677	0.001025	0	0	0.006835	4.796	70.383	2.37

Depth (m)	Na2O	Al2O3	SiO2	K2C			2O3	MnO	FeO	Ab	An	Or
63.85	0.242114	1.718399	2.229988	0.016836	0.763354	0.000683	0	0	0.006835	4.462	71.317	1.997
63.85	0.250038	1.707696	2.236799	0.020797	0.746812	0.000342	0.000718	0.000385	0.007215	4.894	69.897	2.47
63.85	0.242994	1.720539	2.230442	0.015846	0.75557	0.002391	0.000359	0.001154	0.007975	4.866	71.433	1.879
63.85	0.281733	1.658461	2.27812	0.022778	0.708863	0.001025	0	0	0.006076	8.237	64.386	2.713
63.93	0.247396	1.703949	2.230442	0.015846	0.760435	0.001025	0	0.000385	0.007975	5.051	70.299	1.885
63.93	0.250038	1.703949	2.224993	0.017826	0.753623	0	0	0.001538	0.008734	4.645	70.04	2.122
63.93	0.247396	1.713047	2.224085	0.012875	0.750218	0.000683	0	0.000769	0.008734	5.341	71.104	1.537
63.93	0.231549	1.715188	2.204105	0.013865	0.764813	0.001708	0	0	0.008354	4.348	72.864	1.661
63.93	0.242994	1.723215	2.226809	0.017826	0.753623	0.000683	0	0	0.005696	4.612	71.567	2.122
63.93	0.249157	1.699668	2.230896	0.016836	0.750218	0	0.000359	0	0.008734	5.321	69.99	2.009
63.93	0.246516	1.694317	2.228625	0.016836	0.742433	0	0.000359	0.001154	0.006456	5.906	70.208	2.015
63.93	0.241234	1.715188	2.216365	0.017826	0.766273	0.000683	0	0	0.009494	3.709	71.342	2.122
63.93	0.235951	1.70502	2.20683	0.012875	0.761408	0.000342	0	0.000385	0.007975	4.766	72.081	1.542
63.93	0.250918	1.701809	2.23135	0.020797	0.746812	0.000683	0.001436	0	0.009114	4.775	69.623	2.476
63.93	0.253559	1.708231	2.21909	0.009904	0.758975	0.000683	0.000359	0	0.007975	4.953	70.426	1.182
64	0.247396	1.700203	2.23135	0.015846	0.758975	0.001366	0.001077	0	0.010253	5.156	70.11	1.885
64	0.235951	1.714118	2.207284	0.012875	0.76676	0.000683	0	0.000385	0.007975	4.339	72.371	1.537
64	0.23331	1.735524	2.21137	0.015846	0.762867	0.001025	0	0.000385	0.007595	3.804	73.278	1.885
64	0.240353	1.711977	2.225447	0.017826	0.764813	0	0.000718	0	0.008734	4.297	71.212	2.122
64	0.243875	1.700739	2.218182	0.012875	0.753623	0.001366	0.001077	0.000385	0.009873	5.367	70.98	1.537
64	0.250918	1.682008	2.24134	0.017826	0.751191	0.001025	0.000359	0.000385	0.009494	5.973	68.823	2.127
64	0.238592	1.708231	2.210916	0.015846	0.76384	0.000342	0.000718	0	0.009114	4.176	71.605	1.891
64	0.250918	1.691106	2.214549	0.018817	0.75265	0.000683	0.000718	0	0.010633	4.323	69.47	2.252
64	0.228908	1.717328	2.196386	0.014855	0.780382	0.001025	0.000718	0.000769	0.007975	3.106	73.037	1.773
64	0.246516	1.700739	2.227717	0.017826	0.751191	0	0.001077	0	0.009114	5.071	70.264	2.127
64	0.243875	1.725891	2.213187	0.015846	0.7653	0.001366	0.001436	0	0.008354	3.567	71.711	1.879
64	0.237712	1.711442	2.209554	0.012875	0.76384	0.000683	0.001436	0.000385	0.008354	4.471	72.061	1.537
64	0.23419	1.716793	2.208192	0.012875	0.768219	0.000683	0	0	0.004937	4.354	72.66	1.537
64.12	0.239473	1.708766	2.218636	0.016836	0.773084	0	0.000718	0.001154	0.007215	3.934	71.244	2.003
64.12	0.249157	1.714118	2.232712	0.018817	0.752164	0.001708	0	0	0.007975	4.724	70.373	2.234
64.12	0.232429	1.732313	2.22136	0.013865	0.778436	0.001708	0.000718	0	0.008734	3.886	72.99	1.643
64.12	0.242994	1.694852	2.209554	0.015846	0.771138	0.001708	0.001077	0	0.008354	4.006	70.507	1.891
64.12	0.253559	1.690035	2.238615	0.016836	0.757516	0.00205	0.001077	0	0.008734	5.433	68.902	2.003
64.12	0.228027	1.729102	2.21909	0.013865	0.78768	0.003074	0.000718	0	0.008354	3.684	73.209	1.643
64.12	0.251799	1.708231	2.214095	0.016836	0.758002	0.000342	0.000359	0	0.006456	3.976	70.219	2.009
64.12	0.241234	1.692176	2.205467	0.013865	0.762867	0.001025	0	0	0.007595	4.667	70.924	1.661
64.12	0.252679	1.691641	2.214549	0.014855	0.756543	0.000683	0	0.000385	0.007595	4.658	69.573	1.779
64.12	0.248277	1.702879	2.255416	0.013865	0.754596	0.001025	0.001436	0	0.008734	6.517	70.004	1.643
64.12	0.259722	1.688965	2.24588	0.016836	0.739028	0	0.000359	0	0.009114	6.273	68.383	2.003
64.12	0.246516	1.715188	2.235891	0.015846	0.744866	0	0.000359	0	0.008734	5.542	70.964	1.885

APPENDIX II: Major Element Data of Clinopyroxene

Depth (m)	Na2O	MgO	Al2O3	SiO2	K2O	CaO	TiO2	Cr2O3	FeO	Cr/Al	Na/Ca	Mg#	En	Wo	Fs
57.2	0.002563	0.791992	0.02671	1.037984	0	0.057671	0.001847	0.008362	0.180216	0.313061	0.044446	1.180216	76.90141	5.599804	17.49878
57.2	0.001099	0.806632	0.020033	1.014943	0.000824	0.014165	0.001705	0.005674	0.187956	0.283245	0.077555	1.187956	79.96332	1.404196	18.63249
57.2	0.001465	0.810574	0.026042	1.048371	0	0.03784	0.001705	0.006719	0.185902	0.258017	0.038708	1.185902	78.36805	3.658494	17.97345
57.2	0.000366	0.823244	0.021368	1.047805	0	0.016391	0.001421	0.00657	0.190799	0.30747	0.022341	1.190799	79.89297	1.590668	18.51637
57.2	0.000732	0.824088	0.024039	1.047994	0	0.016391	0.001421	0.007167	0.188588	0.298153	0.044682	1.188588	80.08114	1.592781	18.32608
57.2	0.000366	0.824088	0.025375	1.038551	0	0.01457	0.001563	0.005973	0.193168	0.235384	0.025133	1.193168	79.86699	1.412019	18.72099
57.2	0.000366	0.827467	0.025375	1.046483	0	0.018212	0.001847	0.006122	0.192852	0.241269	0.020107	1.192852	79.67667	1.753628	18.5697
57.2	0.000732	0.827748	0.025375	1.044783	0	0.014772	0.002131	0.007018	0.193484	0.276576	0.049578	1.193484	79.89817	1.425856	18.67597
57.2	0.000732	0.829156	0.025375	1.047049	0.000412	0.015986	0.002131	0.006271	0.191115	0.247153	0.045813	1.191115	80.01454	1.542674	18.44279
57.2	0.000366	0.830845	0.022481	1.043272	0	0.014165	0.001705	0.006271	0.190799	0.278965	0.025852	1.190799	80.21222	1.367517	18.42027
57.2	0.000366	0.835632	0.019142	1.045916	0	0.011332	0.002273	0.005973	0.192536	0.312021	0.032314	1.192536	80.38787	1.090129	18.522
57.2	0.000366	0.844923	0.01981	1.054604	0	0.012546	0.001847	0.005525	0.193642	0.27889	0.029187	1.193642	80.38381	1.193597	18.42259
57.51	0.014647	0.441466	0.029381	1.006444	0	0.460358	0.005541	0.010452	0.077709	0.355751	0.031817	1.077709	45.06899	46.9977	7.933312
57.51	0.016844	0.444844	0.040733	0.988125	0.000824	0.433243	0.004973	0.012244	0.085133	0.300597	0.03888	1.085133	46.18306	44.97857	8.838367
57.51	0.016112	0.445689	0.041846	0.999267	0.000824	0.4468	0.005967	0.013737	0.078183	0.328286	0.036061	1.078183	45.91548	46.02997	8.054546
57.51	0.014281	0.449068	0.028713	1.008899	0	0.460358	0.005967	0.009855	0.076288	0.343223	0.031022	1.076288	45.55761	46.70303	7.73936
57.51	0.016844	0.449349	0.03962	1.000401	0.000824	0.449229	0.005541	0.013439	0.080552	0.339191	0.037496	1.080552	45.89269	45.88037	8.226941
57.51	0.01538	0.471873	0.040065	1.000212	0	0.403901	0.00611	0.012394	0.096821	0.309334	0.038078	1.096821	48.5169	41.52819	9.954907
57.59	0.012816	0.430767	0.022704	1.001156	0	0.470678	0.003552	0.01538	0.077236	0.677422	0.02723	1.077236	44.01507	48.09313	7.891807
57.59	0.013549	0.443437	0.028713	1.0038	0	0.459751	0.004547	0.01105	0.076288	0.384826	0.02947	1.076288	45.27286	46.93849	7.78865
57.59	0.015014	0.450475	0.032497	1.004744	0.000824	0.442146	0.005541	0.010303	0.083395	0.317043	0.033956	1.083395	46.15446	45.30107	8.544472
57.59	0.016478	0.450757	0.035168	0.998134	0	0.446598	0.005541	0.012394	0.080868	0.352406	0.036897	1.080868	46.07914	45.65399	8.266862
57.59	0.01538	0.454135	0.047188	0.984914	0.000824	0.423934	0.005257	0.01538	0.091135	0.325929	0.036279	1.091135	46.85652	43.74043	9.403057
57.59	0.013915	0.467087	0.029159	1.004933	0	0.433243	0.004262	0.01105	0.08766	0.37895	0.032118	1.08766	47.27649	43.85094	8.872571
57.59	0.014281	0.483135	0.042291	1.001912	0.000412	0.387713	0.004831	0.013737	0.106772	0.32483	0.036834	1.106772	49.41954	39.65887	10.92159
57.65	0.015014	0.43668	0.032052	0.997379	0	0.47169	0.005541	0.011647	0.072181	0.363374	0.031829	1.072181	44.5341	48.10459	7.361304
57.65	0.014281	0.438087	0.029826	1.001345	0	0.466226	0.004405	0.0109	0.074551	0.36546	0.030631	1.074551	44.75465	47.62933	7.616023
57.65	0.016112	0.440903	0.037617	0.994924	0.000412	0.45368	0.005683	0.01314	0.08308	0.349316	0.035514	1.08308	45.09763	46.40459	8.497778

Depth (m)	Na2O	MgO	Al2O3	SiO2	K2O	CaO	TiO2	Cr2O3	FeO	Cr/Al	Na/Ca	Mg#	En	Wo	Fs
57.65	0.016478	0.463427	0.039397	0.997945	0	0.418268	0.005825	0.014185	0.091767	0.360058	0.039396	1.091767	47.60605	42.96711	9.426839
57.65	0.016112	0.474407	0.040065	0.992657	0	0.385689	0.005825	0.013588	0.105192	0.339149	0.041775	1.105192	49.14667	39.95586	10.89748
58.12	0.016478	0.423728	0.042514	0.992846	0.000412	0.468048	0.004689	0.01538	0.076446	0.361764	0.035206	1.076446	43.76356	48.34095	7.895491
58.12	0.013549	0.426262	0.030272	0.993413	0	0.476749	0.003694	0.011647	0.068707	0.384749	0.028419	1.068707	43.86688	49.06249	7.070625
58.12	0.015014	0.427107	0.034946	0.994168	0.000824	0.467845	0.005541	0.012095	0.076604	0.346105	0.032091	1.076604	43.96112	48.15422	7.884653
58.12	0.016478	0.429359	0.034946	0.997379	0	0.454895	0.006252	0.012543	0.080395	0.358923	0.036224	1.080395	44.50941	47.15651	8.334076
58.12	0.015014	0.430486	0.032943	0.995301	0	0.464405	0.005683	0.011796	0.07613	0.358086	0.032328	1.07613	44.3333	47.8265	7.840202
58.12	0.014281	0.432738	0.030717	1.001156	0.00206	0.465215	0.006394	0.011647	0.076604	0.379173	0.030698	1.076604	44.40358	47.73604	7.860379
58.12	0.011718	0.439213	0.022926	1.007388	0	0.478368	0.003268	0.00657	0.069338	0.286574	0.024496	1.069338	44.50347	48.4708	7.02573
58.54	0.015746	0.430767	0.044294	0.990391	0.000824	0.451252	0.005115	0.015977	0.0815	0.360705	0.034894	1.0815	44.70767	46.83374	8.45859
58.54	0.015014	0.432175	0.034723	0.986425	0.000824	0.450847	0.004831	0.01314	0.085291	0.378425	0.033301	1.085291	44.63172	46.56009	8.80819
58.54	0.012816	0.437524	0.027378	0.998512	0.000412	0.466631	0.004689	0.010303	0.080237	0.376327	0.027466	1.080237	44.44614	47.40299	8.150878
58.54	0.013183	0.438932	0.02582	1.000778	0	0.471488	0.005257	0.00881	0.074866	0.341205	0.02796	1.074866	44.54868	47.85287	7.598445
58.54	0.016112	0.439777	0.040733	0.990958	0	0.42272	0.005967	0.014335	0.090187	0.351918	0.038115	1.090187	46.16186	44.3715	9.466643
58.54	0.012084	0.440621	0.028268	1.0021	0	0.468655	0.004973	0.010751	0.075498	0.380321	0.025785	1.075498	44.74338	47.59007	7.66655
58.54	0.01245	0.441747	0.022036	1.007388	0.000412	0.474118	0.002984	0.007615	0.072181	0.345587	0.02626	1.072181	44.70915	47.9854	7.305455
58.54	0.014647	0.442029	0.035168	0.999645	0	0.4468	0.006394	0.012244	0.083395	0.34816	0.032783	1.083395	45.46571	45.95649	8.5778
58.6	0.015014	0.426825	0.042068	0.992468	0.000824	0.458537	0.005683	0.015081	0.082922	0.358494	0.032742	1.082922	44.0806	47.35563	8.563775
58.6	0.015014	0.430204	0.035614	0.989069	0	0.465619	0.006536	0.011796	0.074866	0.33123	0.032244	1.074866	44.31941	47.96789	7.712703
58.6	0.016112	0.431612	0.042291	0.990013	0	0.460763	0.005825	0.015081	0.081026	0.356607	0.034968	1.081026	44.34059	47.33537	8.324043
58.6	0.011352	0.451883	0.024484	1.002856	0	0.460358	0.004689	0.008661	0.079605	0.353718	0.024658	1.079605	45.5598	46.41428	8.025923
58.6	0.013549	0.458359	0.040733	0.986614	0	0.418471	0.004405	0.014185	0.096031	0.348253	0.032377	1.096031	47.11453	43.01445	9.871013
58.6	0.013549	0.462582	0.041623	1.001156	0	0.40552	0.005967	0.014036	0.100454	0.337216	0.033411	1.100454	47.75998	41.86853	10.37149
58.6	0.009521	0.476941	0.022481	1.024008	0.001648	0.297867	0.008667	0.007466	0.132517	0.332101	0.031963	1.132517	52.56563	32.82915	14.60522
58.67	0.015014	0.42767	0.033833	0.99889	0	0.472095	0.00611	0.011796	0.072655	0.348663	0.031802	1.072655	43.97997	48.54844	7.471584
58.67	0.014281	0.432175	0.028936	0.999645	0	0.469464	0.005399	0.0109	0.075656	0.376705	0.03042	1.075656	44.22153	48.03709	7.741382
58.67	0.013183	0.43668	0.028713	1.003234	0.000412	0.468048	0.004547	0.010452	0.074235	0.364024	0.028165	1.074235	44.60639	47.81061	7.582996
58.67	0.012816	0.439777	0.027378	0.996435	0.000412	0.468655	0.004689	0.010004	0.078815	0.365419	0.027347	1.078815	44.54578	47.4709	7.983323
58.67	0.014647	0.441747	0.033165	0.99549	0	0.445789	0.005683	0.011498	0.08308	0.346678	0.032857	1.08308	45.51209	45.92844	8.559476
59.27	0.01538	0.428233	0.039175	0.996057	0.000412	0.467643	0.005541	0.015828	0.075182	0.404031	0.032888	1.075182	44.09963	48.15807	7.742306
59.27	0.014647	0.430767	0.038952	0.995679	0.000412	0.467441	0.006394	0.013588	0.075024	0.348839	0.031335	1.075024	44.2615	48.02972	7.708785
59.27	0.015014	0.438087	0.035168	0.997379	0	0.462382	0.005825	0.01314	0.077867	0.373635	0.03247	1.077867	44.7788	47.26204	7.959163

Depth (m)	Na2O	MgO	Al2O3	SiO2	K2O	CaO	TiO2	Cr2O3	FeO	Cr/Al	Na/Ca	Mg#	En	Wo	Fs
59.27	0.015014	0.43865	0.03361	1.003045	0.000824	0.468452	0.005399	0.012841	0.070602	0.38207	0.032049	1.070602	44.86533	47.91349	7.221187
59.27	0.013915	0.439495	0.030272	0.999079	0	0.455502	0.005399	0.011647	0.08229	0.384749	0.030549	1.08229	44.97095	46.60881	8.420241
59.27	0.013183	0.44231	0.027378	1.004933	0	0.472095	0.005115	0.008959	0.071707	0.327241	0.027924	1.071707	44.85395	47.87432	7.271734
59.27	0.010253	0.549017	0.045185	1.033263	0.000412	0.289166	0.00341	0.010751	0.080079	0.237935	0.035458	1.080079	59.78875	31.49057	8.720682
59.27	0.002563	0.724984	0.01981	1.042517	0.001236	0.063135	0.002273	0.004778	0.220177	0.241203	0.0406	1.220177	71.90192	6.261541	21.83653
59.33	0.013915	0.434427	0.029826	0.997001	0	0.465619	0.005115	0.010303	0.07534	0.345435	0.029885	1.07534	44.53896	47.7369	7.724141
59.33	0.013915	0.436961	0.030049	0.999645	0.000824	0.459144	0.005683	0.011647	0.07613	0.387599	0.030306	1.07613	44.94397	47.22562	7.830409
59.33	0.013183	0.463427	0.035614	0.99719	0	0.423934	0.005399	0.012244	0.092398	0.343808	0.031096	1.092398	47.30005	43.26923	9.430728
59.33	0.001099	0.768905	0.021146	1.031563	0.000824	0.048768	0.003126	0.00657	0.201697	0.310707	0.022526	1.201697	75.42946	4.784094	19.78645
59.39	0.013549	0.431893	0.031384	0.999079	0	0.473916	0.005115	0.010602	0.073129	0.337801	0.028589	1.073129	44.11854	48.41122	7.470238
59.39	0.013549	0.442874	0.030049	0.991713	0	0.458739	0.005683	0.010602	0.076288	0.352815	0.029535	1.076288	45.28819	46.91062	7.801193
59.44	0.014647	0.427388	0.047411	0.971882	0	0.459549	0.006252	0.014633	0.085133	0.308652	0.031873	1.085133	43.96684	47.27526	8.757898
59.44	0.014647	0.432175	0.032497	1.004556	0.000412	0.476749	0.003836	0.012244	0.068391	0.376776	0.030723	1.068391	44.22065	48.78153	6.997813
59.44	0.013915	0.437243	0.032052	0.999834	0.000412	0.466226	0.005683	0.011647	0.076288	0.363374	0.029846	1.076288	44.62766	47.58593	7.786413
59.44	0.014647	0.43865	0.030939	0.999079	0	0.464405	0.005541	0.012244	0.075814	0.39575	0.03154	1.075814	44.81193	47.44301	7.745065
59.44	0.013549	0.440903	0.029826	1.003045	0	0.470071	0.004831	0.012244	0.073129	0.410517	0.028823	1.073129	44.8025	47.76647	7.431032
59.44	0.012084	0.484824	0.039175	0.994546	0	0.379821	0.005399	0.012991	0.109299	0.331611	0.031815	1.109299	49.77949	38.99823	11.22228
59.44	0.002197	0.76243	0.020478	1.043461	0	0.053826	0.0027	0.006421	0.203119	0.313547	0.040818	1.203119	74.79385	5.280344	19.9258
60.54	0.013183	0.429922	0.032275	1.000967	0	0.475737	0.005399	0.011199	0.071865	0.346989	0.02771	1.071865	43.98071	48.66752	7.351775
60.54	0.014281	0.430767	0.03361	0.993224	0	0.471488	0.004262	0.01314	0.072339	0.390956	0.03029	1.072339	44.19964	48.37786	7.422504
60.54	0.015014	0.43499	0.038507	0.994546	0	0.466834	0.005541	0.013737	0.074077	0.35675	0.03216	1.074077	44.57322	47.83618	7.590598
60.54	0.012084	0.435553	0.029381	1.001345	0.000412	0.474321	0.005257	0.009855	0.070128	0.335422	0.025477	1.070128	44.44413	48.39997	7.155907
60.54	0.013915	0.435835	0.029604	0.997757	0.000412	0.472297	0.005399	0.010154	0.071865	0.342988	0.029462	1.071865	44.47307	48.19371	7.333227
60.54	0.012816	0.446815	0.030939	1.0038	0	0.460763	0.005257	0.011199	0.078025	0.361967	0.027816	1.078025	45.33418	46.74932	7.916504
60.54	0.01245	0.494678	0.039397	1.003045	0	0.383261	0.005399	0.013289	0.108983	0.337317	0.032485	1.108983	50.12335	38.83396	11.04269
60.54	0.008056	0.612083	0.03272	1.021175	0	0.252135	0.003552	0.01105	0.147206	0.337704	0.031951	1.147206	60.51701	24.92868	14.55431
60.59	0.015746	0.425136	0.039397	0.994735	0	0.46825	0.005399	0.01314	0.075814	0.333527	0.033627	1.075814	43.86463	48.31303	7.822335
60.59	0.014647	0.429359	0.035391	0.992091	0	0.481605	0.005825	0.013588	0.070918	0.383943	0.030414	1.070918	43.72818	49.04919	7.222632
60.59	0.014281	0.435835	0.035168	1.000589	0	0.467238	0.004831	0.01314	0.072497	0.373635	0.030565	1.072497	44.67488	47.89385	7.431266
60.59	0.012816	0.43865	0.028713	1.002478	0	0.482213	0.004689	0.012244	0.065706	0.426428	0.026578	1.065706	44.46224	48.87776	6.660009
60.59	0.01538	0.443155	0.038952	0.99719	0.000412	0.456918	0.005683	0.014484	0.075656	0.37184	0.03366	1.075656	45.41783	46.82836	7.753804
60.59	0.013915	0.443718	0.030494	1.000401	0	0.465215	0.005257	0.011498	0.073287	0.377044	0.029911	1.073287	45.17504	47.3636	7.46136

Depth (m)	Na2O	MgO	Al2O3	SiO2	K2O	CaO	TiO2	Cr2O3	FeO	Cr/Al	Na/Ca	Mg#	En	Wo	Fs
60.59	0.010253	0.507911	0.027155	1.017587	0	0.390343	0.00412	0.009109	0.106929	0.335422	0.026267	1.106929	50.52917	38.83303	10.6378
60.61	0.013549	0.430204	0.028046	0.997945	0	0.473511	0.005257	0.010303	0.075024	0.367367	0.028613	1.075024	43.9549	48.3797	7.665406
60.61	0.013915	0.433019	0.040288	0.997757	0	0.467238	0.005967	0.014036	0.075656	0.348394	0.029781	1.075656	44.37066	47.877	7.752339
60.61	0.013915	0.434146	0.03272	0.996057	0	0.46825	0.005257	0.012543	0.075024	0.38334	0.029717	1.075024	44.41751	47.90673	7.675755
60.61	0.013915	0.439495	0.034501	1.001345	0	0.473714	0.005825	0.013588	0.074235	0.393851	0.029374	1.074235	44.50838	47.97375	7.517863
60.61	0.013915	0.452728	0.043404	1.001156	0	0.43648	0.005825	0.013588	0.087344	0.313061	0.03188	1.087344	46.35981	44.69605	8.944136
60.61	0.012816	0.475251	0.037394	0.997757	0.000412	0.415031	0.004831	0.014932	0.098874	0.399312	0.030881	1.098874	48.04615	41.95804	9.995813
60.68	0.012816	0.437243	0.028268	1.000589	0	0.475332	0.004831	0.011498	0.06918	0.406733	0.026963	1.06918	44.53682	48.41658	7.046598
60.68	0.013183	0.451602	0.032943	1.000212	0	0.458335	0.004262	0.011498	0.073603	0.349021	0.028762	1.073603	45.91598	46.60055	7.48347
60.68	0.009887	0.487358	0.024484	1.015887	0	0.410579	0.004831	0.007765	0.096821	0.317127	0.024081	1.096821	48.99264	41.27425	9.733115
60.68	0.009887	0.546201	0.027823	1.002856	0	0.334493	0.003978	0.010452	0.09382	0.375673	0.029558	1.09382	56.04856	34.32409	9.627352
60.68	0.012816	0.437243	0.028268	1.000589	0	0.475332	0.004831	0.011498	0.06918	0.406733	0.026963	1.06918	44.53682	48.41658	7.046598
60.68	0.013183	0.451602	0.032943	1.000212	0	0.458335	0.004262	0.011498	0.073603	0.349021	0.028762	1.073603	45.91598	46.60055	7.48347
60.68	0.009887	0.487358	0.024484	1.015887	0	0.410579	0.004831	0.007765	0.096821	0.317127	0.024081	1.096821	48.99264	41.27425	9.733115
60.68	0.009887	0.546201	0.027823	1.002856	0	0.334493	0.003978	0.010452	0.09382	0.375673	0.029558	1.09382	56.04856	34.32409	9.627352
61.09	0.043576	0.479193	0.130212	0.94582	0.018536	0.246671	0.018613	0.018366	0.115932	0.141049	0.176656	1.115932	56.92506	29.30293	13.77202
61.09	0.050167	0.486513	0.161819	0.921079	0.022655	0.252337	0.022733	0.022697	0.09303	0.140259	0.19881	1.09303	58.48356	30.33332	11.18312
61.09	0.051266	0.491018	0.161819	0.917113	0.025126	0.25092	0.023302	0.023294	0.089555	0.14395	0.20431	1.089555	59.05252	30.17706	10.77042
61.09	0.051266	0.492426	0.161151	0.919568	0.027186	0.248088	0.025717	0.02195	0.091925	0.136207	0.206644	1.091925	59.15466	29.80252	11.04282
61.09	0.051632	0.500309	0.158925	0.925422	0.023479	0.248088	0.024296	0.020158	0.089555	0.12684	0.20812	1.089555	59.70618	29.60641	10.68741
61.09	0.049801	0.500872	0.15069	0.927689	0.023891	0.248695	0.022449	0.020755	0.087186	0.137736	0.200249	1.087186	59.85903	29.72138	10.41959
61.09	0.047238	0.506503	0.146906	0.938454	0.020184	0.249504	0.019323	0.021801	0.087028	0.148399	0.189326	1.087028	60.08089	29.59591	10.3232
61.09	0.038815	0.527056	0.121976	0.966217	0.016064	0.250516	0.016055	0.018516	0.077551	0.151797	0.154942	1.077551	61.6351	29.29586	9.069041
61.13	0.008056	0.486795	0.0276	1.051016	0.001236	0.245457	0.001279	0.00448	0.140414	0.162301	0.032821	1.140414	55.78251	28.12725	16.09024
61.13	0.008056	0.500028	0.029159	1.057626	0.000412	0.238982	0.000426	0.005525	0.122408	0.189475	0.03371	1.122408	58.04708	27.74283	14.21009
61.13	0.008788	0.504532	0.028268	1.055737	0.000412	0.227043	0.000995	0.004778	0.127304	0.169032	0.038708	1.127304	58.7431	26.43474	14.82216
61.13	0.009887	0.512979	0.049636	1.021553	0	0.229471	0.001137	0.006869	0.122092	0.138381	0.043086	1.122092	59.33533	26.54248	14.12219
61.13	0.007324	0.515231	0.032497	1.069713	0.000824	0.236149	0.001137	0.007466	0.125409	0.229741	0.031013	1.125409	58.76343	26.93334	14.30323
61.13	0.012084	0.5569	0.037839	1.081611	0	0.231292	0.001421	0.00657	0.105508	0.17363	0.052246	1.105508	62.31398	25.88027	11.80574
61.13	0.005859	0.633481	0.111515	0.944498	0.000824	0.104415	0.000284	0.009109	0.131727	0.08168	0.056112	1.131727	72.84545	12.00696	15.14759
61.13	0.005127	0.644461	0.164713	0.876885	0.001648	0.093083	0.000568	0.011498	0.142941	0.069804	0.055075	1.142941	73.19383	10.57182	16.23435
61.73	0.030027	0.502562	0.127318	0.955829	0.019772	0.25173	0.009662	0.018964	0.100928	0.148946	0.119283	1.100928	58.76408	29.43456	11.80136

Depth (m)	Na2O	MgO	Al2O3	SiO2	K2O	CaO	TiO2	Cr2O3	FeO	Cr/Al	Na/Ca	Mg#	En	Wo	Fs
61.73	0.029295	0.502843	0.131325	0.961684	0.018948	0.252135	0.012361	0.017172	0.099348	0.130758	0.116187	1.099348	58.85847	29.5127	11.62882
61.73	0.026731	0.509037	0.12487	0.962628	0.0173	0.252135	0.008951	0.019113	0.099506	0.153063	0.10602	1.099506	59.14376	29.29489	11.56135
61.73	0.026365	0.509882	0.120418	0.963384	0.019772	0.253551	0.011367	0.018814	0.097453	0.156241	0.103984	1.097453	59.22759	29.45236	11.32005
61.73	0.025633	0.517484	0.119305	0.980381	0.006179	0.2406	0.005683	0.014783	0.100454	0.123906	0.106537	1.100454	60.275	28.02444	11.70056
61.73	0.023436	0.517765	0.107286	0.979437	0.007414	0.243433	0.006252	0.014036	0.097927	0.130829	0.096272	1.097927	60.26656	28.33503	11.3984
61.73	0.001099	0.783546	0.033833	1.038362	0.000412	0.030556	0.001989	0.008063	0.205172	0.238326	0.035952	1.205172	76.87298	2.997787	20.12924
61.8	0.013549	0.43133	0.030717	1.000589	0	0.476749	0.004831	0.010452	0.074551	0.340283	0.028419	1.074551	43.8955	48.51766	7.586839
61.8	0.009887	0.499465	0.308057	0.733917	0.352182	0	0.07502	0.025534	0.127936	0.082886	#DIV/0!	1.127936	79.60853	0	20.39147
61.8	0.02783	0.508756	0.121976	0.960362	0.016476	0.253551	0.016197	0.017172	0.091609	0.140779	0.109761	1.091609	59.57916	29.69277	10.72808
61.9	0.01538	0.433301	0.038285	1.000401	0.000412	0.459549	0.005967	0.011199	0.082764	0.292519	0.033467	1.082764	44.41318	47.10357	8.483249
61.9	0.014647	0.438369	0.033165	1.003045	0	0.466834	0.005825	0.01105	0.076446	0.333171	0.031376	1.076446	44.65641	47.55609	7.787502
61.9	0.013183	0.455825	0.037617	1.0038	0.000824	0.447003	0.005257	0.009556	0.081974	0.254048	0.029491	1.081974	46.28595	45.39013	8.32391
61.9	0.009155	0.485387	0.301157	0.718808	0.374837	0.000809	0.079993	0.024339	0.126199	0.080819	11.31004	1.126199	79.26041	0.132173	20.60741
61.9	0.000366	0.802128	0.019587	1.045161	0.000412	0.015177	0.00341	0.004181	0.212437	0.213451	0.024128	1.212437	77.89601	1.47383	20.63016
61.9	0.000366	0.803254	0.018252	1.045916	0	0.012748	0.002273	0.00433	0.213859	0.23725	0.028724	1.213859	77.99633	1.237874	20.7658
61.99	0.014281	0.435272	0.034278	0.993224	0.000412	0.470071	0.005115	0.0109	0.074866	0.317998	0.030381	1.074866	44.406	47.9562	7.637798
61.99	0.022337	0.506785	0.111737	0.976604	0.013593	0.250718	0.010088	0.016724	0.095873	0.149671	0.089093	1.095873	59.38586	29.37956	11.23458
61.99	0.021971	0.51692	0.10595	0.982459	0.013181	0.252135	0.007388	0.013737	0.091767	0.129659	0.08714	1.091767	60.04965	29.28999	10.66035
61.99	0.025633	0.519736	0.119528	0.976037	0.005767	0.2406	0.007957	0.015828	0.097453	0.13242	0.106537	1.097453	60.59018	28.0489	11.36092
61.99	0.008788	0.571822	0.043849	1.051393	0.003707	0.249099	0.001421	0.006869	0.081342	0.156644	0.035281	1.081342	63.37639	27.60826	9.015347
61.99	0.006957	0.574638	0.039397	1.055171	0.001648	0.248695	0.003694	0.00881	0.074393	0.223615	0.027976	1.074393	64.01044	27.70276	8.286791
62.08	0.014647	0.418942	0.047856	0.984158	0	0.466834	0.004547	0.011796	0.080552	0.246496	0.031376	1.080552	43.35402	48.31004	8.335934
62.08	0.01538	0.42401	0.046965	0.974527	0.000412	0.459144	0.004547	0.015977	0.08229	0.340191	0.033496	1.08229	43.91865	47.55782	8.523528
62.08	0.017577	0.424291	0.049191	0.985669	0	0.465012	0.003978	0.014185	0.079289	0.288372	0.037799	1.079289	43.80494	48.00907	8.18599
62.08	0.016112	0.44034	0.04652	0.984158	0	0.438908	0.003836	0.014932	0.085923	0.320978	0.036709	1.085923	45.62298	45.4747	8.902325
62.08	0.013549	0.445126	0.048746	0.985858	0	0.435064	0.003836	0.015828	0.092083	0.324701	0.031142	1.092083	45.78203	44.74711	9.470859
62.08	0.013183	0.485669	0.044072	0.999834	0	0.370512	0.005115	0.013289	0.112616	0.301541	0.035579	1.112616	50.13113	38.2446	11.62427
62.08	0.011718	0.566473	0.061879	1.033829	0.004119	0.253956	0.003694	0.008661	0.076604	0.13996	0.046141	1.076604	63.14964	28.31066	8.539694
63.85	0.000732	0.808603	0.02582	1.044783	0	0.01376	0.002984	0.005823	0.193484	0.225543	0.053224	1.193484	79.5989	1.35455	19.04655
63.93	0.011352	0.435835	0.030939	0.99889	0	0.471285	0.003836	0.011348	0.070286	0.366793	0.024087	1.070286	44.59097	48.21796	7.191072
63.93	0.011718	0.437524	0.03272	0.995301	0	0.468655	0.004262	0.011498	0.069812	0.351395	0.025003	1.069812	44.82871	48.01834	7.152949
63.93	0.010253	0.690353	0.073676	1.03043	0.001648	0.012141	0	0.00433	0.087818	0.058775	0.844483	1.087818	87.35193	1.536267	11.1118

Depth (m)	Na2O	MgO	Al2O3	SiO2	K2O	CaO	TiO2	Cr2O3	FeO	Cr/Al	Na/Ca	Mg#	En	Wo	Fs
63.93	0.015014	0.697955	0.057427	1.083689	0.006179	0.012546	0.000995	0.007914	0.090187	0.137809	1.196675	1.090187	87.16939	1.566905	11.2637
63.93	0.013915	0.721605	0.047188	1.122783	0.002883	0.008701	0.001137	0.007317	0.089082	0.155054	1.599187	1.089082	88.06636	1.061924	10.87172
64	0.011352	0.434146	0.028046	1.002667	0	0.483224	0.003552	0.010751	0.064284	0.38334	0.023492	1.064284	44.22593	49.22552	6.548543
64	0.012084	0.435272	0.031162	0.993413	0.000412	0.471285	0.003694	0.011199	0.074866	0.359381	0.025641	1.074866	44.35107	48.02058	7.628349
64	0.011352	0.437243	0.033388	0.994735	0.000412	0.469869	0.00412	0.01105	0.072813	0.33095	0.024159	1.072813	44.62003	47.94949	7.430482
64	0.013183	0.440058	0.034055	0.994168	0	0.470274	0.003694	0.012244	0.072813	0.359538	0.028032	1.072813	44.76026	47.8336	7.406144
64	0.010619	0.445971	0.028713	1.001912	0.000824	0.478165	0.003694	0.011348	0.062073	0.395226	0.022208	1.062073	45.22071	48.48521	6.294082
64.12	0.01245	0.426825	0.034723	0.992468	0.000412	0.470881	0.003694	0.012692	0.080079	0.365524	0.02644	1.080079	43.65229	48.15791	8.189803
64.12	0.01245	0.434709	0.03361	1.000589	0.000824	0.471083	0.003836	0.012244	0.076446	0.3643	0.026429	1.076446	44.25698	47.96019	7.78283
64.12	0.000366	0.791147	0.017139	1.045539	0	0.012748	0.001563	0.005376	0.21149	0.313642	0.028724	1.21149	77.91596	1.255521	20.82852
64.12	0.000732	0.795934	0.020033	1.047427	0	0.013355	0.002557	0.005674	0.210226	0.283245	0.054837	1.210226	78.06981	1.30998	20.62021
64.12	0	0.814234	0.019587	1.057626	0	0.016391	0.001705	0.005226	0.195221	0.266813	0	1.195221	79.37195	1.597781	19.03027

APPENDIX III: Major Element Data of Orthopyroxene

Depth	Na2O	MgO	Al2O3	SiO2	K2O	CaO	TiO2	Cr2O3	FeO	Cr/Al	Al/Si	Mg#	En	Wo	Fs
57.2	0.000722	0.810561	0.022604	1.034379	0.000812	0.015163	0.002241	0.00633	0.192477	0.280061	0.021853	1.192477	79.60718	1.489177	18.90364
57.2	0.001083	0.811116	0.017337	1.034751	0	0.02873	0.001961	0.003533	0.186871	0.203801	0.016755	1.186871	79.00098	2.798196	18.20083
57.2	0.001083	0.811393	0.02414	1.034193	0.000406	0.036311	0.002101	0.00633	0.184379	0.262239	0.023342	1.184379	78.61703	3.518216	17.86476
57.2	0.000722	0.813614	0.023482	1.035496	0.000406	0.017158	0.002381	0.006919	0.189362	0.29467	0.022677	1.189362	79.75557	1.681927	18.5625
57.2	0.000361	0.833323	0.021507	1.044806	0.000406	0.011971	0.002662	0.005594	0.18983	0.260123	0.020584	1.18983	80.50471	1.156446	18.33884
57.2	0.001083	0.819443	0.021068	1.037358	0	0.025737	0.001961	0.005742	0.187961	0.272531	0.020309	1.187961	79.31572	2.491128	18.19315
57.2	0.000722	0.819443	0.022823	1.034565	0	0.01616	0.002101	0.005742	0.190297	0.251567	0.022061	1.190297	79.87552	1.575236	18.54924
57.2	0.000722	0.820276	0.02019	1.033634	0	0.017756	0.001401	0.005153	0.191075	0.255213	0.019533	1.191075	79.70749	1.725421	18.56709
57.2	0.000361	0.820554	0.02414	1.030096	0.000406	0.014365	0.001681	0.00633	0.184224	0.262239	0.023435	1.184224	80.51417	1.409496	18.07633
57.2	0.000361	0.821109	0.023701	1.037358	0	0.016958	0.001821	0.006772	0.184379	0.28573	0.022848	1.184379	80.30825	1.65861	18.03314
57.51	0.000722	0.77614	0.019532	1.022834	0.000406	0.017956	0.002101	0.005889	0.20805	0.301503	0.019096	1.20805	77.44783	1.791752	20.76042
57.51	0.000361	0.778915	0.020848	1.025069	0	0.017557	0.003222	0.005742	0.215992	0.275399	0.020338	1.215992	76.93266	1.73408	21.33326
57.51	0.001083	0.780026	0.023262	1.0314	0.000812	0.015562	0.002662	0.004564	0.212254	0.19619	0.022554	1.212254	77.39566	1.544075	21.06026
57.51	0.000361	0.780859	0.018873	1.02842	0	0.01217	0.002802	0.004564	0.218172	0.241816	0.018352	1.218172	77.22095	1.203535	21.57552
57.51	0.000361	0.782247	0.019093	1.030469	0	0.015163	0.003362	0.00633	0.218172	0.331567	0.018528	1.218172	77.02453	1.493018	21.48245
57.51	0.000722	0.783634	0.022823	1.027117	0	0.018155	0.003922	0.006919	0.216459	0.30317	0.022221	1.216459	76.95905	1.783009	21.25794
57.51	0.000722	0.783912	0.022384	1.030655	0	0.027732	0.003502	0.007067	0.211008	0.315692	0.021719	1.211008	76.65479	2.71177	20.63344
57.51	0.000361	0.78419	0.019532	1.0206	0	0.013168	0.003362	0.004858	0.219106	0.24874	0.019137	1.219106	77.14883	1.295443	21.55573
57.51	0.000722	0.784745	0.02019	1.030655	0	0.012569	0.002802	0.00633	0.219106	0.313547	0.019589	1.219106	77.20674	1.236612	21.55664
57.51	0.000722	0.788076	0.022165	1.027862	0	0.019353	0.003782	0.005742	0.21568	0.259039	0.021564	1.21568	77.0276	1.891542	21.08086
57.51	0.000722	0.792795	0.020848	1.029724	0	0.014365	0.002942	0.006478	0.215369	0.310707	0.020246	1.215369	77.53281	1.404828	21.06236
57.51	0.000361	0.794183	0.020629	1.023765	0	0.014564	0.002802	0.007361	0.214279	0.356832	0.02015	1.214279	77.63078	1.423647	20.94557
57.59	0.000361	0.767812	0.024798	1.019482	0.000406	0.014564	0.002101	0.007067	0.230474	0.284961	0.024325	1.230474	75.80705	1.43795	22.755
57.59	0.000722	0.769477	0.020848	1.028234	0	0.021348	0.003222	0.006625	0.213656	0.317768	0.020276	1.213656	76.6045	2.125241	21.27026
57.59	0.000361	0.776695	0.02831	1.024324	0	0.01237	0.002241	0.006478	0.223778	0.228815	0.027638	1.223778	76.68467	1.221282	22.09405
57.59	0.000361	0.778083	0.023043	1.023951	0	0.018355	0.003642	0.005594	0.218172	0.242782	0.022504	1.218172	76.68791	1.809068	21.50303
57.59	0.000361	0.779471	0.021507	1.021717	0	0.016958	0.003922	0.006625	0.217393	0.308041	0.02105	1.217393	76.88436	1.67272	21.44292
57.59	0.000722	0.783912	0.023043	1.028048	0	0.021348	0.003502	0.006919	0.214279	0.300283	0.022414	1.214279	76.88893	2.093853	21.01722

Depth	Na2O	MgO	Al2O3	SiO2	K2O	CaO	TiO2	Cr2O3	FeO	Cr/Al	Al/Si	Mg#	En	Wo	Fs
57.59	0.000722	0.7853	0.018434	1.025441	0	0.013966	0.002662	0.004417	0.215836	0.239587	0.017977	1.215836	77.36172	1.375798	21.26249
57.59	0.000722	0.785578	0.020409	1.019482	0	0.014764	0.003642	0.007508	0.215057	0.367883	0.020019	1.215057	77.36643	1.453989	21.17958
57.65	0.001805	0.763648	0.019312	1.024324	0.000406	0.042296	0.003082	0.005742	0.205402	0.297306	0.018854	1.205402	75.50805	4.182172	20.30978
57.65	0.000722	0.782247	0.019093	1.025627	0	0.017956	0.003502	0.0053	0.215992	0.277591	0.018616	1.215992	76.97807	1.766981	21.25495
57.65	0.001083	0.783357	0.017118	1.02842	0	0.013567	0.002522	0.004858	0.217393	0.283819	0.016644	1.217393	77.23001	1.337523	21.43247
57.65	0.000722	0.78419	0.01602	1.026372	0	0.014764	0.003082	0.004711	0.21568	0.294069	0.015609	1.21568	77.28797	1.455086	21.25695
57.65	0.000722	0.7853	0.019093	1.032889	0.000406	0.014365	0.002522	0.006183	0.220975	0.323856	0.018485	1.220975	76.94195	1.407428	21.65062
57.65	0.000722	0.790852	0.01997	1.027303	0	0.010973	0.002101	0.005742	0.216926	0.287505	0.01944	1.216926	77.62956	1.077112	21.29332
57.65	0.000361	0.793905	0.02019	1.026558	0.000406	0.014365	0.003362	0.00633	0.21895	0.313547	0.019668	1.21895	77.28675	1.398411	21.31484
57.65	0.000722	0.795293	0.019751	1.025627	0	0.014165	0.003082	0.005889	0.219106	0.298153	0.019257	1.219106	77.32069	1.377187	21.30212
58.12	0.001083	0.7531	0.016459	1.027489	0.000406	0.043493	0.001681	0.005889	0.201042	0.357784	0.016019	1.201042	75.48851	4.359643	20.15185
58.12	0.000722	0.759484	0.020409	1.025627	0.000406	0.027532	0.002101	0.006183	0.210385	0.302962	0.019899	1.210385	76.14624	2.760418	21.09334
58.12	0.000722	0.759484	0.022165	1.019669	0	0.019153	0.003642	0.007803	0.213188	0.352027	0.021737	1.213188	76.57436	1.931087	21.49455
58.12	0.000361	0.770588	0.021068	1.022648	0	0.017756	0.003782	0.005594	0.214434	0.265543	0.020601	1.214434	76.84526	1.770725	21.38401
58.12	0.000361	0.771421	0.018873	1.026744	0.000812	0.023343	0.002802	0.0053	0.211787	0.280819	0.018382	1.211787	76.64004	2.319084	21.04087
58.12	0.000361	0.771421	0.018434	1.022089	0.000406	0.01616	0.003222	0.005447	0.215524	0.295491	0.018036	1.215524	76.90325	1.611033	21.48572
58.12	0.000361	0.771698	0.020848	1.022648	0	0.01616	0.003222	0.005594	0.215369	0.268338	0.020387	1.215369	76.92158	1.610838	21.46759
58.12	0.001083	0.773086	0.01997	1.02302	0.000406	0.023343	0.002381	0.007067	0.210385	0.353852	0.019521	1.210385	76.78537	2.318476	20.89615
58.54	0.000722	0.760039	0.020848	1.020786	0	0.032321	0.003222	0.006772	0.205714	0.32483	0.020424	1.205714	76.15062	3.23831	20.61107
58.54	0.000722	0.761705	0.021068	1.020786	0	0.025737	0.002802	0.005447	0.209607	0.258555	0.020639	1.209607	76.39597	2.581306	21.02273
58.54	0.001083	0.76226	0.019093	1.024137	0.000406	0.023542	0.003642	0.005889	0.20805	0.308434	0.018643	1.20805	76.69755	2.368789	20.93366
58.54	0.001083	0.7692	0.017776	1.024882	0	0.019752	0.002662	0.004417	0.211164	0.248461	0.017344	1.211164	76.9111	1.974927	21.11397
58.54	0.000722	0.772253	0.020629	1.030655	0	0.018355	0.003222	0.006036	0.211631	0.292602	0.020015	1.211631	77.05277	1.831396	21.11583
58.54	0.000361	0.774196	0.017995	1.023951	0	0.014165	0.003222	0.004417	0.211008	0.245431	0.017574	1.211008	77.46845	1.417418	21.11413
58.54	0	0.780581	0.01997	1.025441	0	0.013966	0.002381	0.006625	0.214746	0.331736	0.019475	1.214746	77.33942	1.383716	21.27686
58.54	0.000361	0.787798	0.019312	1.02991	0	0.011971	0.002381	0.005889	0.209295	0.304929	0.018751	1.209295	78.07216	1.186311	20.74153
58.6	0.000722	0.753377	0.022384	1.012965	0	0.029528	0.002381	0.014133	0.216147	0.631383	0.022098	1.216147	75.40921	2.955559	21.63524
58.6	0.000722	0.756431	0.021726	1.0206	0	0.038705	0.003082	0.00633	0.202599	0.291377	0.021288	1.202599	75.8148	3.879293	20.30591
58.6	0.001083	0.760039	0.019093	1.025813	0	0.037907	0.003502	0.005742	0.201821	0.300723	0.018612	1.201821	76.02166	3.791586	20.18676
58.6	0.000722	0.77031	0.02019	1.024324	0	0.014764	0.002942	0.006625	0.210385	0.328131	0.01971	1.210385	77.38238	1.483113	21.13451
58.6	0.000722	0.770588	0.01997	1.027303	0	0.018754	0.003222	0.005153	0.20914	0.258017	0.01944	1.20914	77.17598	1.878252	20.94577
58.6	0.000361	0.771698	0.017118	1.026931	0	0.014963	0.003082	0.005742	0.207115	0.335422	0.016669	1.207115	77.65308	1.5057	20.84122

Depth	Na2O	MgO	Al2O3	SiO2	K2O	CaO	TiO2	Cr2O3	FeO	Cr/Al	Al/Si	Mg#	En	Wo	Fs
58.6	0	0.775584	0.019312	1.028606	0	0.016759	0.002942	0.005742	0.212098	0.297306	0.018775	1.212098	77.21547	1.668478	21.11605
58.6	0.000361	0.782524	0.019751	1.027862	0	0.014165	0.002662	0.006036	0.209295	0.305607	0.019216	1.209295	77.78688	1.408098	20.80502
58.67	0.001444	0.748658	0.020848	1.022834	0	0.0409	0.002241	0.007361	0.196682	0.353076	0.020383	1.196682	75.91039	4.147033	19.94258
58.67	0.001805	0.75421	0.021068	1.023579	0	0.043892	0.002241	0.006625	0.200108	0.314458	0.020582	1.200108	75.55626	4.397105	20.04664
58.67	0.000361	0.759484	0.021726	1.022089	0	0.034316	0.002101	0.006772	0.205246	0.311706	0.021257	1.205246	76.02091	3.434858	20.54424
58.67	0.001083	0.761705	0.018873	1.029351	0	0.029927	0.002802	0.00633	0.204779	0.335422	0.018335	1.204779	76.44487	3.003439	20.55169
58.67	0.000722	0.766979	0.018654	1.029724	0	0.023542	0.002942	0.006183	0.205869	0.331476	0.018115	1.205869	76.97574	2.362753	20.66151
58.67	0.000361	0.767812	0.019532	1.025255	0	0.016759	0.003502	0.005889	0.212254	0.301503	0.01905	1.212254	77.02575	1.681227	21.29302
58.67	0.000722	0.770588	0.020409	1.024882	0	0.025936	0.003082	0.00633	0.205091	0.310175	0.019914	1.205091	76.93454	2.589456	20.47601
58.67	0.000361	0.779193	0.019312	1.028048	0	0.017756	0.002942	0.006036	0.20914	0.312553	0.018785	1.20914	77.44772	1.764898	20.78739
59.27	0.001444	0.749769	0.021068	1.020972	0.000406	0.046286	0.002522	0.008097	0.19964	0.384338	0.020635	1.19964	75.301	4.648657	20.05034
59.27	0.000722	0.758651	0.024798	1.020227	0	0.015562	0.002241	0.007361	0.213344	0.296834	0.024307	1.213344	76.82099	1.57579	21.60322
59.27	0.000722	0.759762	0.021507	1.026186	0	0.038705	0.003502	0.005742	0.201353	0.266969	0.020958	1.201353	75.98984	3.871202	20.13895
59.27	0.001083	0.765314	0.019751	1.029724	0	0.034515	0.003362	0.006478	0.20805	0.327968	0.019181	1.20805	75.93312	3.424554	20.64232
59.27	0.001083	0.766979	0.018434	1.024696	0	0.020749	0.002802	0.005594	0.203689	0.303477	0.01799	1.203689	77.36187	2.092873	20.54525
59.27	0.001083	0.769755	0.02019	1.021344	0	0.022146	0.003642	0.007655	0.209607	0.379173	0.019768	1.209607	76.85964	2.211235	20.92913
59.27	0.000722	0.782524	0.016679	1.027489	0.000406	0.013567	0.002802	0.004564	0.211008	0.273634	0.016232	1.211008	77.7008	1.347109	20.95209
59.27	0.000722	0.787521	0.019312	1.03382	0	0.015961	0.002802	0.006183	0.21023	0.320176	0.01868	1.21023	77.68689	1.574497	20.73862
59.33	0.000722	0.729227	0.018215	1.007006	0	0.039304	0.005884	0.006919	0.201042	0.379876	0.018088	1.201042	75.21119	4.053704	20.73511
59.33	0.002166	0.753932	0.021946	1.024137	0	0.051274	0.002662	0.007067	0.195124	0.322005	0.021428	1.195124	75.3683	5.125727	19.50597
59.33	0.001444	0.756431	0.02019	1.019669	0	0.03651	0.003082	0.005742	0.201509	0.28438	0.0198	1.201509	76.06522	3.67142	20.26336
59.33	0.000722	0.763093	0.020848	1.022089	0	0.04908	0.002802	0.005594	0.19964	0.268338	0.020398	1.19964	75.41838	4.850661	19.73096
59.33	0.000722	0.767534	0.017776	1.029351	0	0.018754	0.002942	0.006183	0.20914	0.347845	0.017269	1.20914	77.10596	1.884014	21.01002
59.33	0.001083	0.768922	0.019093	1.01911	0	0.030725	0.002802	0.006772	0.203689	0.354699	0.018735	1.203689	76.63656	3.062248	20.3012
59.33	0.000722	0.771143	0.019312	1.018737	0	0.019752	0.003222	0.006625	0.209295	0.343046	0.018957	1.209295	77.09966	1.97478	20.92556
59.33	0	0.774474	0.021287	1.023951	0	0.015562	0.002802	0.007067	0.210385	0.331964	0.020789	1.210385	77.41479	1.555528	21.02968
59.39	0.001083	0.752544	0.022165	1.020786	0	0.044491	0.003222	0.007803	0.19964	0.352027	0.021714	1.19964	75.50545	4.463926	20.03062
59.39	0.000722	0.76226	0.020409	1.029165	0	0.030924	0.002241	0.006478	0.207271	0.317389	0.019831	1.207271	76.19133	3.091008	20.71766
59.39	0.000722	0.766702	0.023921	1.019296	0	0.019552	0.003642	0.007803	0.212721	0.32619	0.023468	1.212721	76.74883	1.957211	21.29396
59.39	0.001083	0.767812	0.022823	1.027303	0.000406	0.034515	0.003502	0.007508	0.199952	0.328972	0.022217	1.199952	76.6066	3.443686	19.94971
59.39	0.000361	0.780026	0.018215	1.032517	0	0.015163	0.003362	0.005153	0.20805	0.282886	0.017641	1.20805	77.75081	1.511387	20.7378
59.39	0.000722	0.781136	0.018215	1.030282	0	0.014165	0.003082	0.005742	0.20805	0.315216	0.017679	1.20805	77.85274	1.411795	20.73547

Depth	Na2O	MgO	Al2O3	SiO2	K2O	CaO	TiO2	Cr2O3	FeO	Cr/Al	Al/Si	Mg#	En	Wo	Fs
59.39	0.000361	0.785855	0.02414	1.026372	0	0.017557	0.003362	0.007803	0.211164	0.323225	0.02352	1.211164	77.4565	1.73047	20.81303
59.39	0.000361	0.786688	0.018654	1.032517	0	0.012569	0.002802	0.004858	0.20805	0.260446	0.018066	1.20805	78.09816	1.2478	20.65404
59.44	0.001444	0.749491	0.022384	1.022834	0	0.045289	0.003082	0.00633	0.202132	0.282807	0.021885	1.202132	75.18127	4.54292	20.27581
59.44	0.001444	0.756153	0.01997	1.018179	0.000406	0.03252	0.003222	0.005594	0.208361	0.280133	0.019614	1.208361	75.84023	3.261696	20.89808
59.44	0.000722	0.773641	0.018434	1.02842	0.000406	0.016759	0.002802	0.005742	0.20805	0.311464	0.017925	1.20805	77.48425	1.678491	20.83726
59.44	0.000361	0.775307	0.019312	1.028979	0	0.01616	0.003362	0.006478	0.210385	0.335422	0.018768	1.210385	77.38731	1.613048	20.99964
59.44	0.000361	0.775862	0.019751	1.026744	0	0.015961	0.003082	0.00633	0.209607	0.320515	0.019237	1.209607	77.47544	1.593806	20.93076
59.44	0.000361	0.780859	0.019751	1.025627	0	0.013966	0.002802	0.006183	0.20914	0.313061	0.019257	1.20914	77.77755	1.39106	20.83139
59.44	0.000361	0.781691	0.017337	1.02991	0	0.019752	0.008265	0.0053	0.207271	0.305701	0.016834	1.207271	77.49387	1.958093	20.54804
59.44	0.000361	0.790574	0.016459	1.032331	0	0.013766	0.002662	0.005594	0.212098	0.339895	0.015944	1.212098	77.77883	1.354359	20.86681
60.54	0.002166	0.737832	0.02019	1.019669	0	0.07342	0.002942	0.006036	0.186404	0.298963	0.0198	1.186404	73.95659	7.359242	18.68417
60.54	0.001444	0.756431	0.020629	1.030096	0	0.046685	0.002381	0.00633	0.192633	0.306876	0.020026	1.192633	75.96601	4.68848	19.34551
60.54	0.001444	0.756431	0.021507	1.028793	0	0.04489	0.002522	0.00633	0.19528	0.29435	0.020905	1.19528	75.90109	4.504301	19.59461
60.54	0.001805	0.76337	0.020848	1.024696	0	0.043693	0.003082	0.007214	0.197927	0.346015	0.020346	1.197927	75.95797	4.347585	19.69445
60.54	0.000361	0.770588	0.025018	1.023393	0	0.017357	0.003222	0.006036	0.212254	0.241269	0.024446	1.212254	77.04342	1.735397	21.22118
60.54	0.000361	0.782524	0.023701	1.025069	0	0.019552	0.003082	0.007361	0.207271	0.310576	0.023122	1.207271	77.52775	1.937098	20.53515
60.54	0.000361	0.783079	0.021287	1.031027	0	0.019153	0.002662	0.006478	0.204468	0.304301	0.020647	1.204468	77.78675	1.902555	20.3107
60.54	0.000361	0.788909	0.01624	1.035496	0	0.012569	0.003502	0.0053	0.207894	0.326357	0.015683	1.207894	78.15839	1.245247	20.59636
60.59	0.000722	0.764758	0.020848	1.028048	0.000406	0.026934	0.006724	0.005889	0.201198	0.282461	0.020279	1.201198	77.02348	2.712681	20.26384
60.59	0.000722	0.77031	0.017995	1.027862	0.000406	0.037508	0.002522	0.00633	0.194813	0.351784	0.017508	1.194813	76.82888	3.740957	19.43016
60.59	0.000361	0.773919	0.021946	1.026558	0	0.019153	0.002662	0.006183	0.204312	0.281755	0.021378	1.204312	77.59487	1.920326	20.4848
60.59	0.001083	0.774196	0.020409	1.027489	0	0.031922	0.002942	0.00633	0.203222	0.310175	0.019863	1.203222	76.70322	3.16263	20.13415
60.59	0.000722	0.778915	0.018873	1.026186	0	0.027732	0.002522	0.00633	0.200575	0.335422	0.018392	1.200575	77.33304	2.753313	19.91365
60.59	0	0.781414	0.021946	1.02842	0.000406	0.02035	0.003362	0.00795	0.207894	0.362256	0.021339	1.207894	77.39393	2.015543	20.59053
60.59	0.000361	0.782247	0.021726	1.026558	0	0.013567	0.002381	0.006036	0.211008	0.277825	0.021164	1.211008	77.69465	1.34748	20.95787
60.59	0.000361	0.789741	0.017337	1.036427	0.000406	0.012569	0.002662	0.0053	0.200886	0.305701	0.016728	1.200886	78.72249	1.252912	20.0246
60.61	0.001083	0.7692	0.01997	1.028979	0	0.037308	0.002662	0.005594	0.198706	0.280133	0.019408	1.198706	76.52098	3.711496	19.76753
60.61	0.001083	0.775307	0.019751	1.028606	0.000406	0.036311	0.002802	0.005594	0.198395	0.283245	0.019202	1.198395	76.76212	3.595098	19.64279
60.61	0.001083	0.780859	0.020629	1.033634	0	0.026934	0.002101	0.006919	0.204779	0.335422	0.019958	1.204779	77.11637	2.659953	20.22368
60.61	0.000361	0.785022	0.020629	1.027117	0.000406	0.019951	0.002522	0.005889	0.201821	0.285466	0.020084	1.201821	77.9725	1.981643	20.04586
60.61	0	0.788631	0.021726	1.030282	0	0.020949	0.002522	0.006036	0.204935	0.277825	0.021088	1.204935	77.73481	2.06489	20.2003
60.61	0.000361	0.791407	0.016898	1.028979	0.000406	0.019552	0.002802	0.005889	0.202911	0.348491	0.016422	1.202911	78.05806	1.928457	20.01348

Depth	Na2O	MgO	Al2O3	SiO2	K2O	CaO	TiO2	Cr2O3	FeO	Cr/Al	Al/Si	Mg#	En	Wo	Fs
60.61	0.000722	0.791685	0.020629	1.032144	0	0.013367	0.003502	0.005594	0.204468	0.271192	0.019986	1.204468	78.42191	1.324116	20.25397
60.61	0.000361	0.79335	0.020629	1.030282	0.000406	0.016559	0.002942	0.006183	0.200419	0.299739	0.020023	1.200419	78.52398	1.63901	19.83701
60.68	0.001083	0.775862	0.01997	1.025069	0	0.039104	0.002241	0.006478	0.193411	0.324364	0.019482	1.193411	76.94163	3.877921	19.18045
60.68	0.000722	0.778083	0.023921	1.026931	0.000406	0.031523	0.002101	0.007214	0.199796	0.301572	0.023293	1.199796	77.08357	3.122908	19.79352
60.68	0.000361	0.786966	0.021946	1.030282	0.000406	0.017956	0.001961	0.006625	0.201042	0.30188	0.021301	1.201042	78.23004	1.784951	19.98501
60.68	0	0.787798	0.02019	1.027675	0	0.018355	0.003502	0.006036	0.199796	0.298963	0.019646	1.199796	78.31391	1.824642	19.86144
60.68	0.000361	0.788631	0.022384	1.019296	0	0.017357	0.002942	0.006478	0.19746	0.289384	0.021961	1.19746	78.59207	1.729777	19.67816
60.68	0	0.791685	0.019532	1.034379	0	0.012769	0.002662	0.00633	0.200108	0.324116	0.018882	1.200108	78.80903	1.271071	19.9199
60.68	0	0.793905	0.019312	1.033448	0	0.014963	0.002241	0.006036	0.20073	0.312553	0.018687	1.20073	78.6357	1.482103	19.88219
60.68	0.000361	0.796959	0.017776	1.035869	0	0.022944	0.002241	0.004858	0.196059	0.273307	0.01716	1.196059	78.44382	2.258327	19.29785
60.68	0.001083	0.775862	0.01997	1.025069	0	0.039104	0.002241	0.006478	0.193411	0.324364	0.019482	1.193411	76.94163	3.877921	19.18045
60.68	0.000722	0.778083	0.023921	1.026931	0.000406	0.031523	0.002101	0.007214	0.199796	0.301572	0.023293	1.199796	77.08357	3.122908	19.79352
60.68	0.000361	0.786966	0.021946	1.030282	0.000406	0.017956	0.001961	0.006625	0.201042	0.30188	0.021301	1.201042	78.23004	1.784951	19.98501
60.68	0	0.787798	0.02019	1.027675	0	0.018355	0.003502	0.006036	0.199796	0.298963	0.019646	1.199796	78.31391	1.824642	19.86144
60.68	0.000361	0.788631	0.022384	1.019296	0	0.017357	0.002942	0.006478	0.19746	0.289384	0.021961	1.19746	78.59207	1.729777	19.67816
60.68	0	0.791685	0.019532	1.034379	0	0.012769	0.002662	0.00633	0.200108	0.324116	0.018882	1.200108	78.80903	1.271071	19.9199
60.68	0	0.793905	0.019312	1.033448	0	0.014963	0.002241	0.006036	0.20073	0.312553	0.018687	1.20073	78.6357	1.482103	19.88219
60.68	0.000361	0.796959	0.017776	1.035869	0	0.022944	0.002241	0.004858	0.196059	0.273307	0.01716	1.196059	78.44382	2.258327	19.29785
61.09	0.000361	0.809173	0.021068	1.034193	0	0.014365	0.002241	0.006625	0.182043	0.314458	0.020371	1.182043	80.46819	1.428504	18.1033
61.09	0.000361	0.815002	0.019312	1.037731	0	0.011971	0.001961	0.005742	0.181109	0.297306	0.01861	1.181109	80.84683	1.187467	17.96571
61.09	0.000722	0.818056	0.023701	1.04071	0	0.01616	0.002381	0.006478	0.182043	0.273307	0.022774	1.182043	80.49674	1.590181	17.91308
61.09	0.000361	0.820554	0.022823	1.041641	0	0.015761	0.001961	0.006183	0.180175	0.270918	0.021911	1.180175	80.72426	1.550565	17.72518
61.09	0.000361	0.824995	0.021946	1.03922	0.000406	0.016759	0.002241	0.006036	0.175191	0.275046	0.021117	1.175191	81.12482	1.647964	17.22722
61.09	0.000722	0.831935	0.018873	1.041455	0	0.017357	0.002522	0.0053	0.173478	0.280819	0.018122	1.173478	81.34129	1.697098	16.96161
61.13	0.010109	0.492443	0.028968	1.047227	0.000812	0.2446	0.001961	0.005594	0.124581	0.193122	0.027662	1.124581	57.15293	28.38826	14.45881
61.13	0.007582	0.558787	0.106875	0.927496	0.000812	0.166591	0.0007	0.009275	0.133613	0.086783	0.115229	1.133613	65.05156	19.39384	15.5546
61.13	0.006499	0.604312	0.016679	1.068827	0.002031	0.115916	0.000981	0.004417	0.097484	0.264807	0.015605	1.097484	73.90279	14.17562	11.9216
61.13	0.001083	0.70119	0.304165	0.697531	0	0.001197	0.0007	0.005742	0.171143	0.018877	0.43606	1.171143	80.2709	0.137037	19.59206
61.13	0.000361	0.717568	0.324136	0.610758	0.000812	0.001796	0	0.010747	0.177839	0.033156	0.530711	1.177839	79.9784	0.200133	19.82147
61.13	0.000722	0.740331	0.324355	0.63031	0	0.001596	0	0.005742	0.176281	0.017702	0.514597	1.176281	80.62775	0.173826	19.19842
61.13	0.002888	0.768922	0.027871	1.029351	0.000406	0.063644	0.002662	0.008539	0.174101	0.30637	0.027076	1.174101	76.38294	6.322236	17.29482
61.13	0.000361	0.805009	0.022823	1.032331	0	0.019353	0.002522	0.00633	0.183445	0.277368	0.022109	1.183445	79.87734	1.920263	18.2024

Depth	Na2O	MgO	Al2O3	SiO2	K2O	CaO	TiO2	Cr2O3	FeO	Cr/Al	Al/Si	Mg#	En	Wo	Fs
61.13	0.000722	0.805564	0.025237	1.033634	0.000406	0.019951	0.001541	0.006478	0.182355	0.256671	0.024416	1.182355	79.92738	1.979528	18.09309
61.13	0	0.811671	0.019312	1.035869	0.000406	0.013766	0.002381	0.005889	0.186404	0.304929	0.018643	1.186404	80.21726	1.360514	18.42223
61.13	0.000361	0.815835	0.020409	1.035869	0.000406	0.013766	0.001681	0.004564	0.18033	0.223615	0.019703	1.18033	80.78121	1.363086	17.8557
61.73	0.004693	0.695083	0.027871	1.013524	0	0.152027	0.002241	0.008392	0.15993	0.301088	0.027499	1.15993	69.02237	15.09642	15.88121
61.73	0.001083	0.771143	0.022165	1.026558	0	0.029727	0.002381	0.006919	0.201042	0.312175	0.021592	1.201042	76.96714	2.967036	20.06582
61.73	0.000722	0.776972	0.023262	1.033075	0	0.02853	0.002381	0.007214	0.197772	0.310107	0.022518	1.197772	77.44368	2.843692	19.71263
61.73	0.000722	0.77836	0.019751	1.030282	0	0.016559	0.002522	0.005447	0.201665	0.275792	0.01917	1.201665	78.10279	1.661614	20.23559
61.73	0.000361	0.781969	0.014923	1.032517	0	0.014365	0.001961	0.004269	0.207894	0.286095	0.014453	1.207894	77.86771	1.430429	20.70186
61.73	0.000361	0.786133	0.023262	1.031772	0.000406	0.019951	0.002241	0.006036	0.205869	0.259478	0.022546	1.205869	77.6847	1.97154	20.34376
61.73	0.000361	0.788631	0.016898	1.030282	0.001218	0.013367	0.002101	0.004269	0.208828	0.252656	0.016401	1.208828	78.01844	1.322404	20.65915
61.73	0.000722	0.800845	0.011851	1.039406	0	0.001995	0.00042	0.001914	0.213188	0.1615	0.011401	1.213188	78.82111	0.196363	20.98253
61.8	0.001083	0.773919	0.021068	1.029724	0	0.03671	0.002662	0.005889	0.197304	0.279519	0.02046	1.197304	76.78275	3.642102	19.57515
61.8	0.001083	0.774196	0.023043	1.022648	0.000406	0.019353	0.002101	0.006919	0.198239	0.300283	0.022533	1.198239	78.06069	1.951277	19.98803
61.8	0.000361	0.775862	0.020848	1.028606	0.000406	0.019552	0.003362	0.004564	0.206648	0.218907	0.020268	1.206648	77.42654	1.951181	20.62228
61.8	0.001083	0.782524	0.02809	1.030655	0	0.031323	0.002101	0.008244	0.188895	0.293495	0.027255	1.188895	78.03839	3.12375	18.83786
61.8	0.000361	0.788353	0.017118	1.035682	0	0.012968	0.002241	0.004269	0.206181	0.249417	0.016528	1.206181	78.24829	1.287162	20.46455
61.8	0.000361	0.788631	0.023701	1.030096	0	0.013966	0.002522	0.005447	0.204468	0.229826	0.023009	1.204468	78.30987	1.386777	20.30335
61.8	0.000722	0.79446	0.022165	1.030841	0.000406	0.010175	0.001541	0.006625	0.193878	0.298891	0.021502	1.193878	79.56428	1.019018	19.4167
61.9	0.002166	0.764758	0.028529	1.02302	0	0.041498	0.001961	0.008392	0.199017	0.29414	0.027887	1.199017	76.07462	4.128049	19.79733
61.9	0.000722	0.779748	0.01624	1.026558	0	0.010574	0.002802	0.003975	0.200419	0.244768	0.01582	1.200419	78.70352	1.067288	20.22919
61.9	0.000722	0.783357	0.016459	1.03531	0	0.014564	0.002942	0.003828	0.206181	0.232559	0.015898	1.206181	78.01567	1.450478	20.53385
61.9	0.000361	0.788353	0.013167	1.037731	0	0.012569	0.000841	0.002356	0.206492	0.178892	0.012689	1.206492	78.25509	1.247666	20.49724
61.9	0.000361	0.789464	0.026115	1.032144	0	0.013966	0.001541	0.006919	0.21132	0.264955	0.025302	1.21132	77.7989	1.376275	20.82482
61.9	0.000361	0.790297	0.026115	1.027117	0.000406	0.014365	0.001821	0.007067	0.208984	0.270593	0.025426	1.208984	77.9658	1.417139	20.61706
61.9	0.000361	0.791685	0.025018	1.028234	0	0.011971	0.002381	0.007067	0.202755	0.282461	0.024331	1.202755	78.66421	1.189439	20.14635
61.9	0.000722	0.791685	0.019093	1.032703	0	0.012968	0.002241	0.004858	0.21023	0.254458	0.018488	1.21023	78.00751	1.277802	20.71468
61.99	0.001083	0.754488	0.026335	1.020227	0.000406	0.03671	0.001541	0.007067	0.201821	0.268338	0.025813	1.201821	75.97924	3.696806	20.32395
61.99	0.001805	0.760317	0.024579	1.027489	0.000406	0.042496	0.002101	0.006625	0.197927	0.269536	0.023921	1.197927	75.97547	4.246434	19.7781
61.99	0.000722	0.7692	0.026115	1.02842	0.000406	0.02454	0.001821	0.006036	0.203533	0.231131	0.025394	1.203533	77.13031	2.460691	20.409
61.99	0.001444	0.770865	0.022823	1.032889	0	0.034515	0.003082	0.005594	0.196214	0.245116	0.022097	1.196214	76.96377	3.446037	19.59019
61.99	0.000722	0.773919	0.023921	1.028234	0	0.023941	0.002101	0.007361	0.204935	0.307727	0.023264	1.204935	77.17617	2.387454	20.43638
61.99	0.001083	0.778915	0.026115	1.026372	0	0.030326	0.001541	0.007508	0.194813	0.287505	0.025444	1.194813	77.57705	3.020317	19.40263

Depth	Na2O	MgO	Al2O3	SiO2	K2O	CaO	TiO2	Cr2O3	FeO	Cr/Al	Al/Si	Mg#	En	Wo	Fs
61.99	0.000722	0.784745	0.026774	1.032517	0	0.022146	0.002101	0.007508	0.202132	0.280435	0.02593	1.202132	77.77278	2.194766	20.03245
61.99	0.000361	0.795571	0.025896	1.031027	0	0.013168	0.002381	0.007361	0.206648	0.284256	0.025116	1.206648	78.35152	1.296817	20.35166
62.08	0.001444	0.757263	0.023701	1.025627	0	0.043294	0.002802	0.006036	0.199485	0.254672	0.023109	1.199485	75.72317	4.329199	19.94763
62.08	0.000361	0.775029	0.020409	1.022834	0	0.014764	0.002522	0.005742	0.206648	0.281322	0.019954	1.206648	77.77974	1.481652	20.73861
62.08	0.000361	0.778638	0.022823	1.02451	0	0.014963	0.003082	0.005742	0.214746	0.251567	0.022277	1.214746	77.21924	1.483943	21.29681
62.08	0	0.783079	0.025018	1.0314	0	0.014165	0.002662	0.006478	0.208361	0.258922	0.024256	1.208361	77.87142	1.408629	20.71995
62.08	0.000722	0.785022	0.025896	1.024137	0	0.009976	0.001961	0.006919	0.203378	0.267201	0.025285	1.203378	78.62996	0.999176	20.37086
62.08	0.000361	0.786688	0.013606	1.027117	0	0.013367	0.002381	0.003239	0.206648	0.238042	0.013247	1.206648	78.14498	1.327821	20.5272
62.08	0.000361	0.796681	0.014704	1.034379	0	0.014963	0.002241	0.003386	0.206959	0.23029	0.014215	1.206959	78.21305	1.469001	20.31795
62.08	0.000361	0.798347	0.015801	1.032144	0.000406	0.013567	0.002802	0.003239	0.207271	0.20498	0.015309	1.207271	78.33192	1.331135	20.33694
62.57	0.001083	0.793628	0.024798	1.034565	0	0.041897	0.002101	0.006772	0.17052	0.273087	0.02397	1.17052	78.88594	4.16455	16.94951
62.57	0.001444	0.795016	0.025018	1.031027	0.000406	0.041299	0.001821	0.008244	0.175036	0.329538	0.024265	1.175036	78.60935	4.083522	17.30713
62.57	0.001444	0.8014	0.022823	1.037358	0	0.036909	0.001681	0.006625	0.170675	0.290269	0.022001	1.170675	79.42637	3.658079	16.91555
62.57	0.001083	0.811949	0.025237	1.034937	0	0.033518	0.001961	0.005594	0.173011	0.22167	0.024385	1.173011	79.72179	3.290969	16.98724
62.57	0.000722	0.811949	0.021287	1.037917	0	0.026335	0.001541	0.006772	0.171765	0.318132	0.02051	1.171765	80.38701	2.607338	17.00565
62.57	0.001083	0.820554	0.02436	1.036986	0	0.026734	0.002381	0.006183	0.165381	0.253833	0.023491	1.165381	81.02883	2.639996	16.33117
62.57	0	0.827216	0.023262	1.034751	0	0.012968	0.001961	0.007361	0.181888	0.316436	0.022481	1.181888	80.93521	1.268814	17.79597
62.57	0	0.833878	0.022604	1.041641	0	0.012569	0.001961	0.0053	0.17161	0.23447	0.0217	1.17161	81.90878	1.234623	16.85659
62.65	0.001805	0.773641	0.026774	1.032703	0	0.06524	0.001961	0.006772	0.159463	0.252941	0.025926	1.159463	77.49243	6.534817	15.97276
62.65	0.002527	0.785855	0.02831	1.027862	0.000406	0.065639	0.002101	0.007361	0.160397	0.260017	0.027542	1.160397	77.66199	6.486761	15.85125
62.65	0.001083	0.810005	0.027651	1.041455	0	0.034316	0.001961	0.00633	0.173323	0.228939	0.026551	1.173323	79.59615	3.372086	17.03176
62.65	0.001083	0.816668	0.025018	1.0422	0	0.038306	0.002101	0.00633	0.166938	0.253038	0.024005	1.166938	79.91568	3.748469	16.33585
62.65	0.001083	0.819721	0.026115	1.041082	0	0.03671	0.002381	0.007214	0.162422	0.27623	0.025085	1.162422	80.45529	3.603067	15.94164
62.65	0.000361	0.82555	0.026554	1.040524	0	0.019353	0.001681	0.006625	0.166471	0.249488	0.02552	1.166471	81.62664	1.91349	16.45987
62.65	0.000722	0.835266	0.025237	1.046482	0	0.014365	0.001961	0.006036	0.169274	0.239171	0.024116	1.169274	81.97686	1.409824	16.61331
62.65	0	0.838597	0.026115	1.043689	0	0.014165	0.001821	0.005889	0.165692	0.225494	0.025022	1.165692	82.34016	1.390858	16.26898
62.78	0.002527	0.762815	0.037307	1.023206	0	0.067036	0.002662	0.009864	0.166782	0.264392	0.036461	1.166782	76.53923	6.726204	16.73457
62.78	0.001805	0.771143	0.029407	1.028606	0	0.064841	0.002101	0.00795	0.160242	0.27034	0.028589	1.160242	77.40645	6.508661	16.08488
62.78	0.001805	0.780303	0.032918	1.02302	0.000812	0.038905	0.001541	0.008244	0.175036	0.250449	0.032178	1.175036	78.48211	3.912982	17.60491
62.78	0.001805	0.786688	0.02831	1.03531	0.000812	0.043493	0.001681	0.007361	0.164602	0.260017	0.027344	1.164602	79.08134	4.37214	16.54652
62.78	0.001083	0.8014	0.026774	1.038103	0	0.041299	0.001541	0.006772	0.171454	0.252941	0.025791	1.171454	79.02163	4.072236	16.90613
62.78	0.001083	0.801955	0.029627	1.033634	0.000406	0.027931	0.001681	0.007508	0.17815	0.25343	0.028662	1.17815	79.55614	2.770879	17.67298

Depth	Na2O	MgO	Al2O3	SiO2	K2O	CaO	TiO2	Cr2O3	FeO	Cr/Al	Al/Si	Mg#	En	Wo	Fs
62.78	0.000722	0.806119	0.02831	1.030841	0	0.023742	0.001261	0.005742	0.175036	0.202813	0.027463	1.175036	80.21911	2.362608	17.41828
62.78	0.000361	0.807507	0.02436	1.037731	0.000406	0.029328	0.002522	0.006625	0.175191	0.271964	0.023474	1.175191	79.7911	2.897954	17.31095
62.84	0.002527	0.758929	0.027651	1.028793	0	0.081999	0.002101	0.007361	0.162422	0.266208	0.026878	1.162422	75.63953	8.17251	16.18796
62.84	0.001444	0.778083	0.029188	1.02842	0	0.050077	0.002241	0.007067	0.1727	0.242109	0.028381	1.1727	77.74144	5.003415	17.25515
62.84	0.001444	0.790574	0.031821	1.027675	0	0.029727	0.001681	0.00898	0.181888	0.282217	0.030964	1.181888	78.88475	2.966216	18.14904
62.84	0.001805	0.795571	0.028529	1.032331	0	0.043493	0.001961	0.006036	0.163668	0.211574	0.027636	1.163668	79.34034	4.337482	16.32218
62.84	0.001444	0.802233	0.02809	1.031586	0.000812	0.027931	0.001961	0.008097	0.177683	0.288254	0.02723	1.177683	79.59865	2.7714	17.62995
62.84	0.000722	0.814169	0.027651	1.035496	0.000406	0.015562	0.001821	0.007655	0.181888	0.276857	0.026704	1.181888	80.48183	1.53831	17.97986
62.84	0.000722	0.819721	0.027651	1.0368	0	0.014764	0.001681	0.007067	0.178462	0.25556	0.02667	1.178462	80.92442	1.457509	17.61807
62.84	0.000361	0.821942	0.02809	1.039034	0	0.017357	0.001401	0.006772	0.17597	0.241085	0.027035	1.17597	80.95801	1.709638	17.33235
63.79	0.000361	0.807507	0.023262	1.0314	0.000406	0.011771	0.002381	0.006625	0.189674	0.284793	0.022554	1.189674	80.03423	1.166668	18.7991
63.79	0	0.808895	0.022604	1.034937	0	0.011572	0.002662	0.007067	0.190453	0.312627	0.021841	1.190453	80.0158	1.144663	18.83954
63.79	0	0.808895	0.023262	1.032703	0	0.009776	0.001821	0.00633	0.188895	0.272135	0.022526	1.188895	80.28206	0.970261	18.74768
63.79	0.000361	0.814447	0.025896	1.034751	0	0.011771	0.002381	0.005889	0.181109	0.227405	0.025026	1.181109	80.85228	1.168551	17.97917
63.93	0.012636	0.680094	0.064959	1.055606	0.003655	0.013966	0.0007	0.006036	0.088608	0.092921	0.061537	1.088608	86.89435	1.784378	11.32128
63.93	0.014802	0.697304	0.062325	1.054489	0.003249	0.007781	0.0007	0.006183	0.088764	0.099209	0.059105	1.088764	87.83842	0.980151	11.18143
63.93	0.00686	0.71396	0.120481	0.971069	0.001624	0.008379	0.00028	0.006036	0.106828	0.0501	0.124071	1.106828	86.10566	1.010586	12.88376
64	0.000722	0.778638	0.022384	1.020041	0.000812	0.015163	0.002101	0.005889	0.208361	0.263076	0.021945	1.208361	77.69583	1.51301	20.79116
64	0.000361	0.785022	0.017995	1.027117	0	0.014165	0.001961	0.005447	0.211475	0.302698	0.01752	1.211475	77.67399	1.40158	20.92443
64	0.000361	0.825273	0.024798	1.0314	0	0.013766	0.002381	0.007214	0.171454	0.290897	0.024044	1.171454	81.67031	1.362328	16.96736
64	0.000361	0.839707	0.026335	1.041641	0.000812	0.014365	0.001961	0.005742	0.172388	0.218024	0.025282	1.172388	81.80611	1.399446	16.79444
64	0.000361	0.843871	0.023921	1.041827	0.000406	0.010175	0.002381	0.004564	0.161176	0.190791	0.02296	1.161176	83.12181	1.002247	15.87594
64.12	0.000361	0.771143	0.021287	1.019296	0	0.01636	0.002241	0.006919	0.217237	0.325048	0.020884	1.217237	76.75048	1.628269	21.62125
64.12	0	0.771143	0.020629	1.033262	0	0.01237	0.002522	0.004564	0.221442	0.221236	0.019965	1.221442	76.73411	1.230867	22.03502
64.12	0.000361	0.775307	0.020629	1.023765	0.000406	0.02055	0.002101	0.005889	0.208984	0.285466	0.02015	1.208984	77.15722	2.045061	20.79772
64.12	0.000361	0.775584	0.019751	1.028793	0	0.015961	0.001961	0.005153	0.214434	0.260884	0.019198	1.214434	77.09743	1.586598	21.31597
64.12	0.000722	0.776972	0.018873	1.026186	0.000812	0.015362	0.002381	0.005742	0.21241	0.30422	0.018392	1.21241	77.33034	1.528978	21.14068
64.12	0.000722	0.77836	0.018215	1.021717	0.000406	0.014564	0.001961	0.004858	0.208672	0.266721	0.017828	1.208672	77.71192	1.454105	20.83397

* In Appendix I, MgO and BaO were analyzed for but not displayed because they were not used in data interpretation.

* In Appendix II and III, MnO and BaO were analyzed for but not displayed because they were not used in data interpretation.